Latest Higgs physics results from the ATLAS experiment

UNIVERSITY of GLASGOW

Dr. Adrian Buzatu

10th edition of the international conference

Hadron Structure and QCD: from low to high energies

27 June – 1 July, Gatchina, St. Petersburg, Russia

Observing and measuring all Higgs boson couplings is essential to confirm SM or discover BSM.

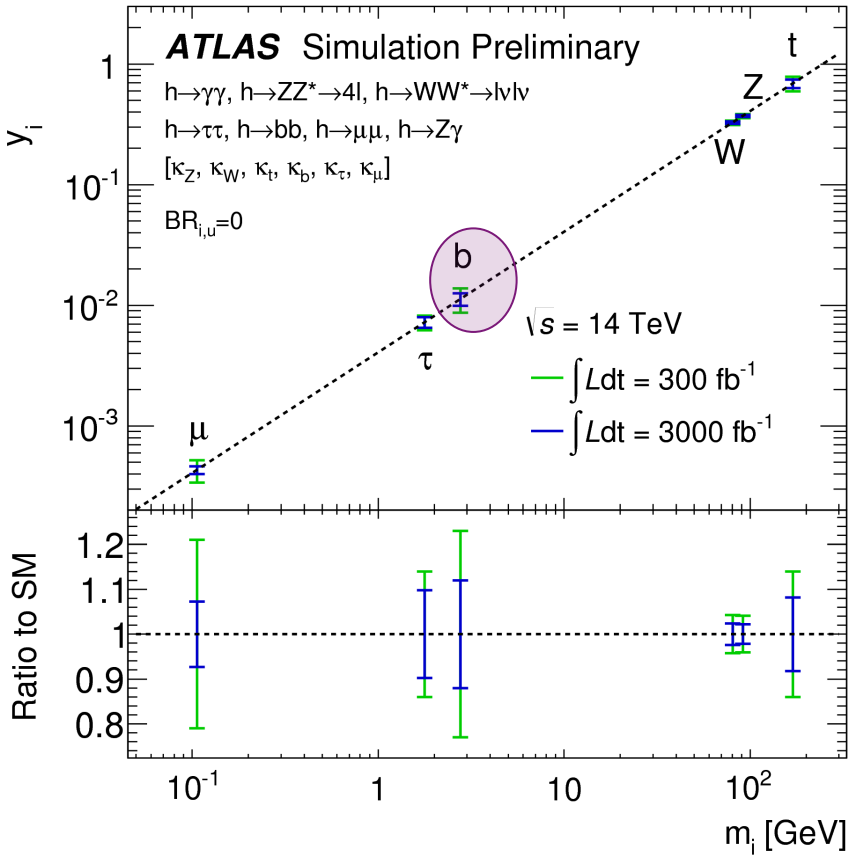

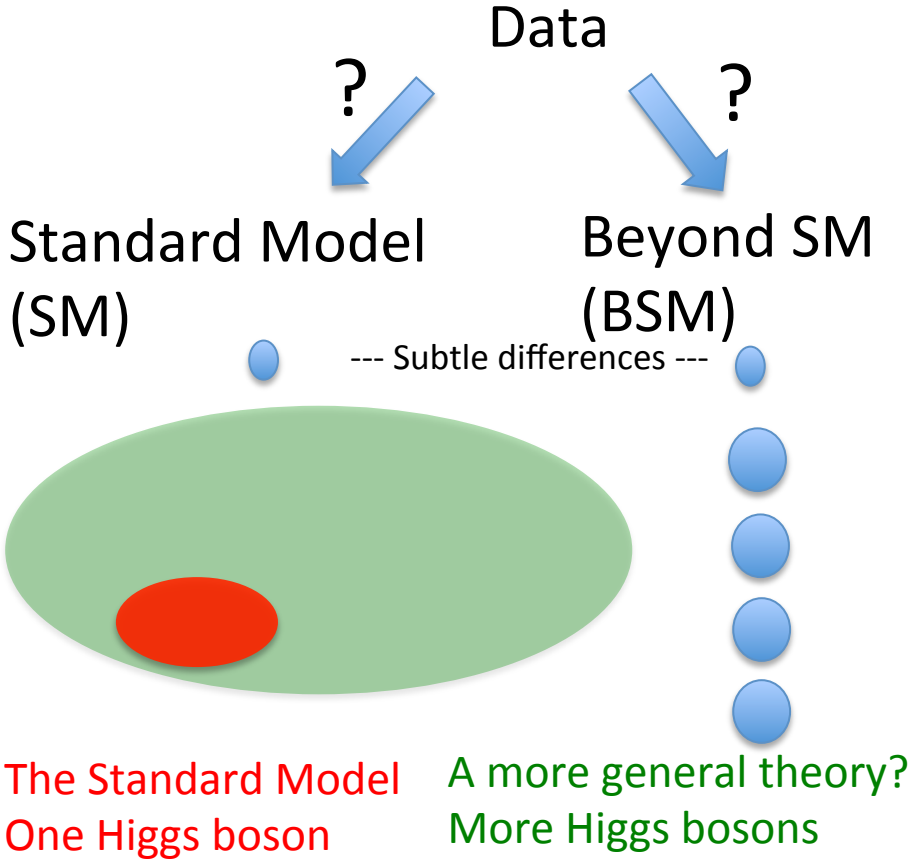

We need to study the Higgs couplings to all particles.

A straight line (SM) or not (BSM)?

The Higgs boson (SM) or **a** Higgs boson (BSM)?

ggF cross-section is ~13x that of VBF, which in turn is ~2x that of WH and ~4x that of ZH.

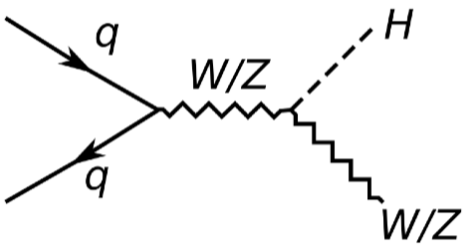

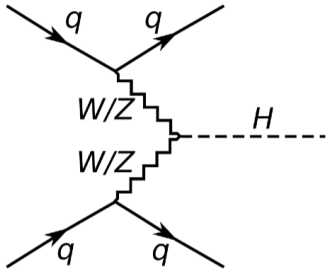

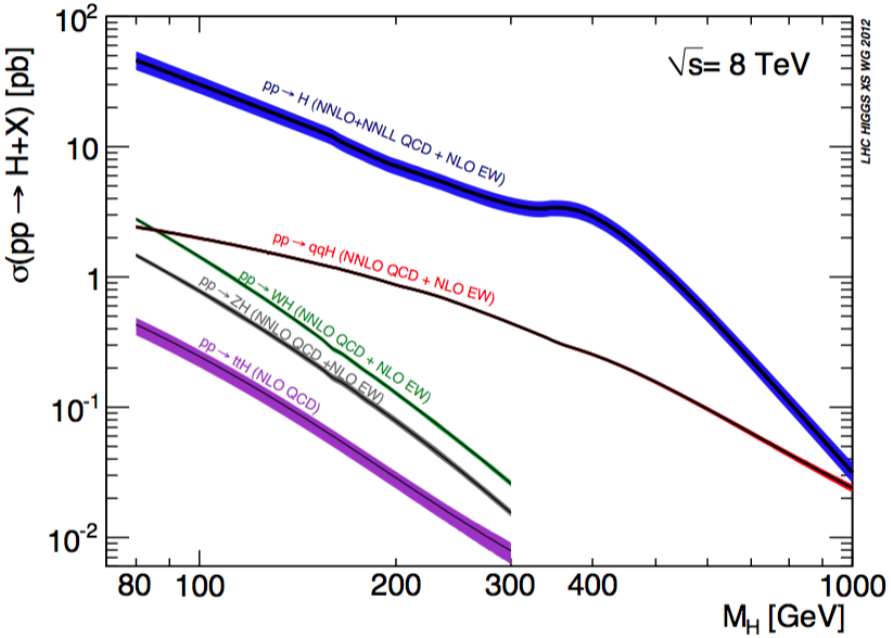

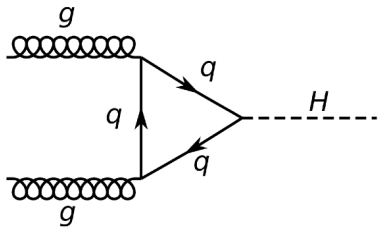

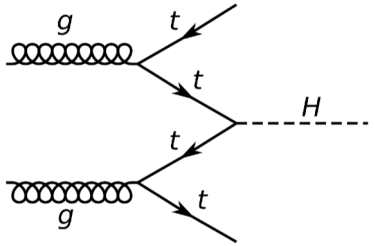

	σ at 7 TeV	σ at 8 TeV	σ at 13 TeV	σ at 14 TeV
ggF	15.3 pb ± 8 %	19.4 pb ± 8 %	44.1 pb ± 8 %	49.6 pb ± 8 %
VBF	1.24 pb ± 2 %	1.60 pb ± 2 %	3.78 pb ± 2 %	4.28 pb ± 2 %
WH	0.58 pb ± 3 %	0.70 pb ± 3 %	1.38 pb ± 3 %	1.51 pb ± 3 %
ZH	0.34 pb ± 4 %	0.42 pb ± 4 %	0.88 pb ± 5 %	0.99 pb ± 5 %
ttH	0.09 pb +8% -13%	0.13 pb 8% -13%	0.51 pb 10% -13%	0.61 pb 9% -13%

Higgs bosons at m_H=125 GeV decay in many ways.

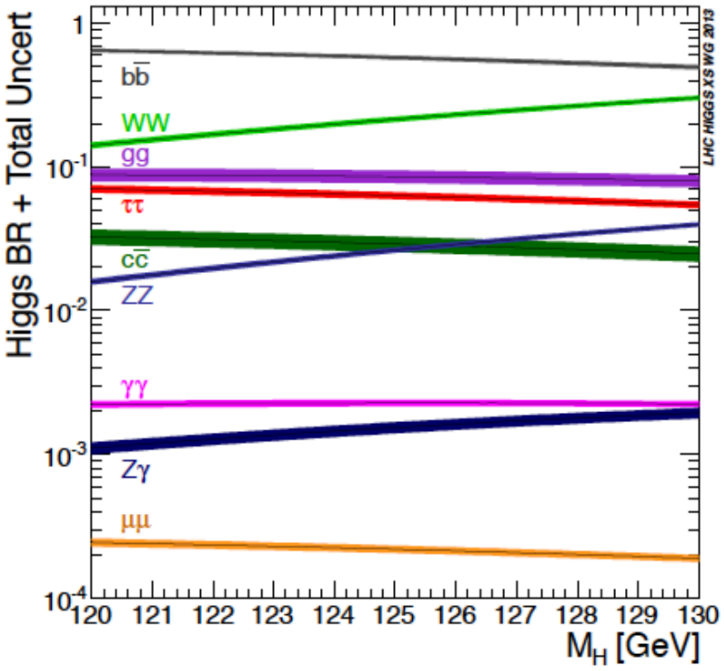

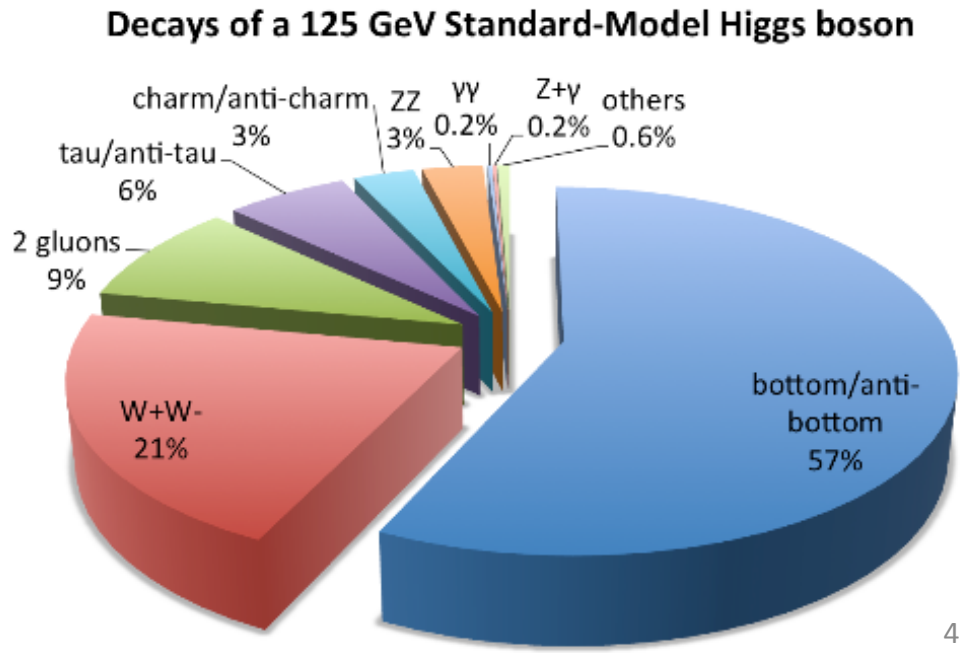

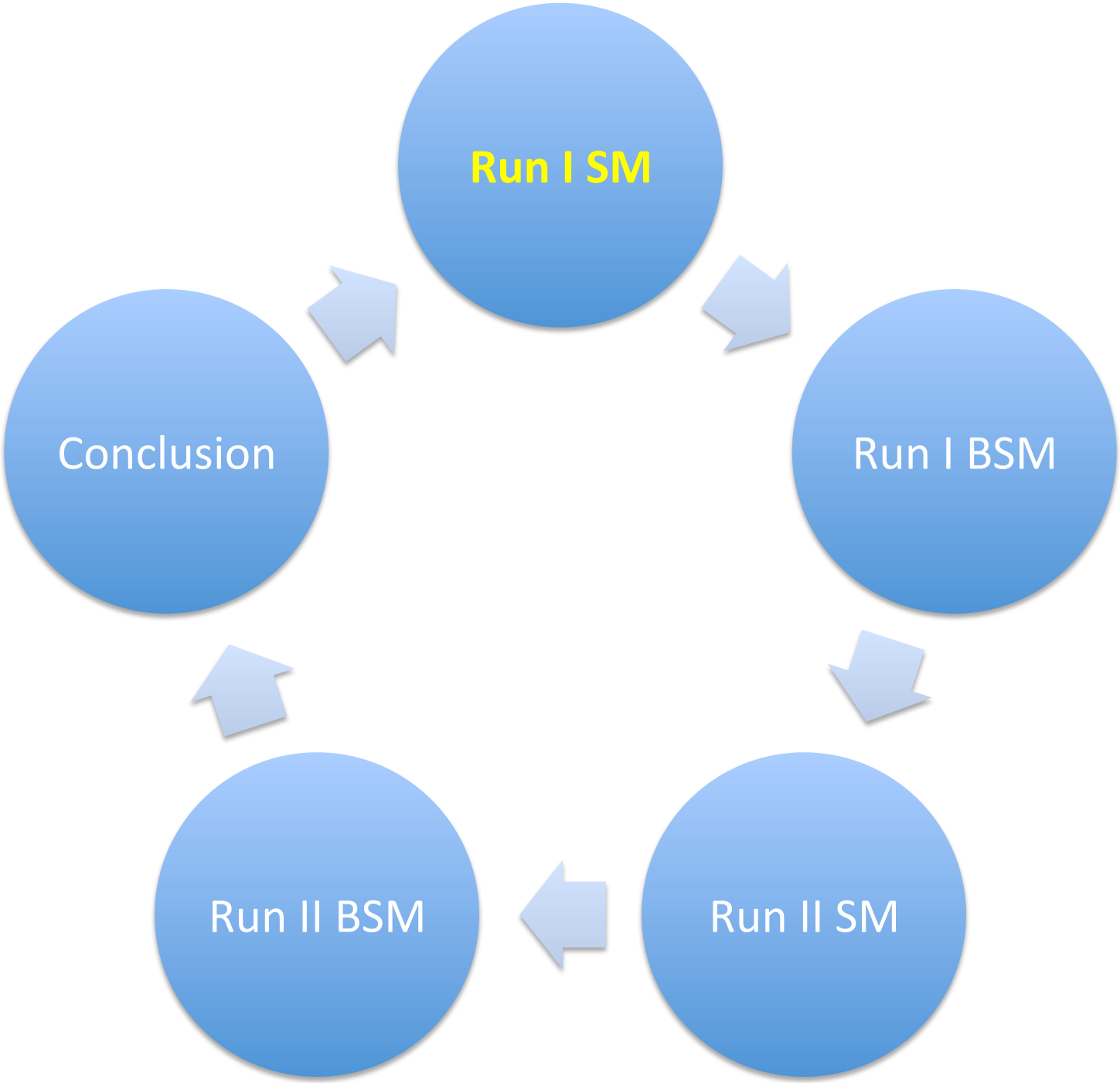
Run I SM
Run I BSM
Run II SM
Run II BSM
Conclusion

Run I VBF, H->bb.

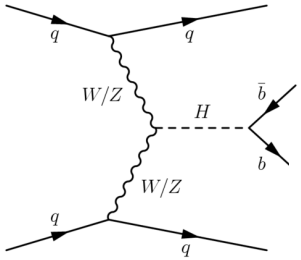

VH, H->bb, 7 TeV, published in PLB (2012).
VH, H->bb, 8 TeV, published in JHEP (2015).

mbb the key S/B discriminant.

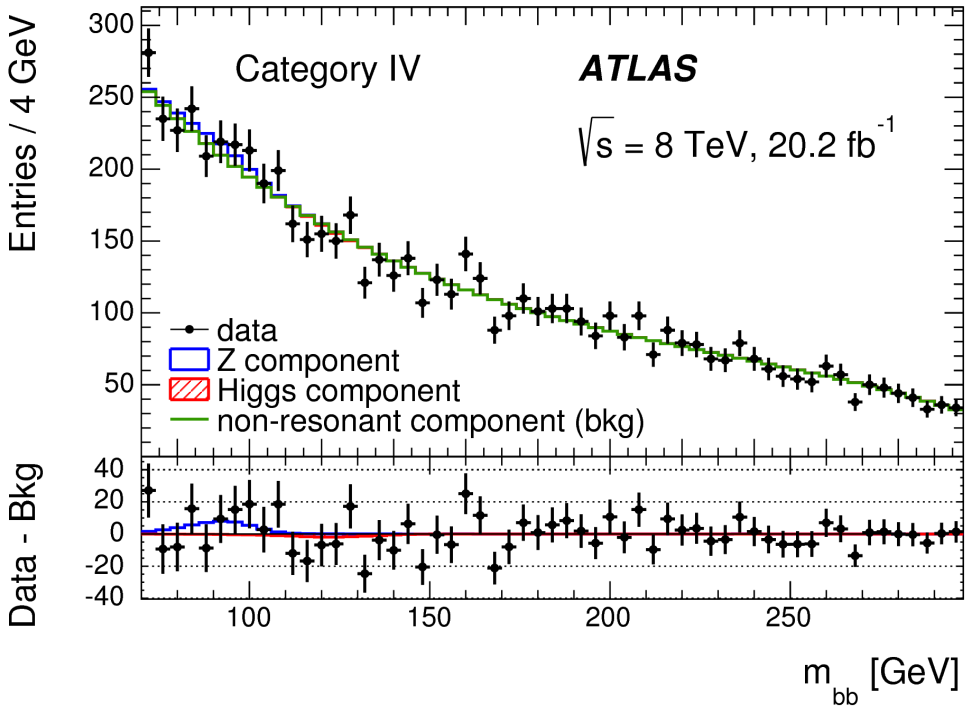

Submitted to JHEP
arXiv:1606.02181

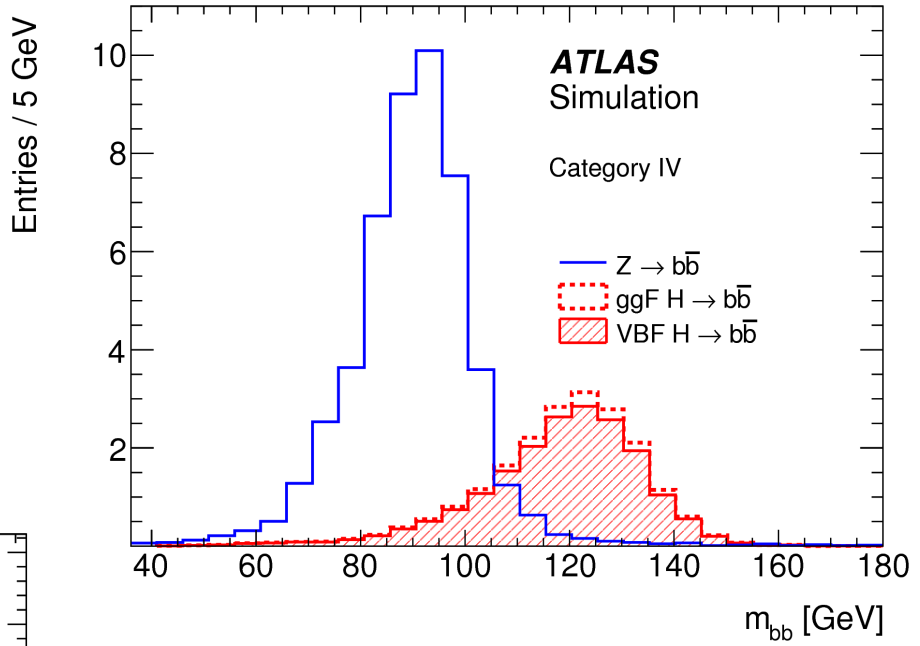

Signal yield μ = -0.8 ± 2.3
Observed: σ*BR < 4.4 x SM
Expected: σ*BR < 5.4 x SM

Run I ttH all hadronic, H->bb.

[Published in JHEP](#)
[arXiv:1604.03812](#)

Analysis is split in many categories based on the number of jets and b-tags.
S/B increases with nr jets and b-tags.
Dominant background is multijet. For best category, it is tt+bb.

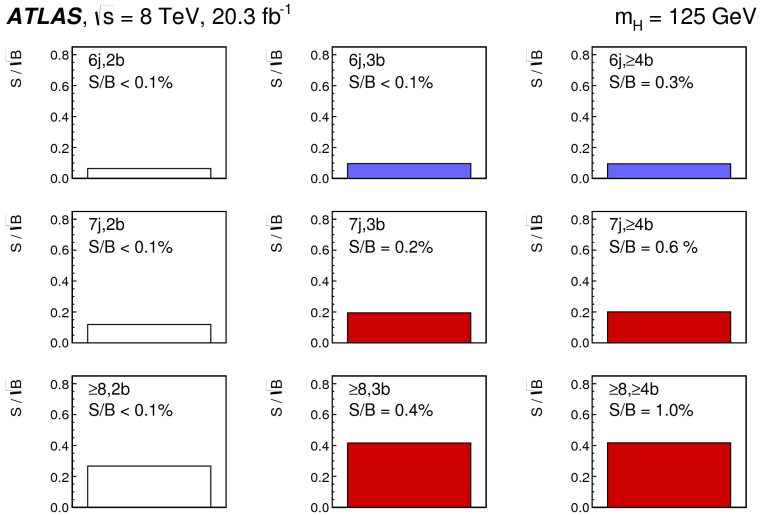

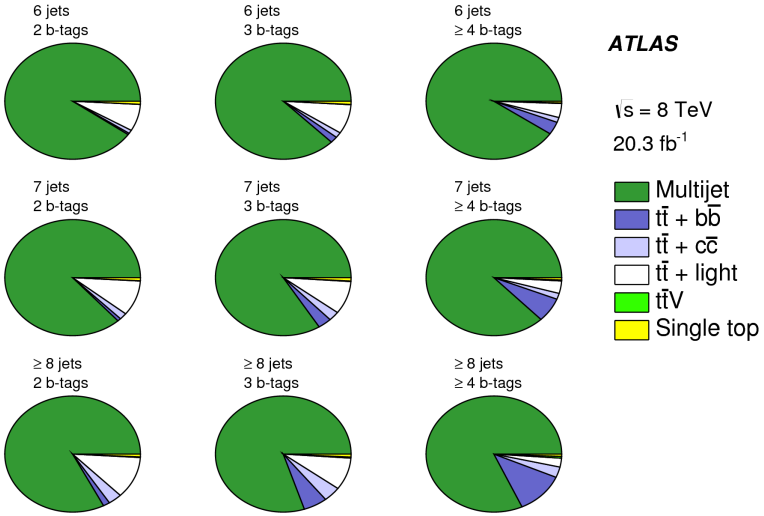

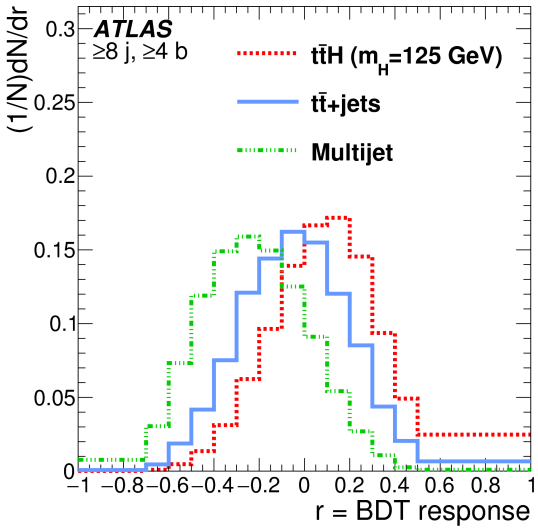

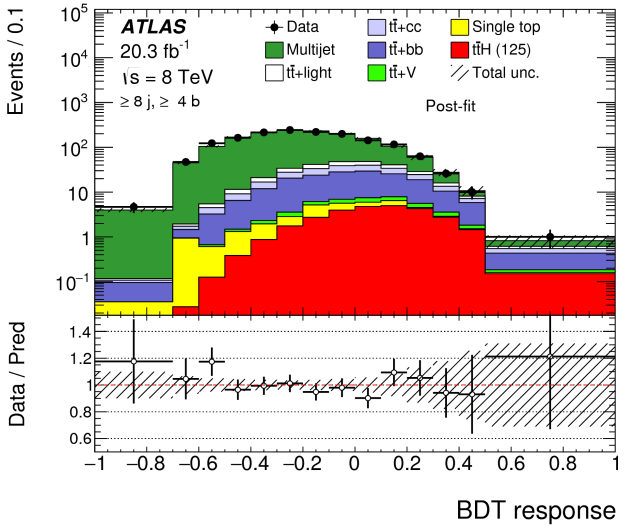

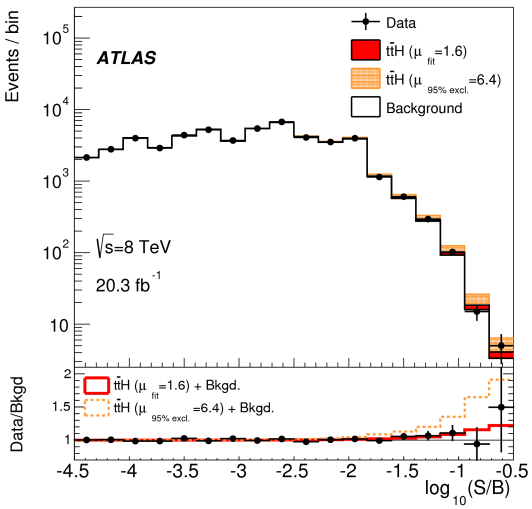

ttH hadronic H->bb sensitivity σ = 5.4xSM.
Combining all 8 TeV, ttH, H->bb, σ = 3.0xSM.

Published in JHEP
arXiv:1604.03812

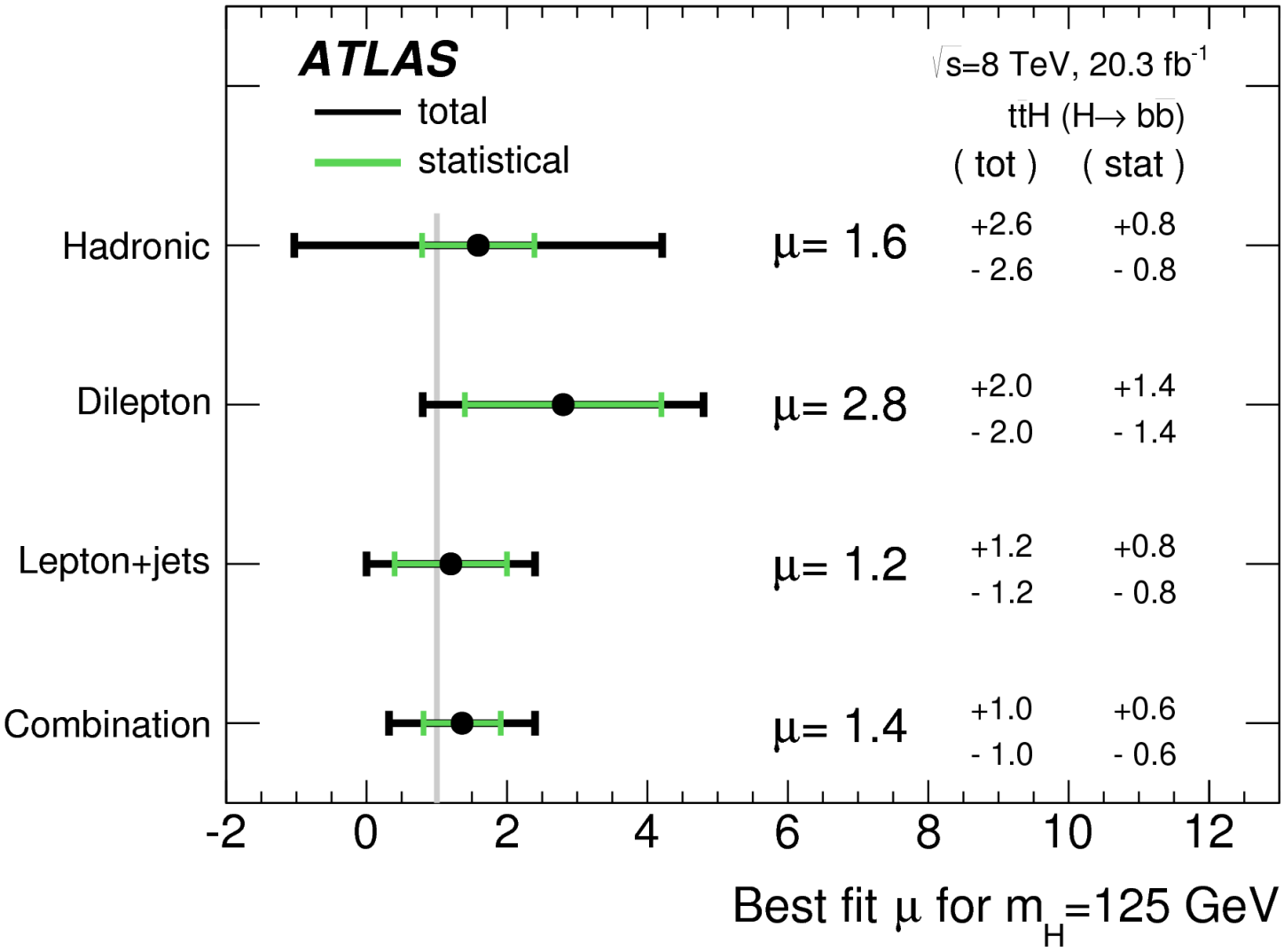

Run I combining all ttH channels, sensitivity is improved from 3.0xSM to σ = 2.0xSM.

Published in JHEP
arXiv:1604.03812

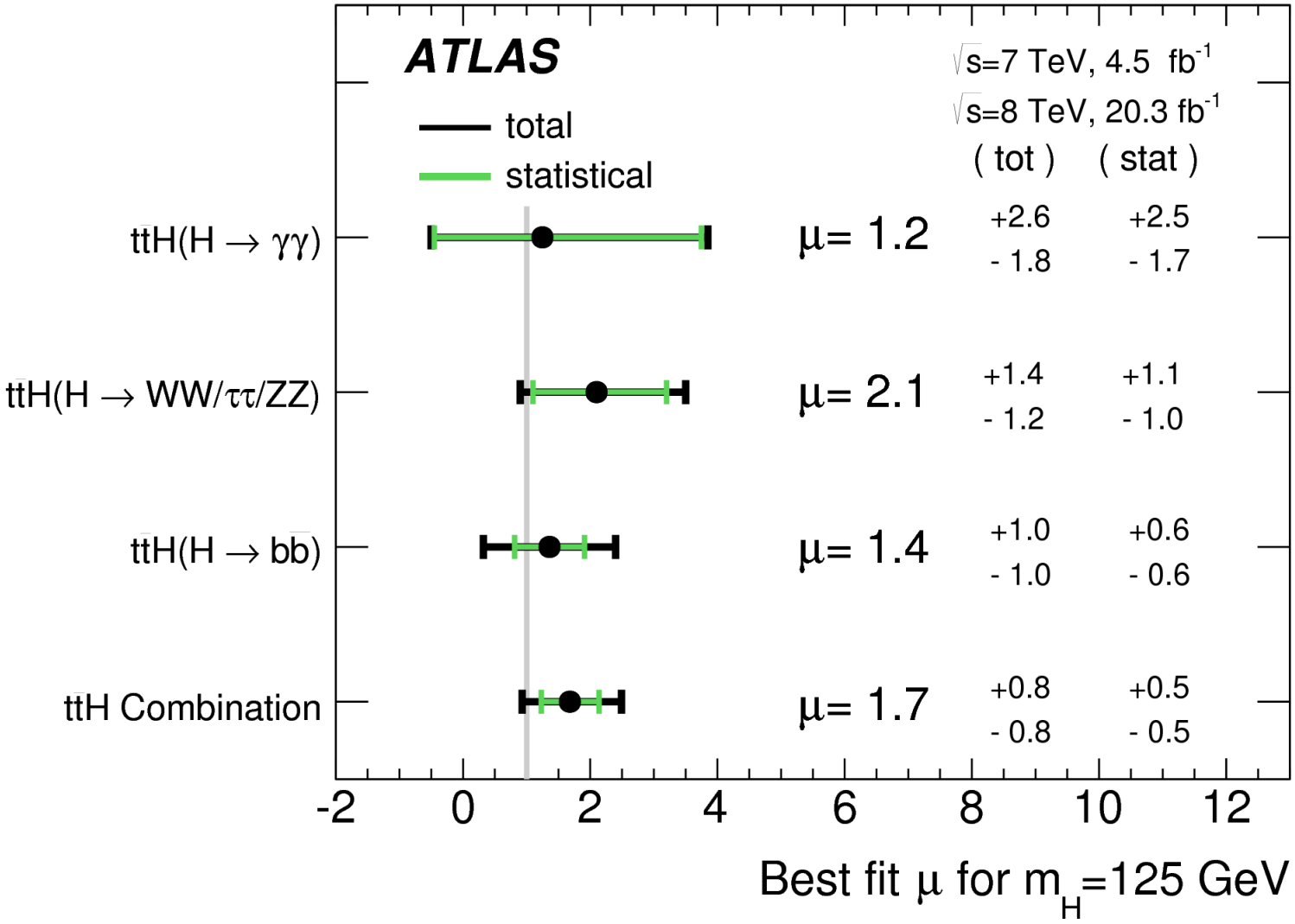

H->WW->evμv differential σ at 8 TeV. Consistent with the SM prediction.

[Submitted to JHEP arXiv:1604.02997]

In categories of number of additional jets.
As a function of number of jets, pT of Higgs, dilepton rapidity, pT of leading jet.

Measured: $\sigma^{\text{fid}}_{\text{ggF}} = 36.0 \pm 7.2(\text{stat}) \pm 6.4(\text{sys}) \pm 1.0(\text{lumi})$ fb

Predicted: $\sigma^{\text{fid}}_{\text{ggF}} = 25.1 \pm 2.6$ fb.

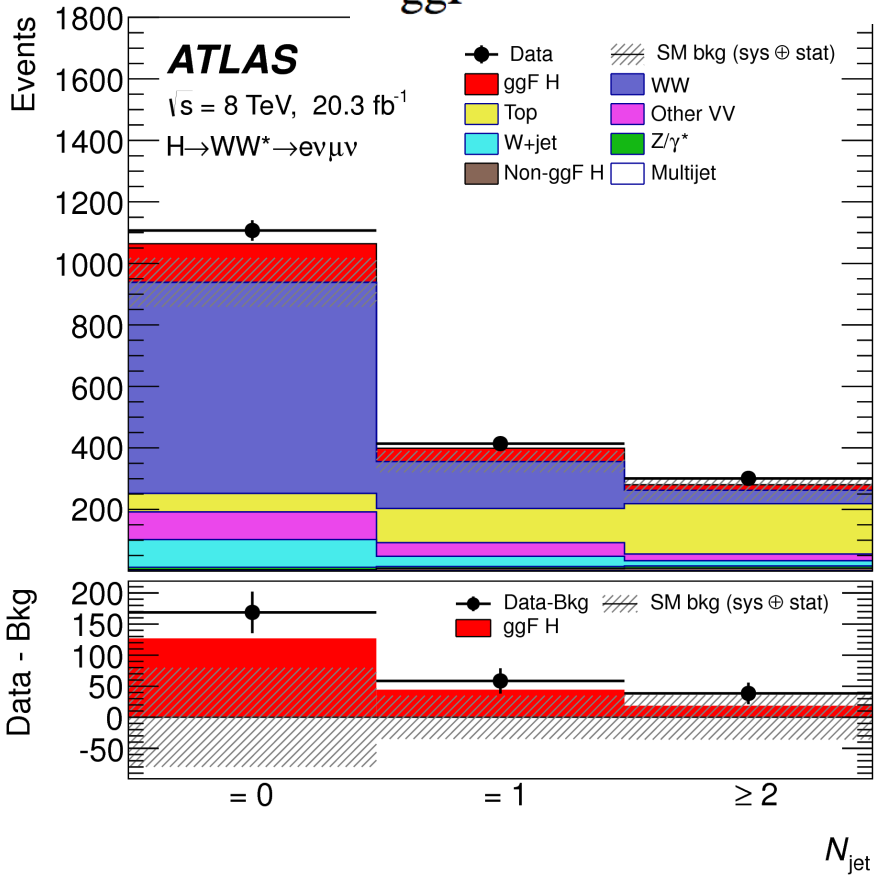

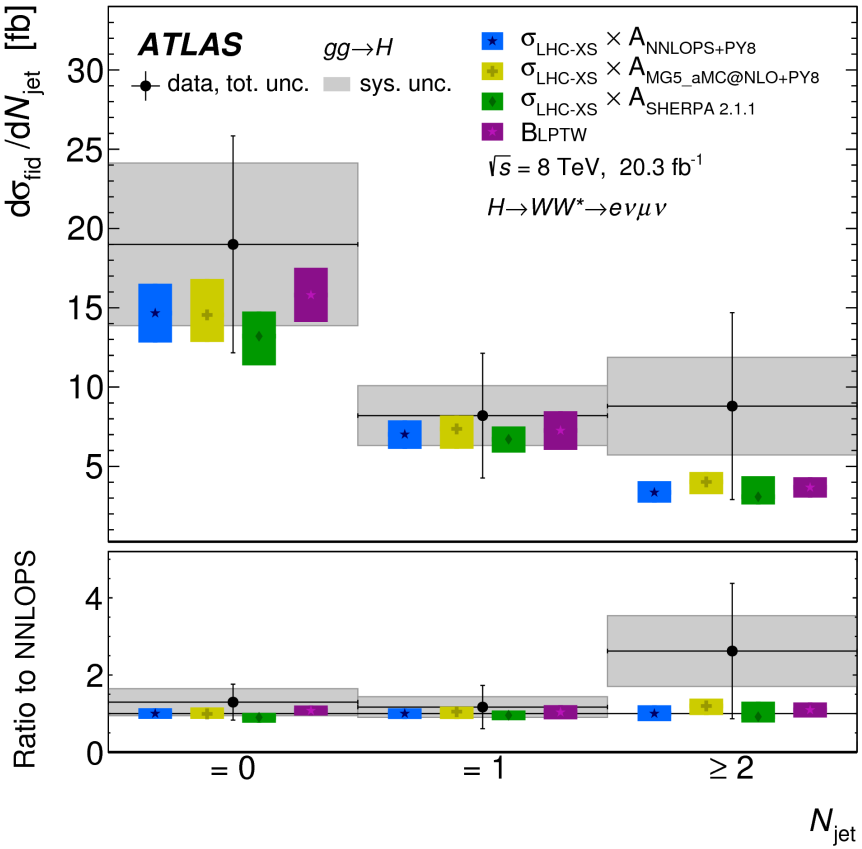

ATLAS+CMS Run I 7+8 TeV combination.

[Submitted to JHEP arXiv:1606.02266]

Data consistent with SM. Total μ = 1.09 ± 0.11.

	Best fit μ	Uncertainty				
		Total	Stat	Expt	Thbgd	Thsig
ATLAS + CMS (measured)	1.09	$^{+0.11}_{-0.10}$	$^{+0.07}_{-0.07}$	$^{+0.04}_{-0.04}$	$^{+0.03}_{-0.03}$	$^{+0.07}_{-0.06}$
ATLAS + CMS (expected)		$^{+0.11}_{-0.10}$	$^{+0.07}_{-0.07}$	$^{+0.04}_{-0.04}$	$^{+0.03}_{-0.03}$	$^{+0.07}_{-0.06}$
ATLAS (measured)	1.20	$^{+0.15}_{-0.14}$	$^{+0.10}_{-0.10}$	$^{+0.06}_{-0.06}$	$^{+0.04}_{-0.04}$	$^{+0.08}_{-0.07}$
ATLAS (expected)		$^{+0.14}_{-0.13}$	$^{+0.10}_{-0.10}$	$^{+0.06}_{-0.05}$	$^{+0.04}_{-0.04}$	$^{+0.07}_{-0.06}$
CMS (measured)	0.97	$^{+0.14}_{-0.13}$	$^{+0.09}_{-0.09}$	$^{+0.05}_{-0.05}$	$^{+0.04}_{-0.03}$	$^{+0.07}_{-0.06}$
CMS (expected)		$^{+0.14}_{-0.13}$	$^{+0.09}_{-0.09}$	$^{+0.05}_{-0.05}$	$^{+0.04}_{-0.03}$	$^{+0.08}_{-0.06}$

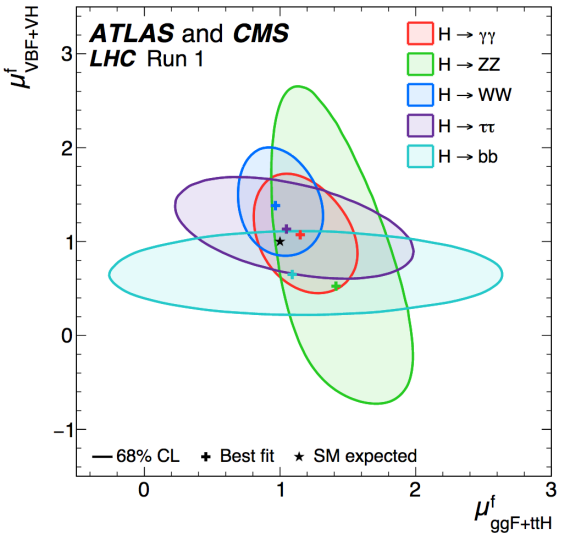

Production process	Measured significance (σ)	Expected significance (σ)
VBF	5.4	4.6
WH	2.4	2.7
ZH	2.3	2.9
VH	3.5	4.2
ttH	4.4	2.0
Decay channel		
$H \to \tau\tau$	5.5	5.0
$H \to bb$	2.6	3.7

ATLAS+CMS Run I 7+8 TeV combination.

[Submitted to JHEP arXiv:1606.02266]

Data consistent with SM. Total μ = 1.09 ± 0.11.

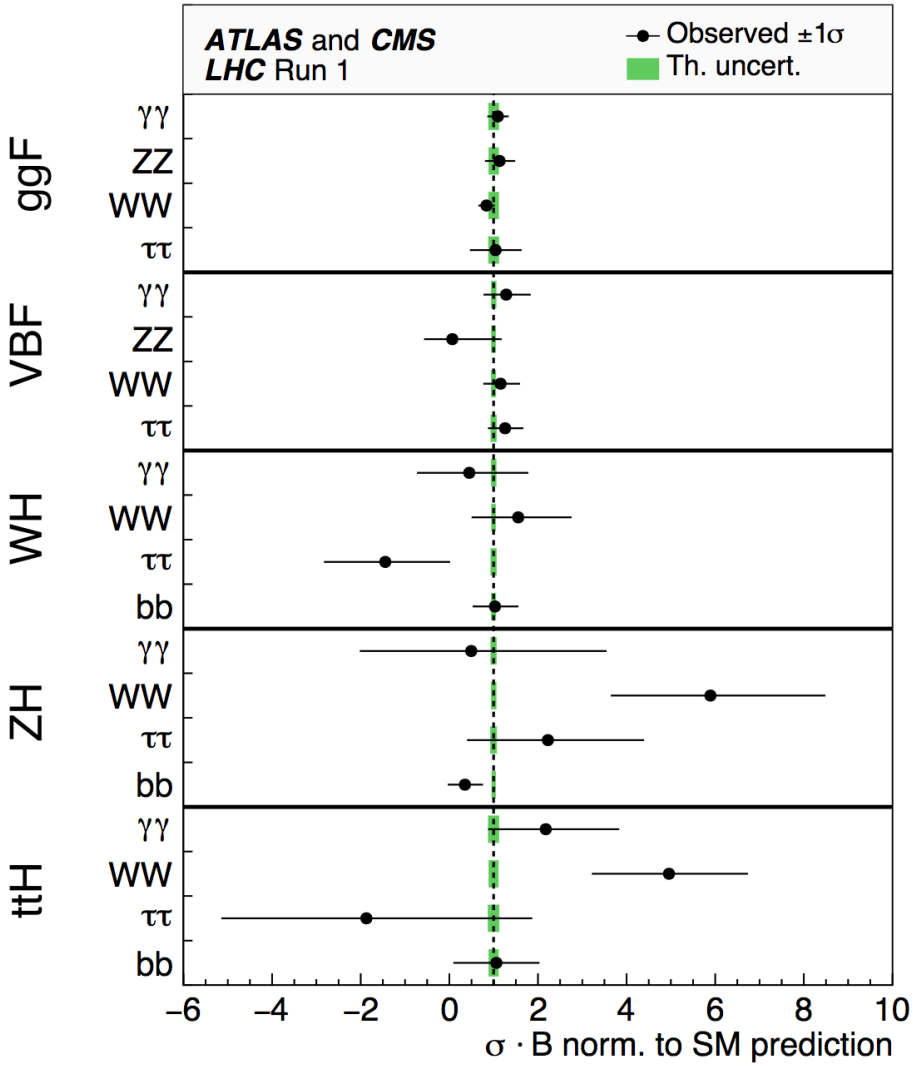

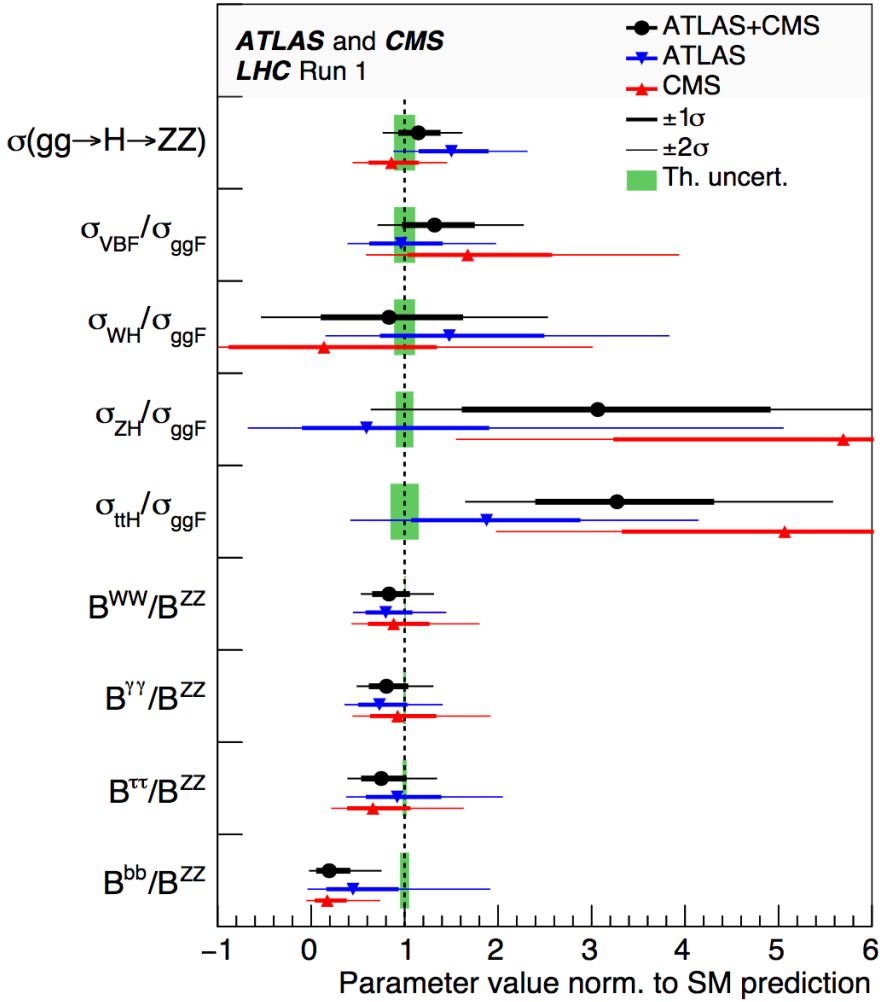

ATLAS+CMS Run I 7+8 TeV combination.

Submitted to JHEP
arXiv:1606.02266

Data consistent with SM. Total μ = 1.09 ± 0.11.

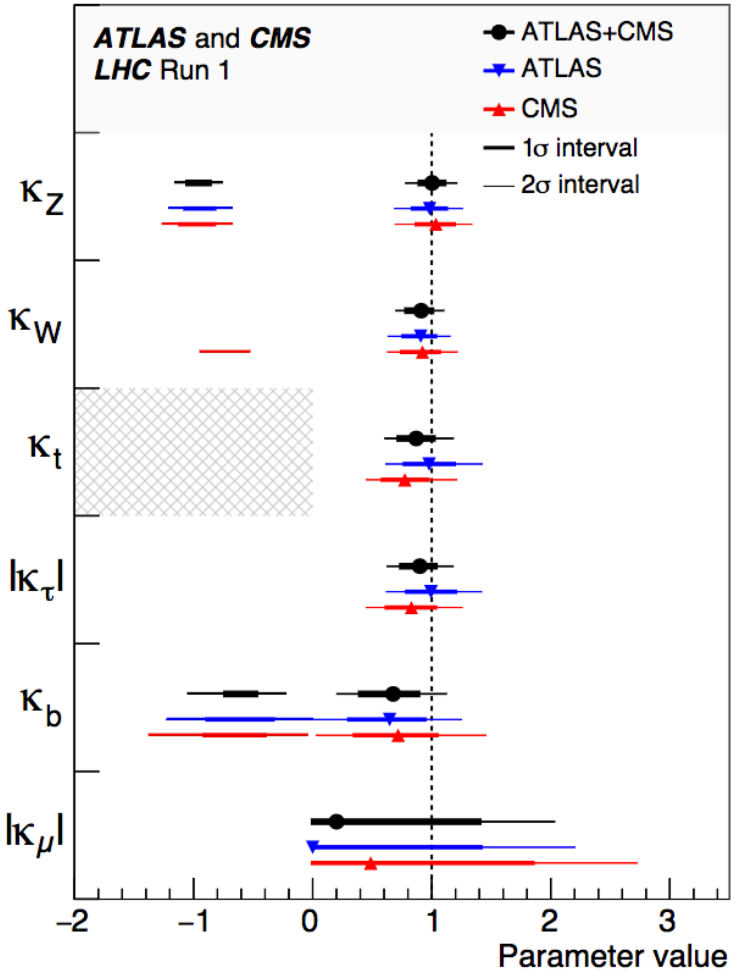

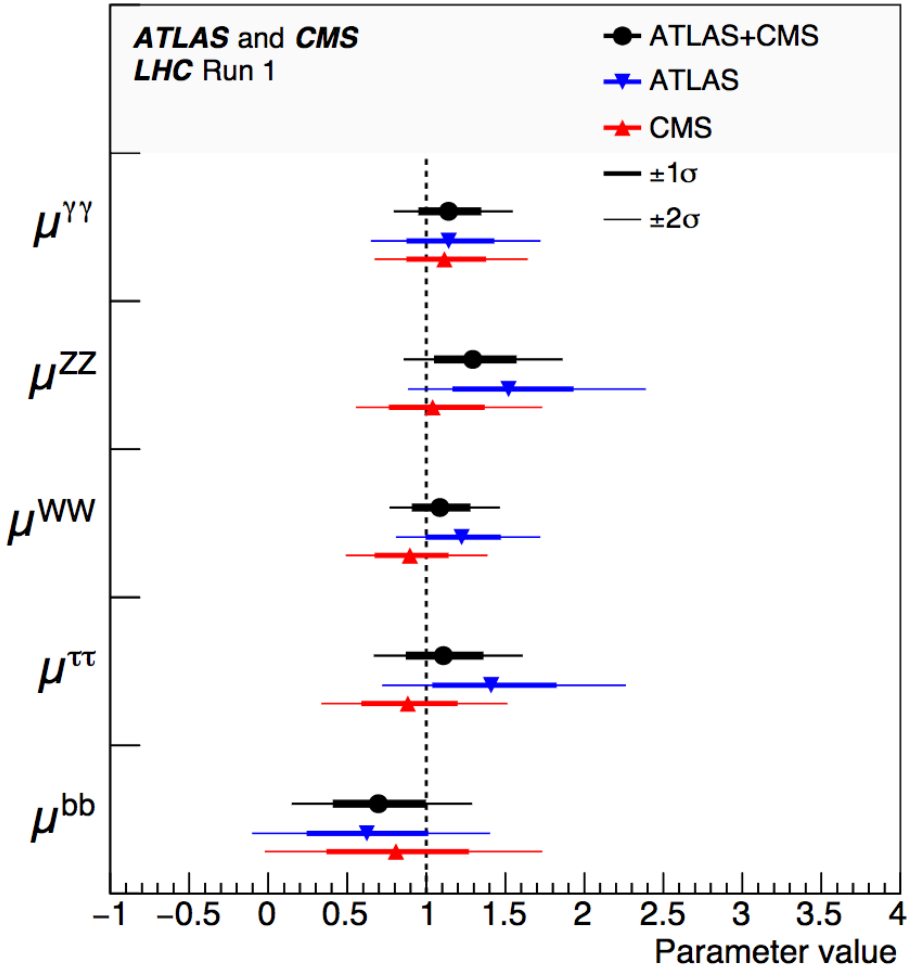

ATLAS+CMS Run I 7+8 TeV combination.

Submitted to JHEP
arXiv:1606.02266

Data consistent with SM. Total μ = 1.09 ± 0.11.

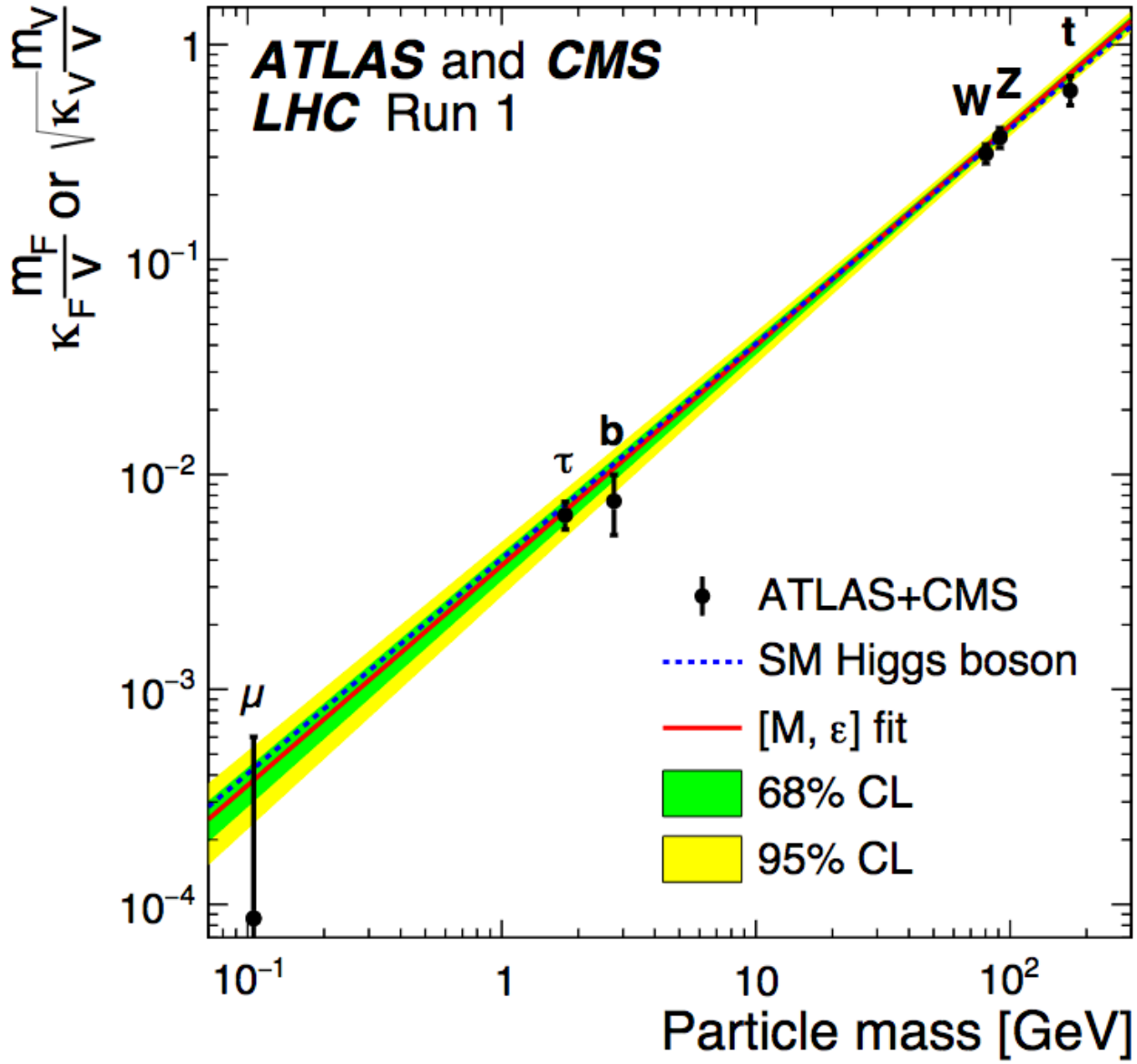

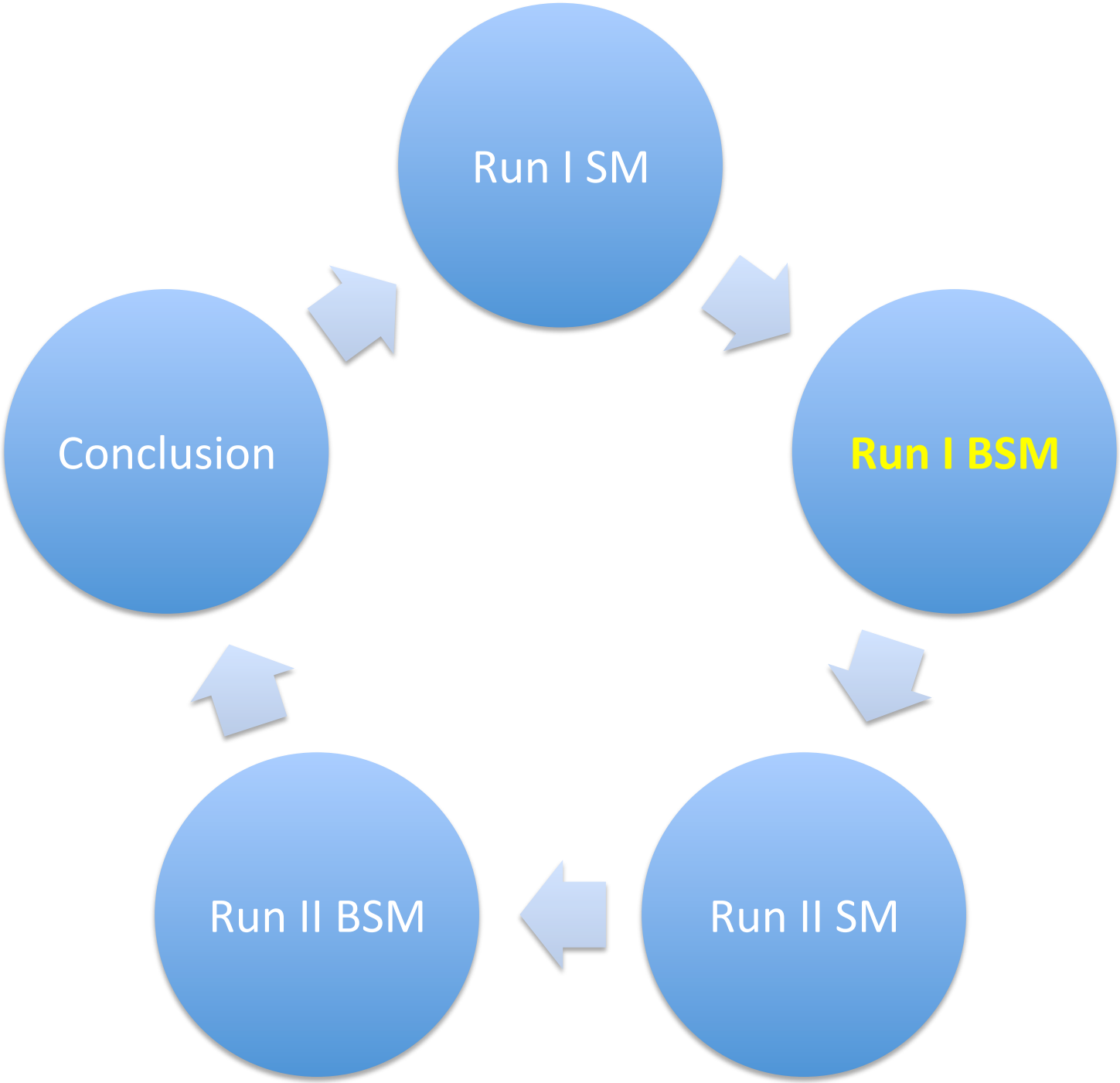
Run I SM
Run I BSM
Run II SM
Run II BSM
Conclusion

First direct CP violation test in Higgs 8 TeV. No sensitive, need more statistics.

[Submitted to EPJC arXiv:1602.04516]

In SM no CP violation involving Higgs.
If observed, it means physics BSM.
EFT framework
Optimum Variable d sensitive
to interference of SM and CP-odd couplings
d=0 (SM), d!=0 (BSM).
H -> $\tau_{lep}\tau_{lep}$, H->$\tau_{lep}\tau_{had}$
d measured in [-0.11, 0.05] at 68% CL.
x10 better than previous ATLAS H->WW search.

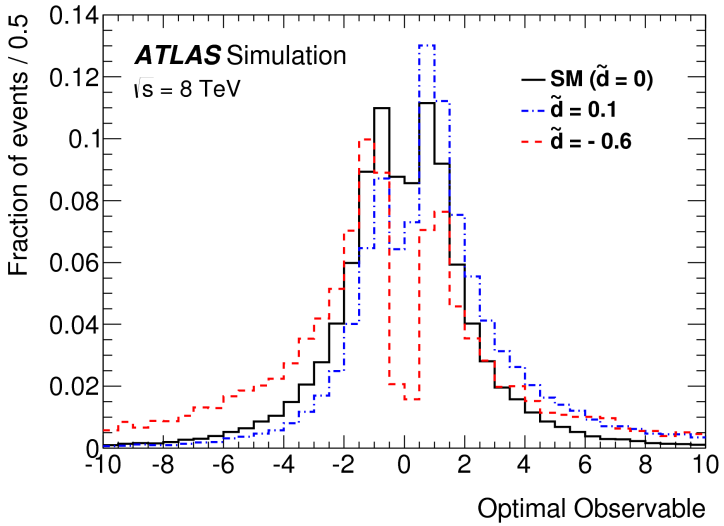

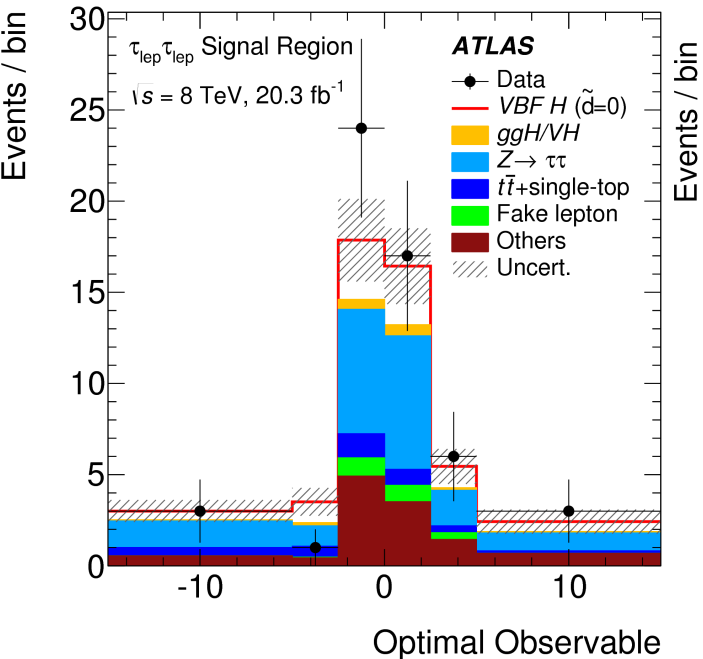

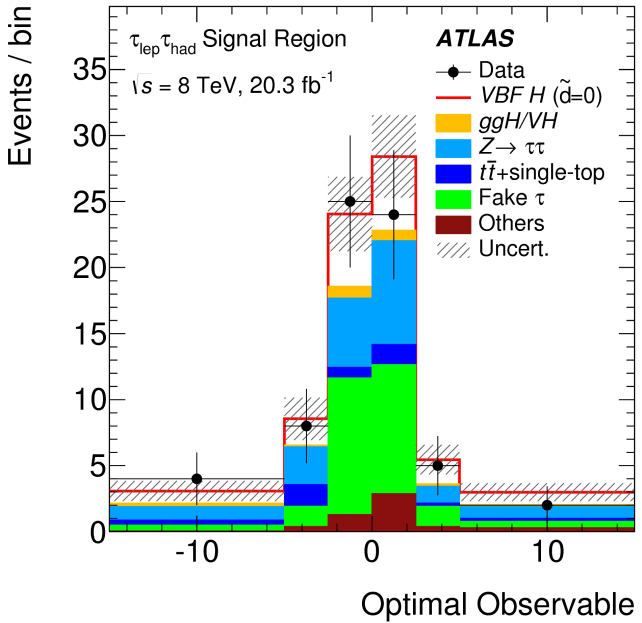

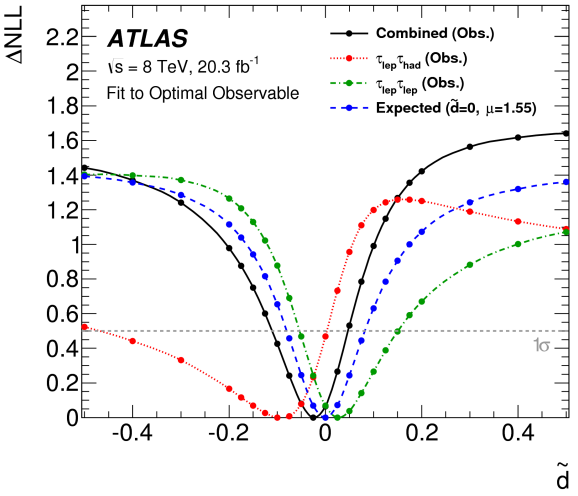

Direct searches for lepton flavor violations.

[Submitted to EPJC arXiv:1604.07730]

No data excess, over bkg limits set σ*BR < 1%.

Run I 8 TeV: H->eτ, H->μτ, Z->μτ.

For H, τ is hadronic or leptonic decay.

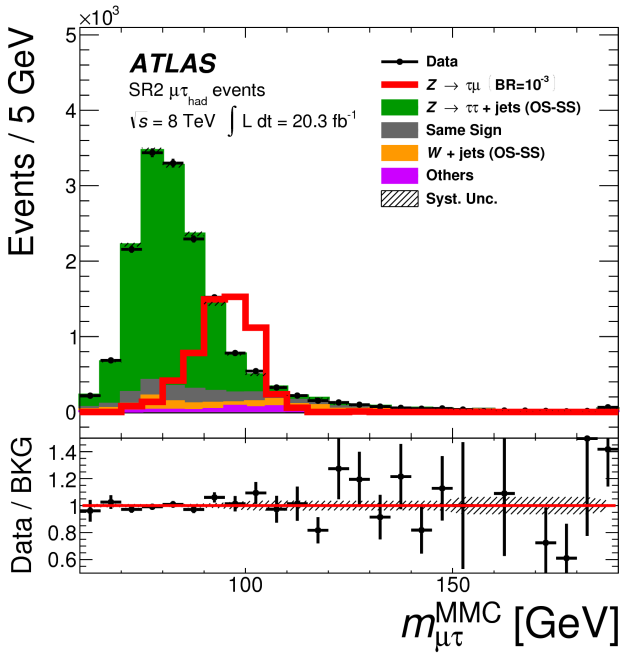

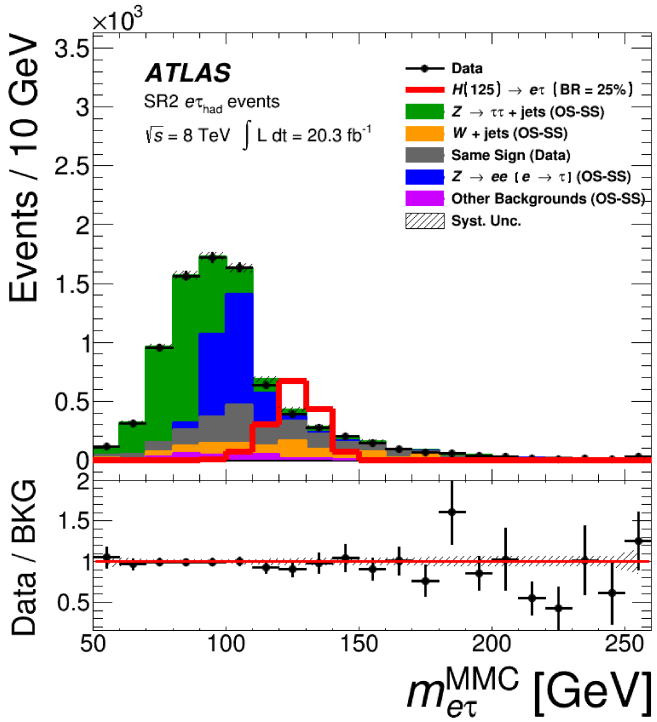

$\mathrm{Br}(Z \to \mu\tau)[10^{-5}]$	SR1	SR2	Combined
Expected limit	$2.6^{+1.1}_{-0.7}$	$6.4^{-1.8}_{+2.8}$	$2.6^{+1.1}_{-0.7}$
Observed limit	1.5	7.9	1.7
Best fit	$-2.1^{+1.2}_{-1.3}$	$2.6^{+2.9}_{-2.6}$	$-1.6^{+1.3}_{-1.4}$

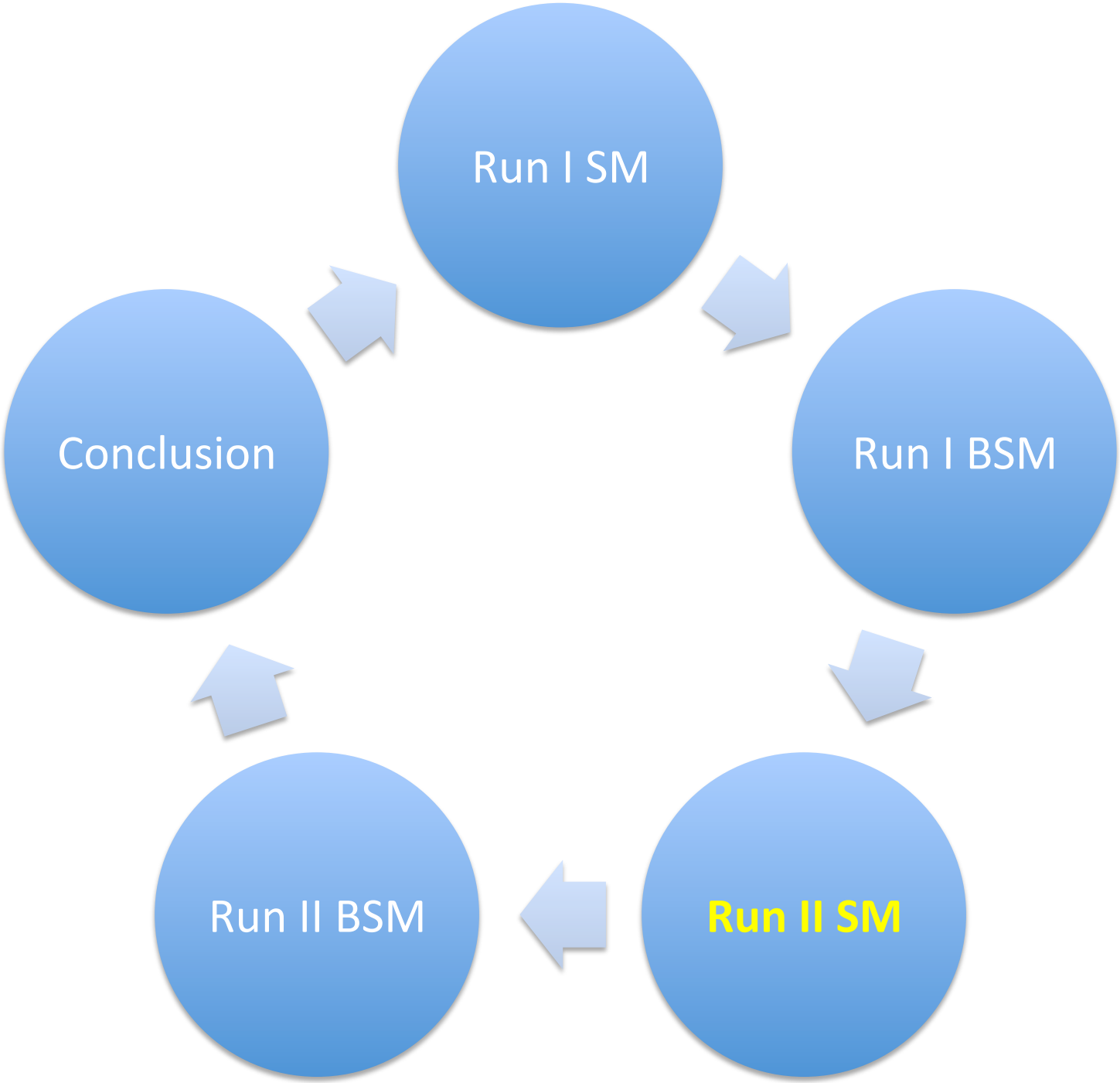
Run I SM
Run I BSM
Run II SM
Run II BSM
Conclusion

Total cross section for H at 7, 8 and 13 TeV.

[Conference note 14 dec ATLAS-CONF-2015-069]

From H->ϒϒ and H->ZZ*->4l

Measurements compatible with the SM

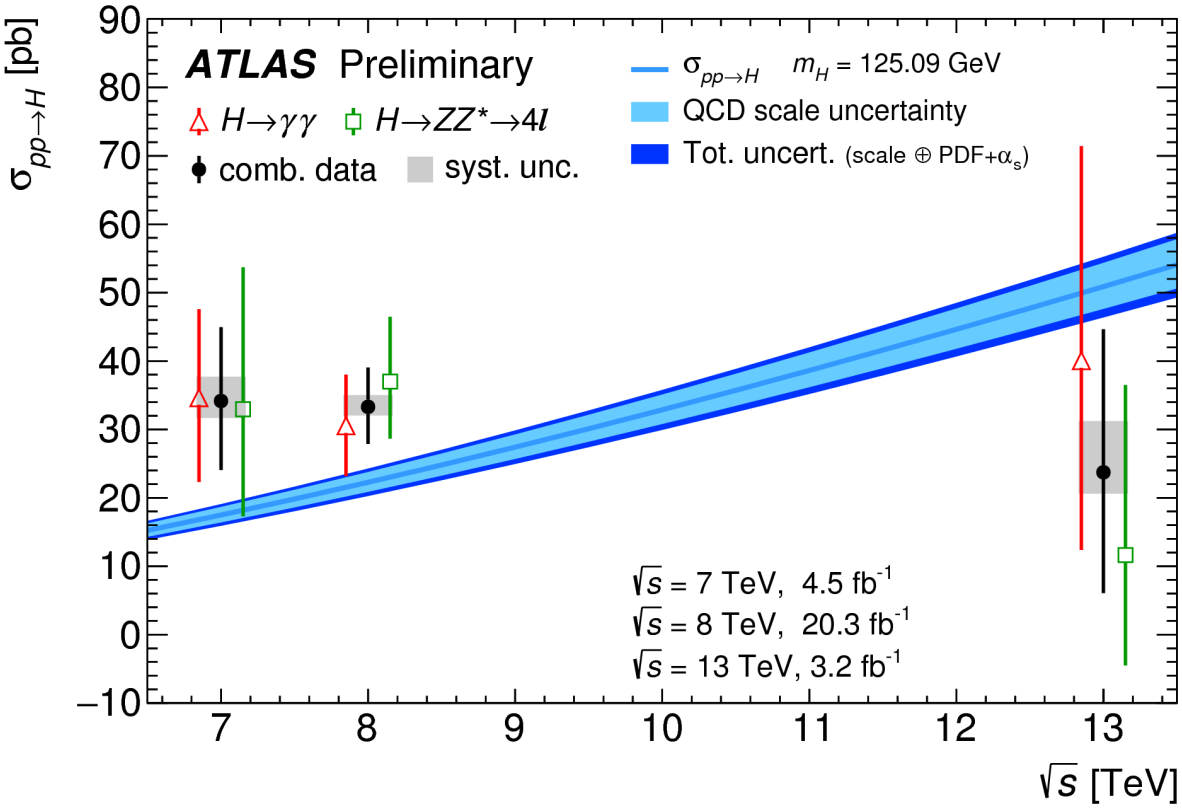

Total cross section [pb]	7 TeV	8 TeV	13 TeV
$H \to \gamma\gamma$	35^{+13}_{-12}	$30.5^{+7.5}_{-7.4}$	40^{+31}_{-28}
$H \to ZZ^* \to 4\ell$	33^{+21}_{-16}	37^{+9}_{-8}	12^{+25}_{-16}
Combination	34 ± 10 (stat.) $^{+4}_{-2}$ (syst.)	$33.3^{+5.5}_{-5.3}$ (stat.) $^{+1.7}_{-1.3}$ (syst.)	24^{+20}_{-17} (stat.) $^{+7}_{-3}$ (syst.)
LHC-XS	17.5 ± 1.6	22.3 ± 2.0	$50.9^{+4.5}_{-4.4}$

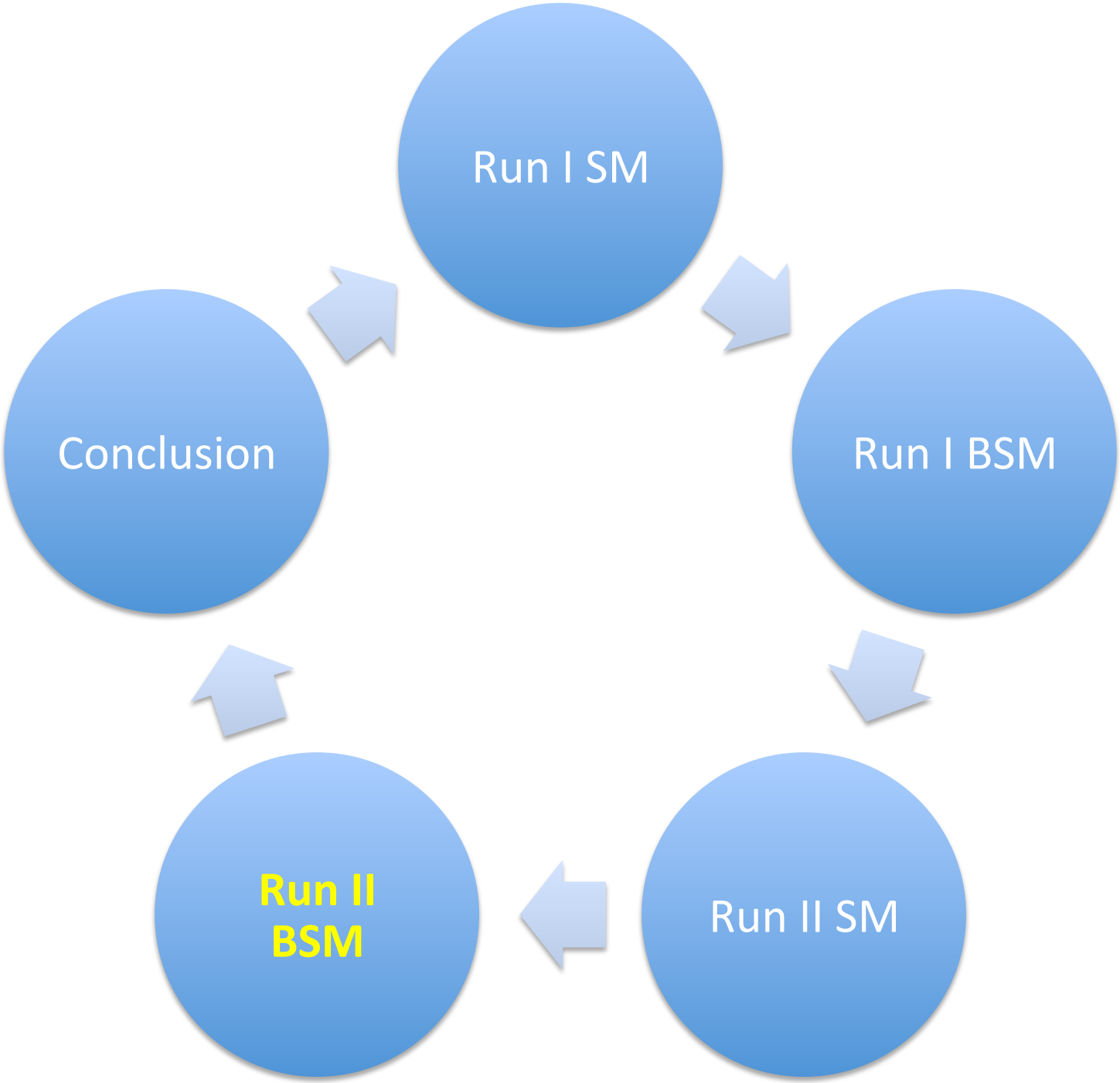
Run I SM
Run I BSM
Run II SM
Run II BSM
Conclusion

X->HH->bb bb.

No excess seen, limits are set.

[Submitted to PRD
arXiv:1606.04782]

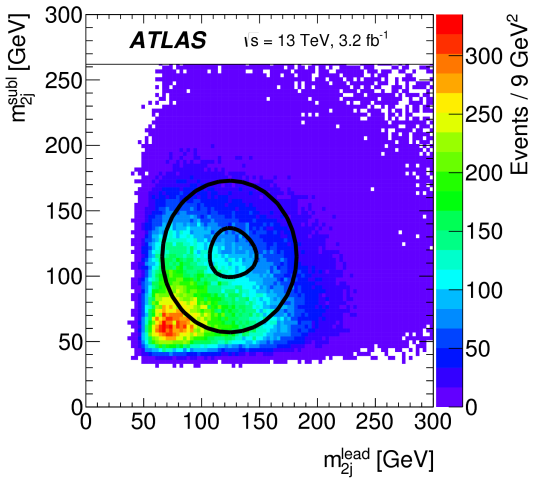

SM non resonant HH->bbbb:

- to small to see now

BSM resonant X ->hh->bbbb:

- RSG*
- 2HDM

Most sensitive for m_X>500 GeV from all HH searches.

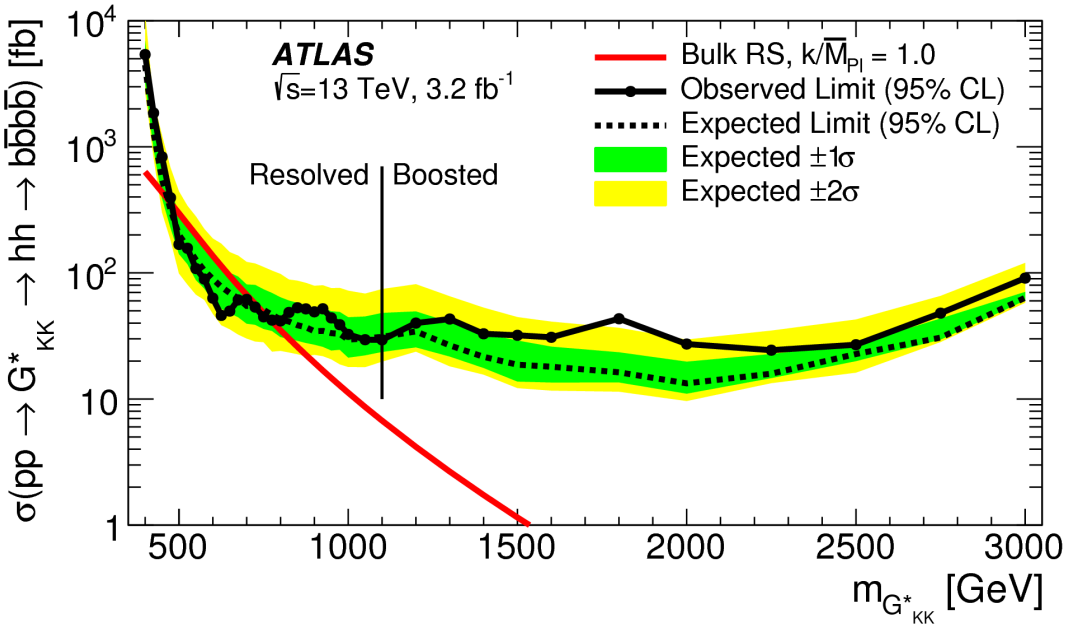

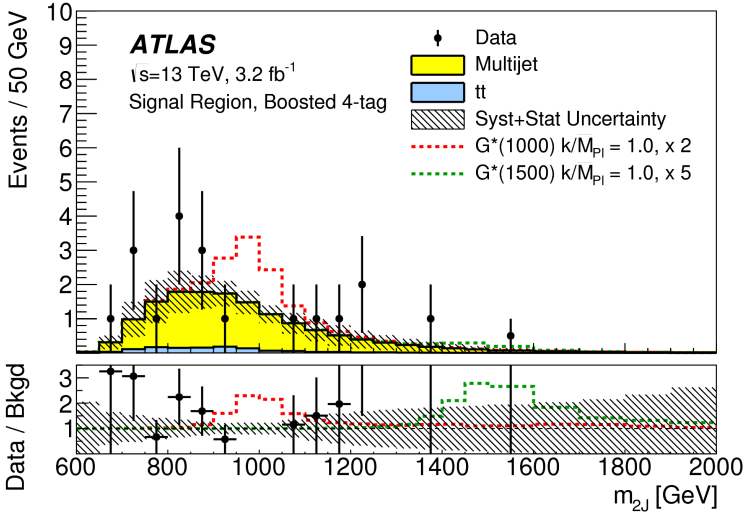

New heavy A->Zh (llbb, vvbb). No excess seen, limits are set.

[Conference note 16 March ATLAS-CONF-2016-015]

CP-odd spin 0 Higgs boson A from 2H2D.
m(Vh) for 2-lep and m_T(Vh) for 0-lep discriminant.
b-jet energy correction key for mbb measurement.

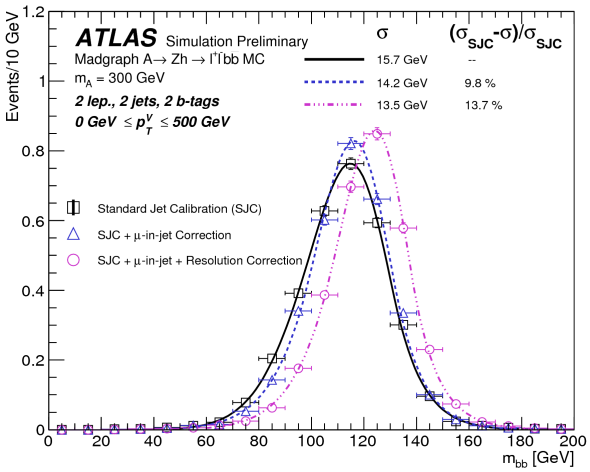

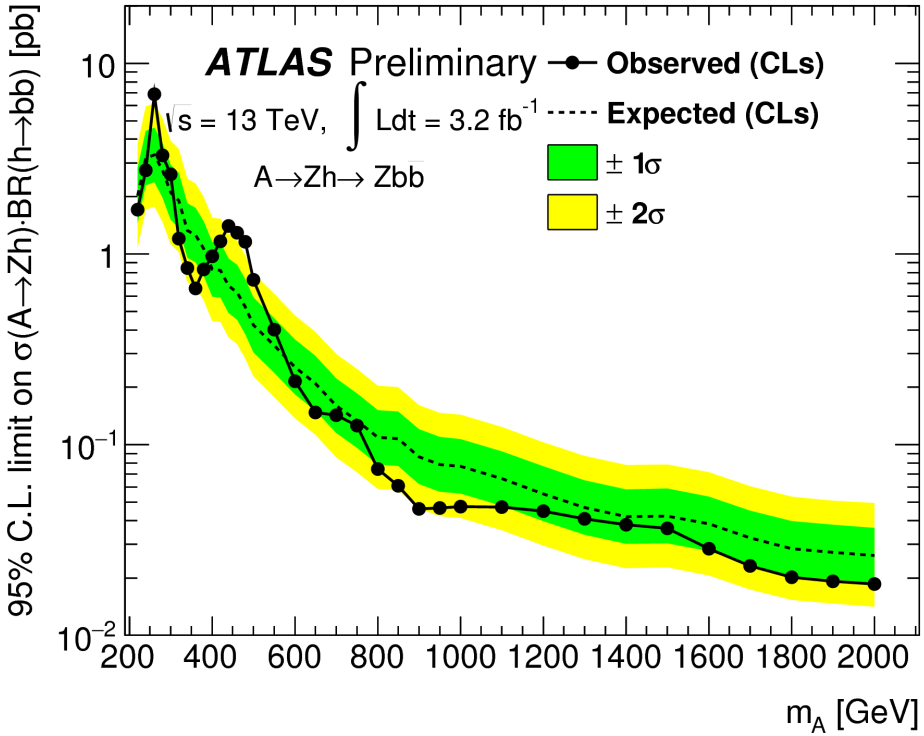

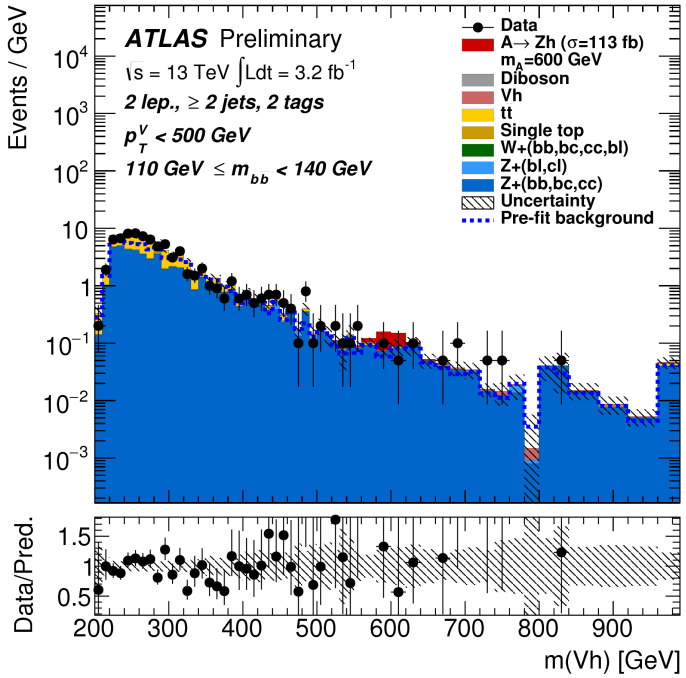

New heavy H->WW (lvlv and lvqq). No excess seen, limits are set.

[Conference note 19 April ATLAS-CONF-2016-021]

+0 +1 jet enhanced in ggF
+2 enhanced in VBF
m_T as discriminator

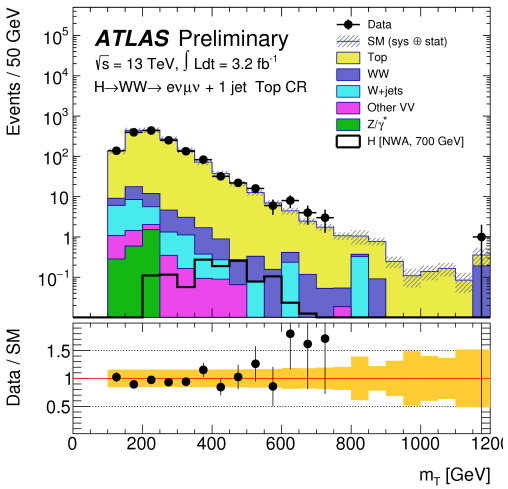

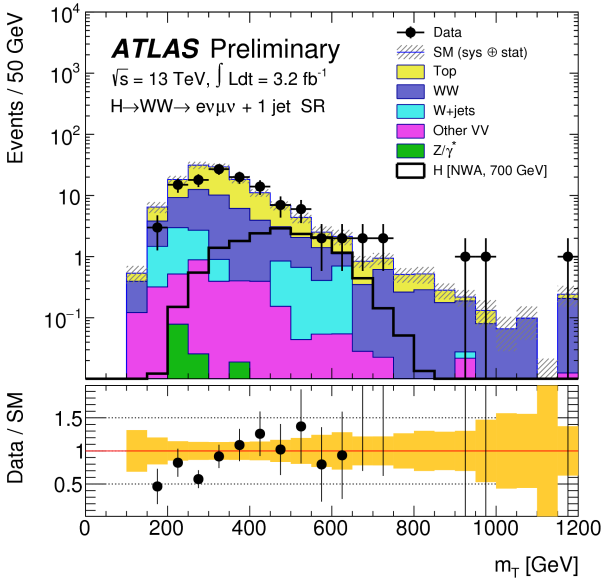

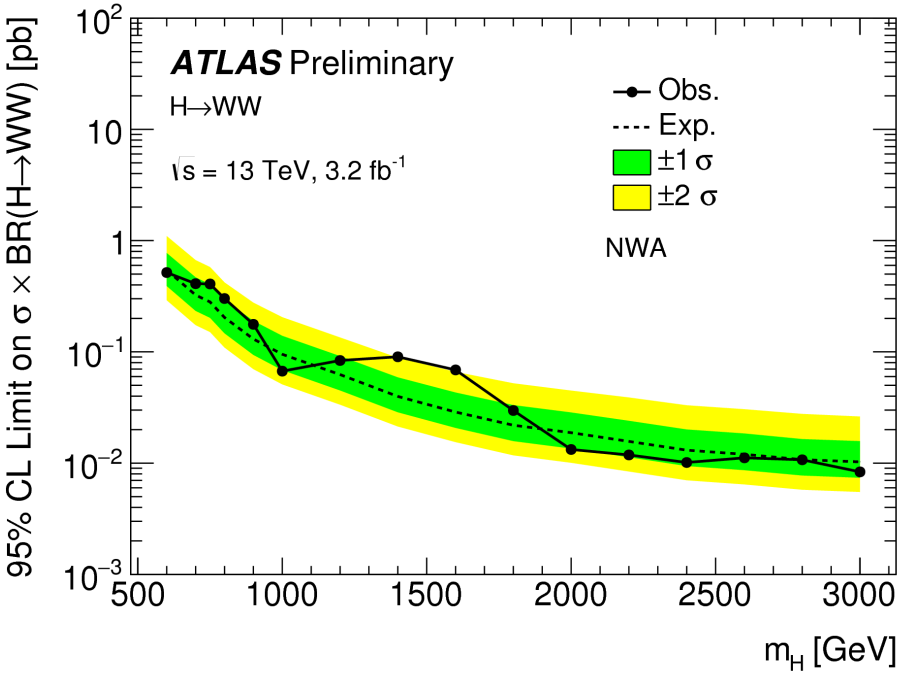

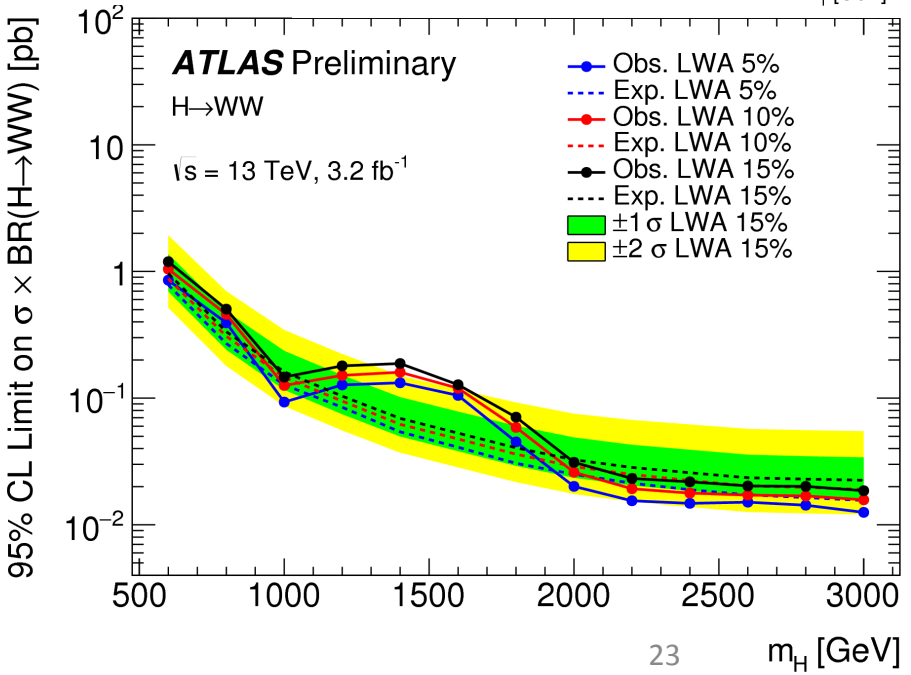

New heavy H->ZZ (llqq).
No excess seen, limits are set.

[Conference note 18 March ATLAS-CONF-2016-016]

Two regular-R jets or one large-R jet.
With or without b-tagging.
Optimised for spin 0 Higgs boson.
Looking also at spin 2 RSG*.

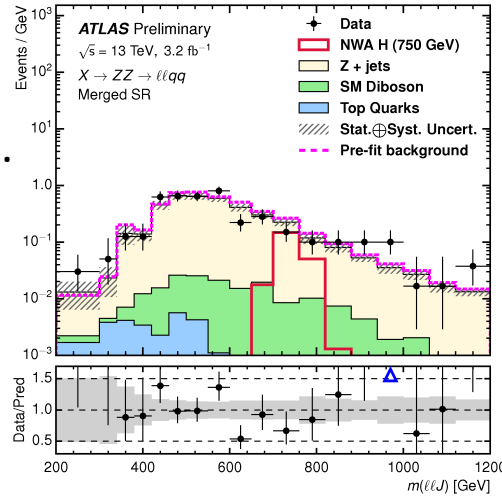

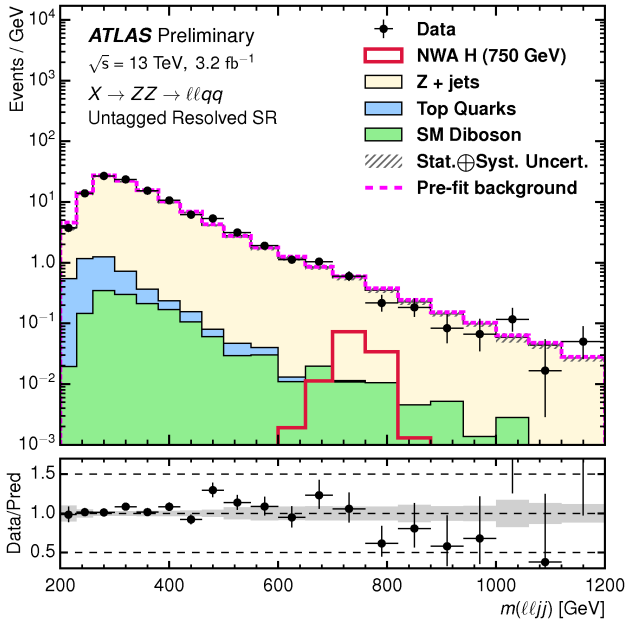

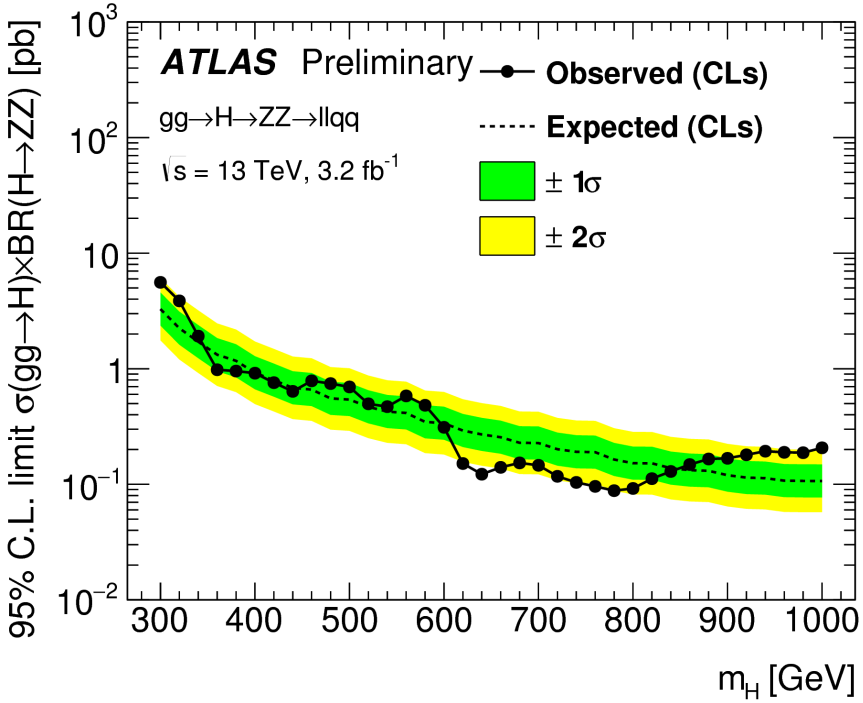

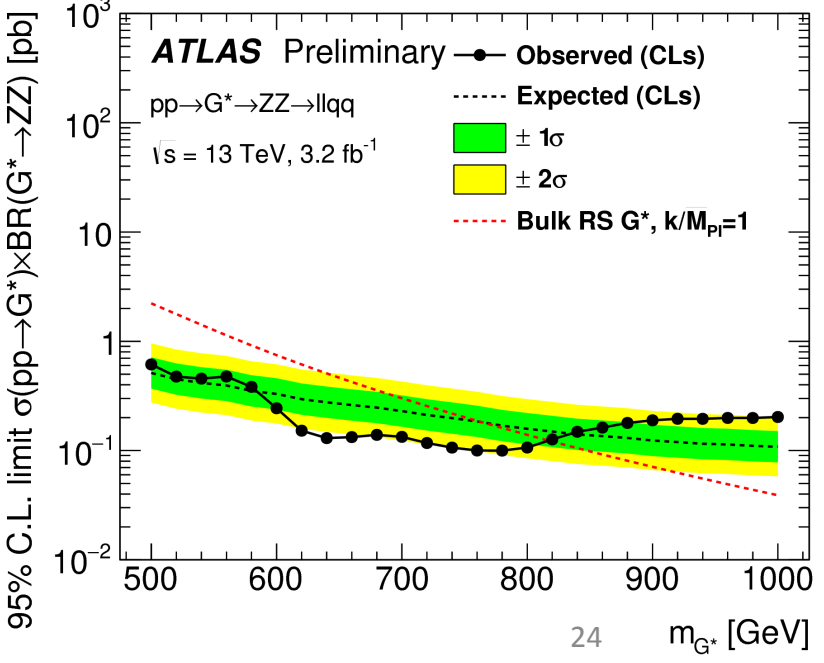

H->hχχ or Z'->hZ' with ->ϒϒ+MET

[Conference note 15 March ATLAS-CONF-2016-011]

No excess is seen, limits are set.

Two models with Dark Matter (DM) checked:

1. Heavy Higgs -> 125 GeV Higgs + two DM.

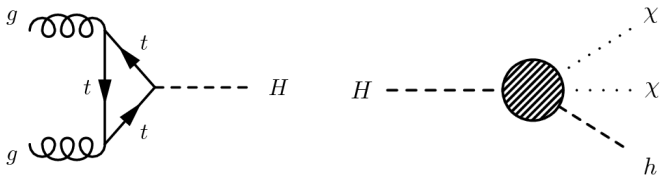

2. Heavy vector boson radiation a 125 GeV Higgs, and decaying to two DM.

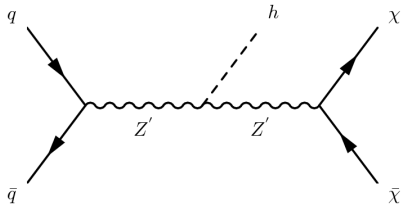

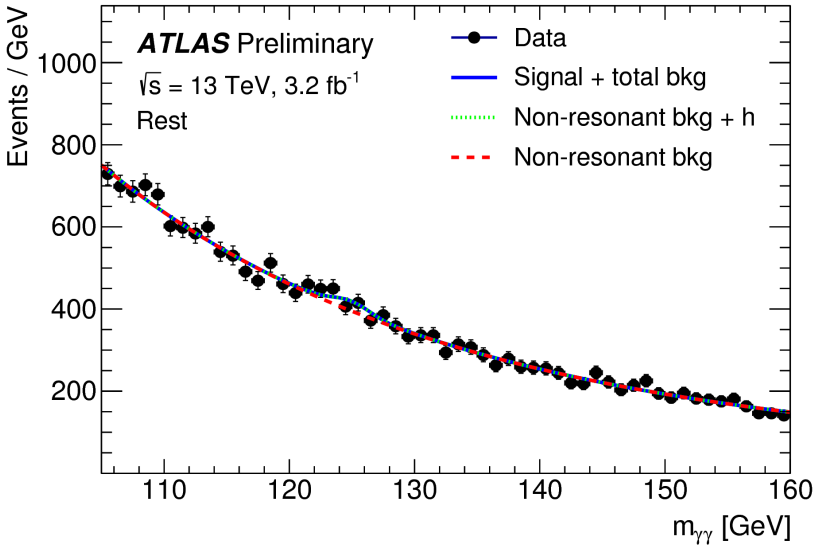

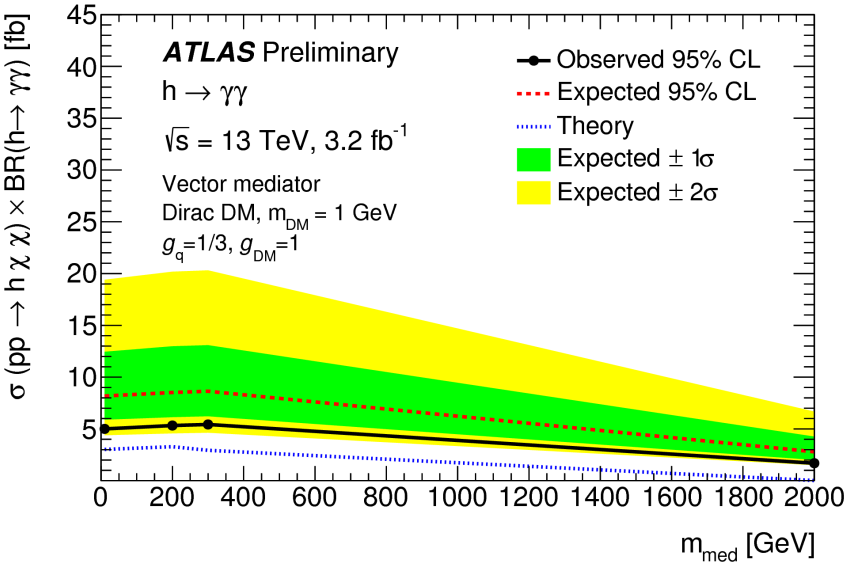

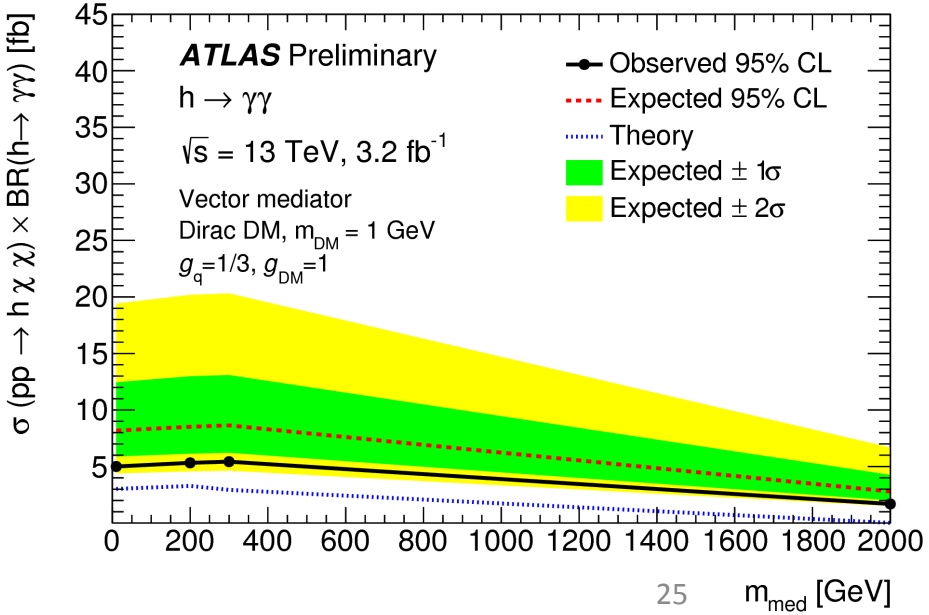

Higgs-like spin-0 X->ZϒΥ (llΥ + JΥ)
Two about 2 sigma excesses.

[Conference note 15 March ATLAS-CONF-2016-010]

Z->ee, electron trigger
Z->μμ, muon triggger
Z->qq (merged in large-R jet), photon trigger
Together 77% of Z BR.
Leptonic Z sensitive m_X 250 – 1500 GeV
Hadronic Z sensitive m_X 720 – 2750 GeV
No visible excess of data over bkg.
2.0σ local excess 350 GeV leptonic channel.
1.8σ local excess 1900 GeV hadronic channel.

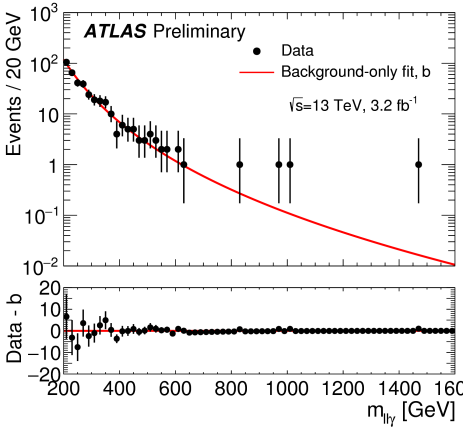

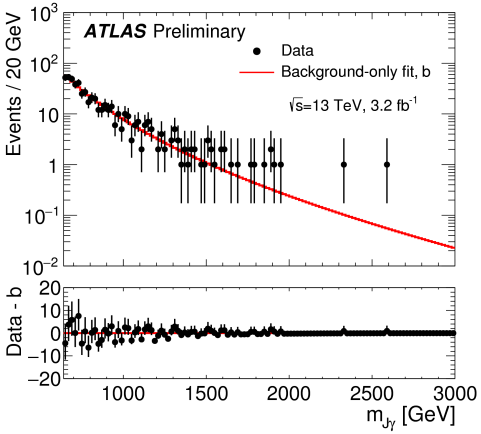

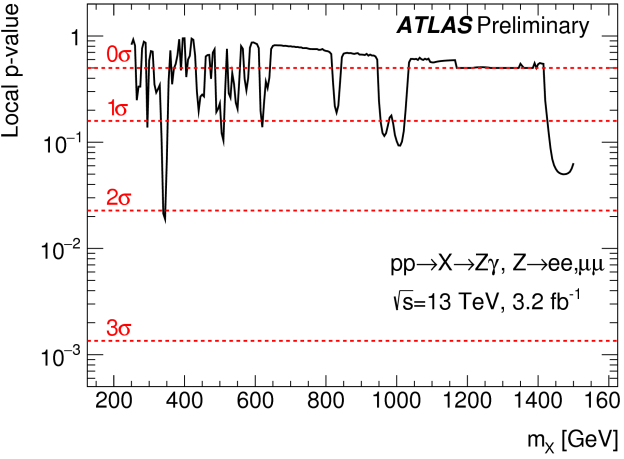

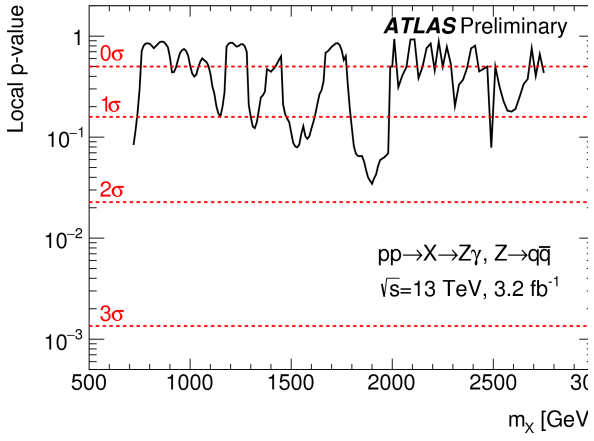

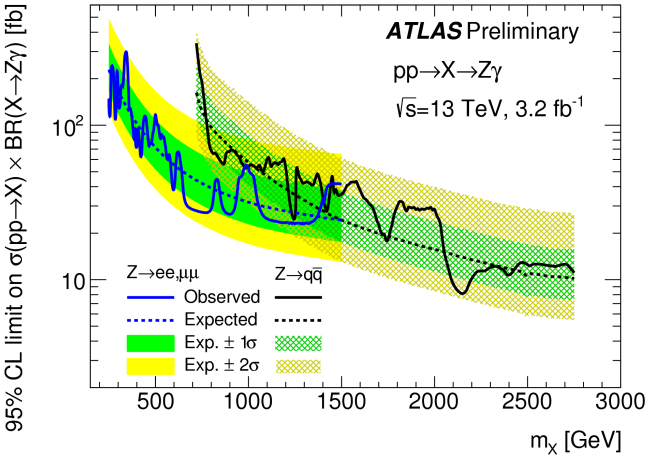

H/A -> ττ, several MSSM scenarios.
No excess seen, limits are set.

[Conference note 14 Dec ATLAS-CONF-2015-061]

At large tan β, increase BR of decay to bb and ττ, as well as increased bH production.
If $m_A >> m_Z$, m_h about 125 GeV and $m_H \approx m_A$.
For m_A>700 GeV, better limits than with 8 TeV.
For m_A=200 GeV, exclude tan β > 10.

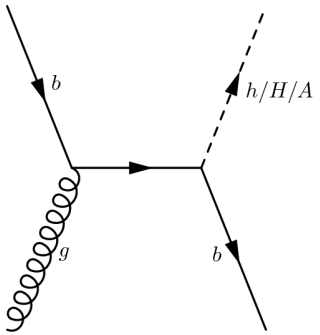

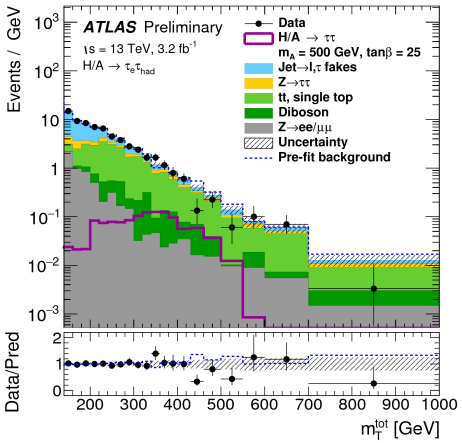

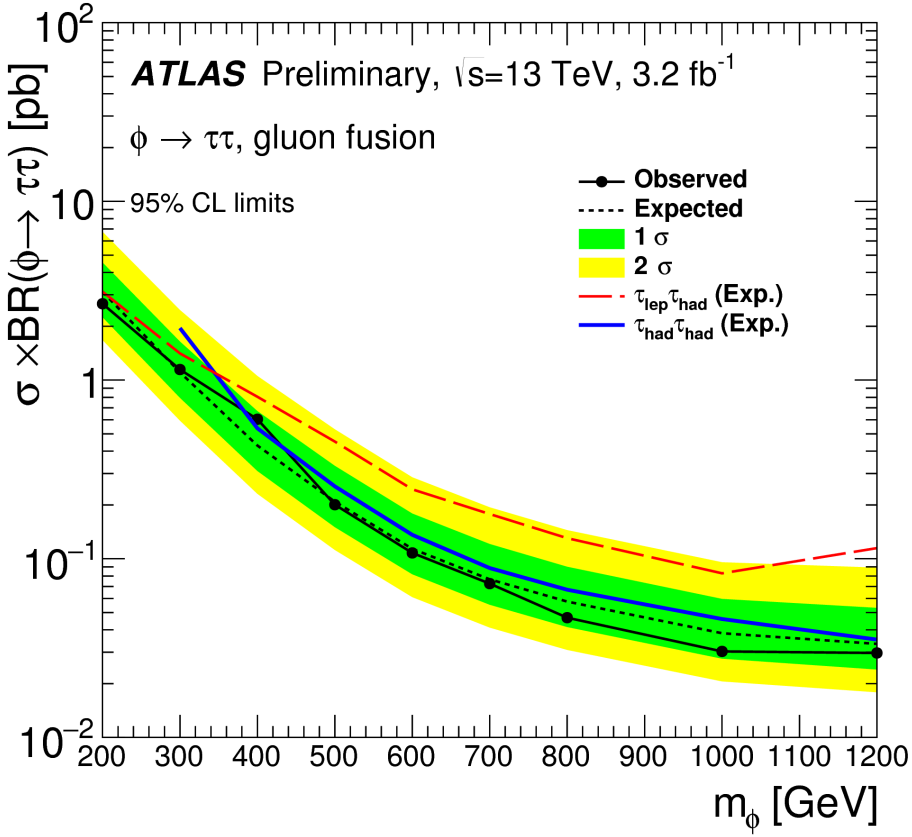

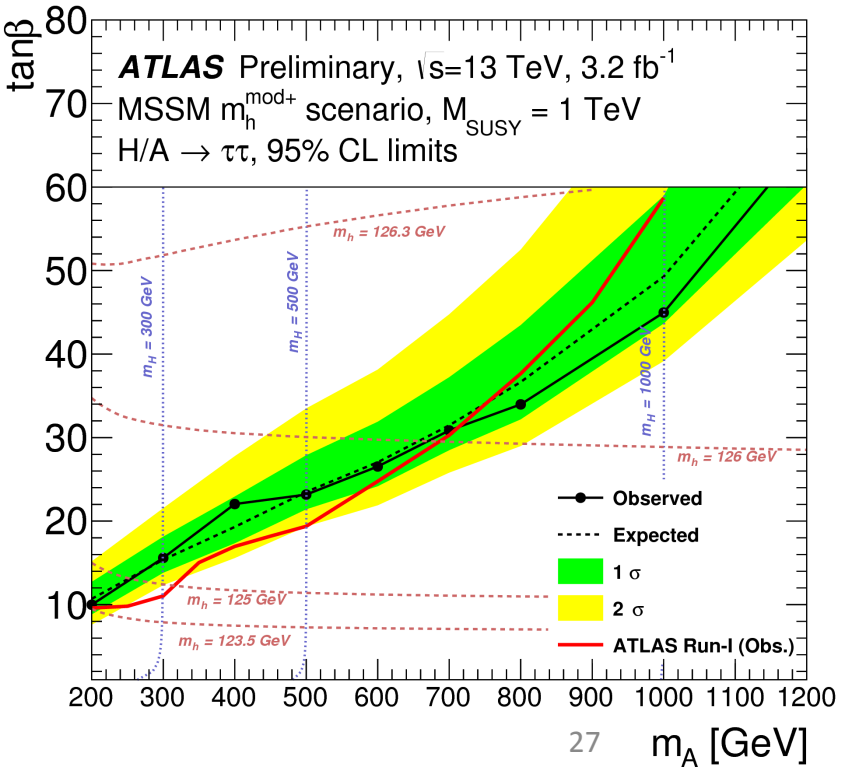

tH^+, with t hadronic $H^+ \to \tau_{had}\nu$ 13 TeV. No excess, but run I limits are surpassed.

[Accepted to PLB](#)
[arXiv:1603.09203](#)

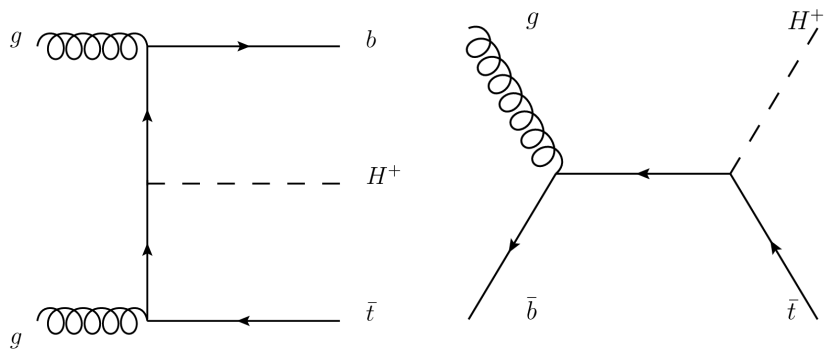

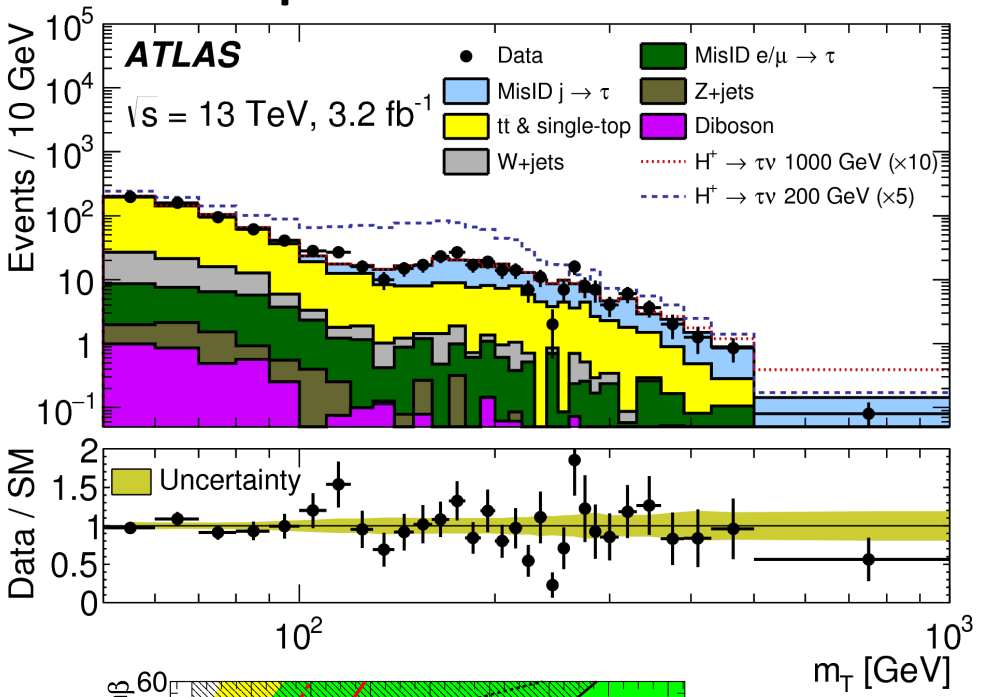

Only MET comes from prompt neutrino.
MET trigger used.
Key background jet faking hadronic τ.
8 TeV searches stop at m_H = 1 TeV.
13 TeV search extended to m_H = 2 TeV.
σ*BR < 1.9 pb – 15 fb for m_H 200 – 2000 GeV.

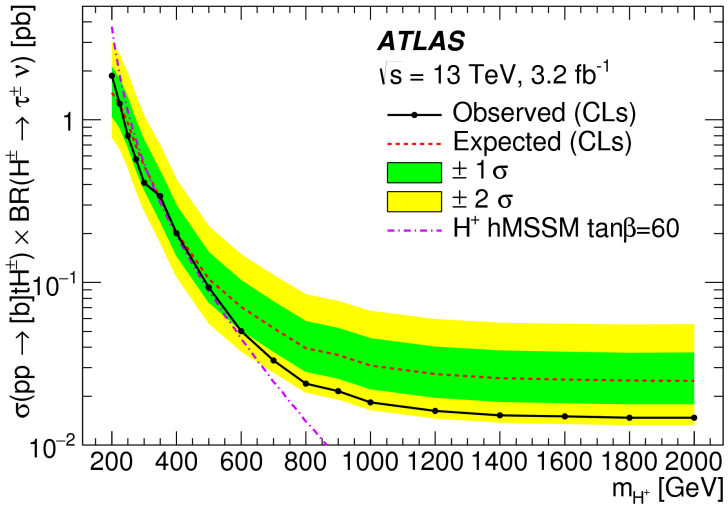

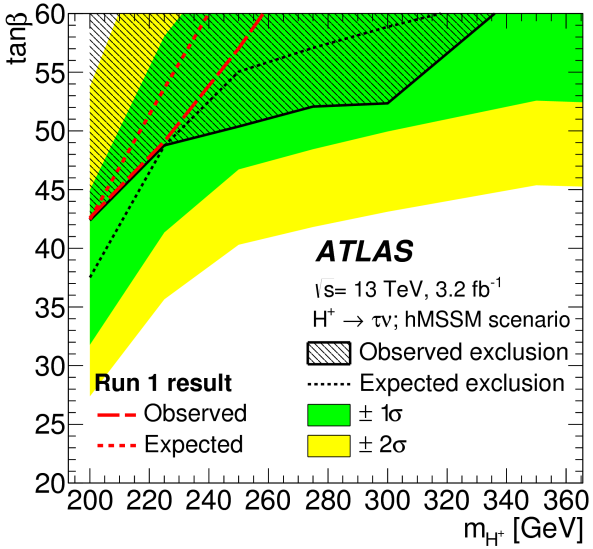

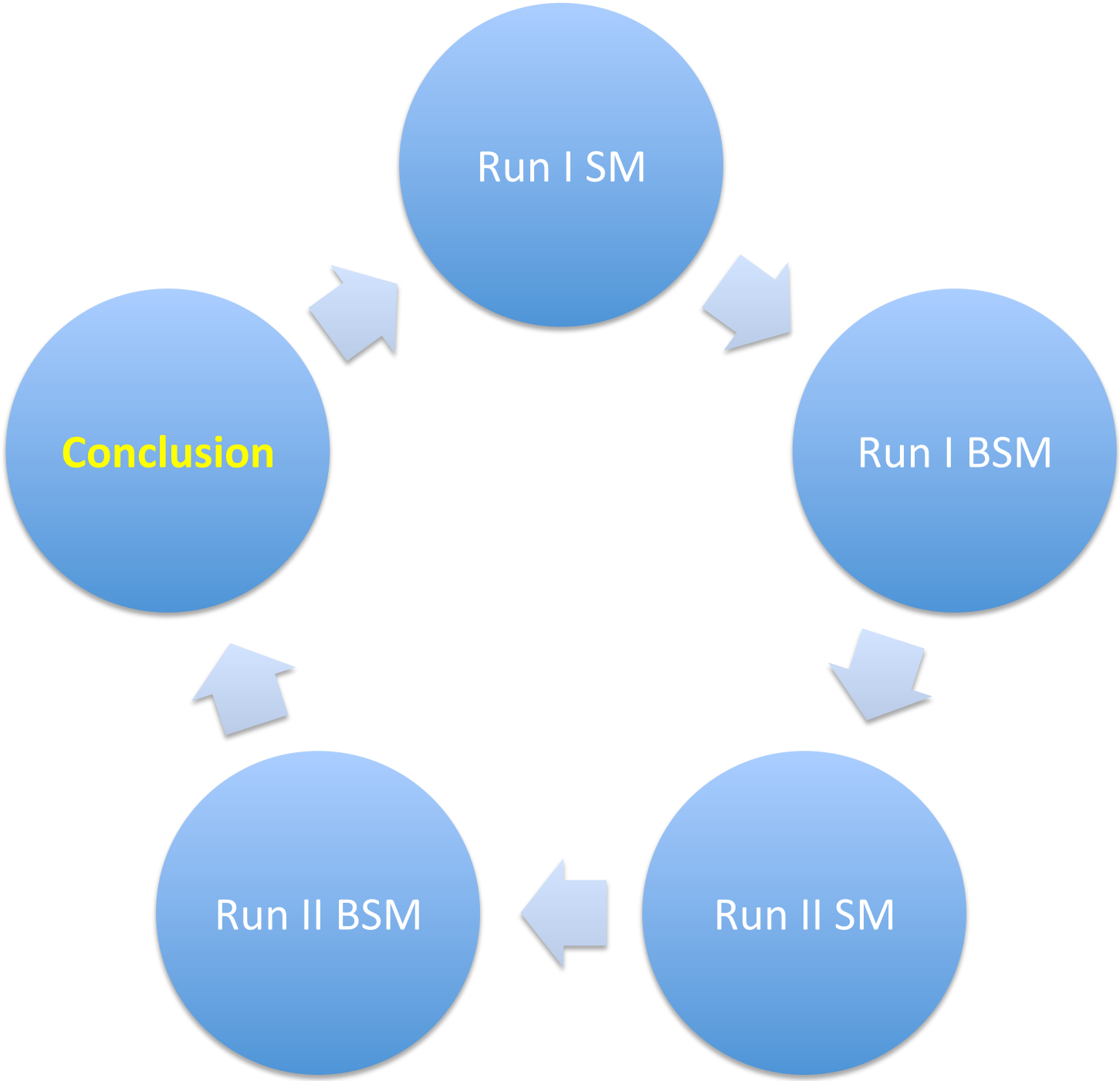
Run I SM
Run I BSM
Run II SM
Run II BSM
Conclusion

Conclusion

ATLAS has a strong program of measuring precisely the properties of the 125 GeV Higgs boson.

- All production mechanisms (ggF, VBF, VH, ttH)
- Most of the decay channels (ϒϒ,ZZ,Zϒ,WW,bb,ττ,μμ)
- Higgs boson couplings to fermions/gauge bosons
- Higgs boson mass
- Total and differential cross sections

… and to search for BSM physics using the 125 GeV Higgs boson.

- Search of an extended Higgs boson family
- Search for new particles decaying to a 125 GeV Higgs boson

No deviations from the SM yet, but …

- Run II searches extend Run I limits to higher mass due to 8 TeV -> 13 TeV.
- But most searches still limited by statistics.
- The 2016 data will help a lot!

…. stay tuned for next summer 2016 conference!

- https://twiki.cern.ch/twiki/bin/view/AtlasPublic/HiggsPublicResults#Higgs_Group_Publications

Backup slides

SM non resonant HH->bbbb.

[Submitted to PRD arXiv:1606.04782]

BSM resonant RSG or 2HDM HH, both ->hh->bbbb.

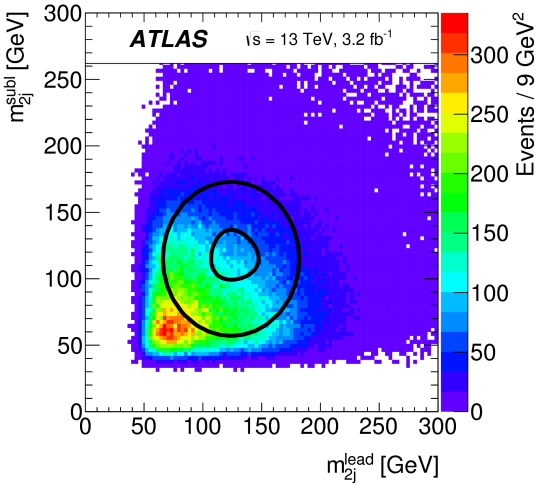

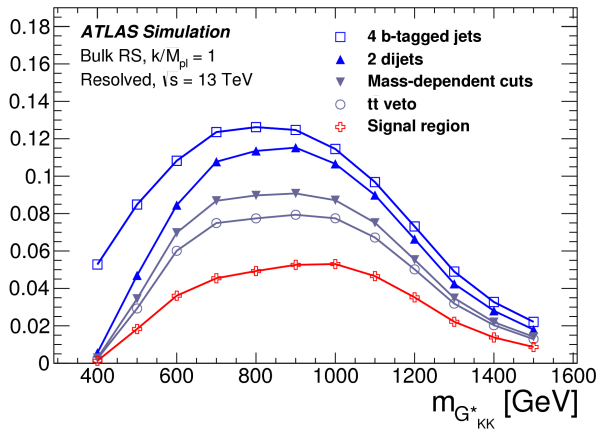

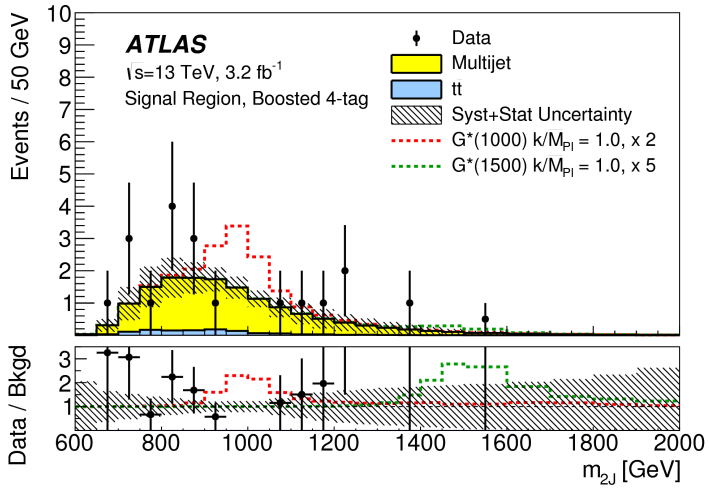

4 resolved R=0.4 b jets, or
2 boosted R=1.0 jets with 3 or 4 b-tagged track jets inside.
Limiting factor: b-tagging efficiency drops for high pT jets.
m_{2j} leading around 124 GeV, m_{2j} subleading around 115 GeV.

Sample	Signal Region Yield
Multijet	43.3 ± 2.3
$t\bar{t}$	4.3 ± 3.0
Z+jets	–
Total	47.6 ± 3.8
Data	46
SM hh	0.22 ± 0.05
G^*_{KK} $(800GeV)$, $k/\bar{M}_{Pl} = 1$	5.7 ± 1.5

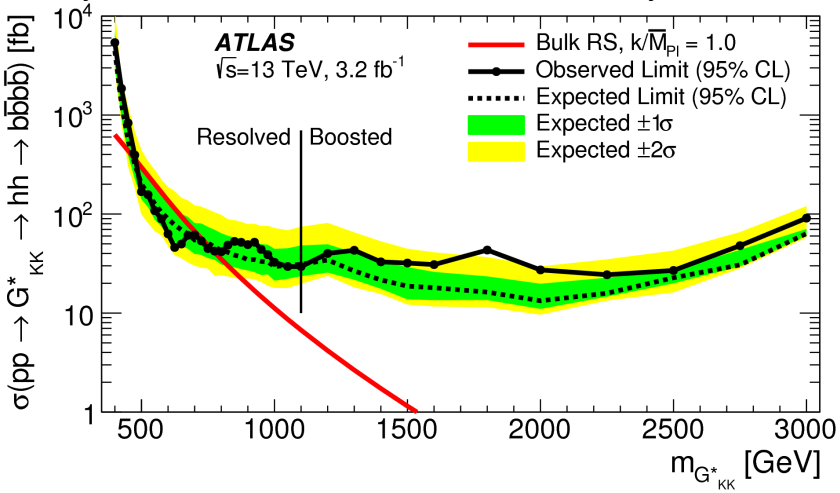

Similar approach to Run I 8 TeV searches,
but enhanced sensitivity at large m_X.
Most sensitive for m_X>500 GeV from all HH searches.
No data excess over background observed.
Limits were set:
SM σ*BR < 1.22 fb
BSM σ*BR < 24-91 fb for m_X=600-3000 GeV.

H->WW->eνμν differential σ at 8 TeV. Consistent with the SM prediction.

[Submitted to JHEP arXiv:1604.02997]

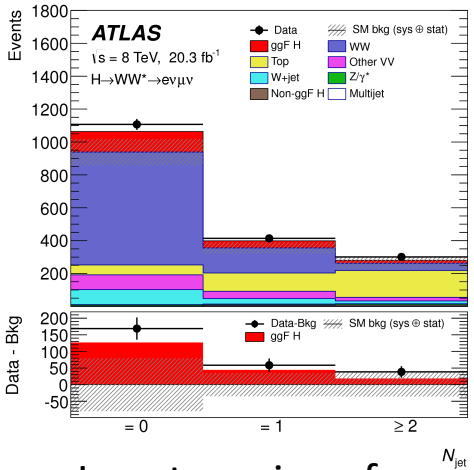

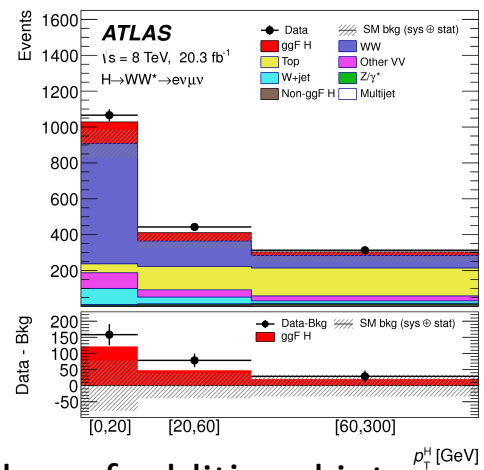

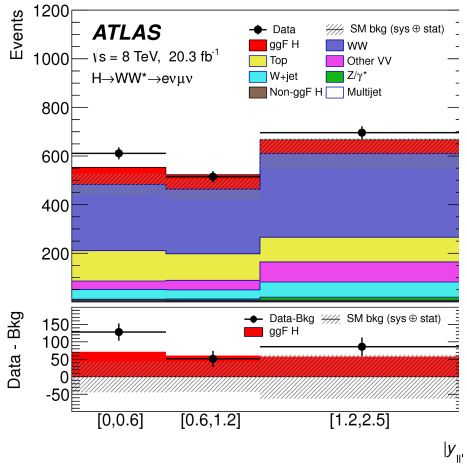

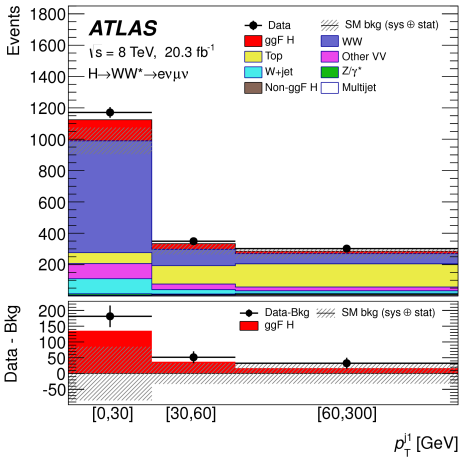

In categories of number of additional jets.

As a function of number of jets, pT of Higgs, dilepton rapidity, pT of leading jet.

Measured: $\sigma^{\text{fid}}_{\text{ggF}} = 36.0 \pm 7.2(\text{stat}) \pm 6.4(\text{sys}) \pm 1.0(\text{lumi})$ fb

Predicted: $\sigma^{\text{fid}}_{\text{ggF}} = 25.1 \pm 2.6$ fb.

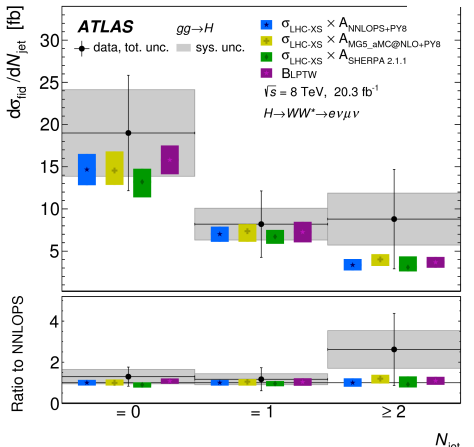

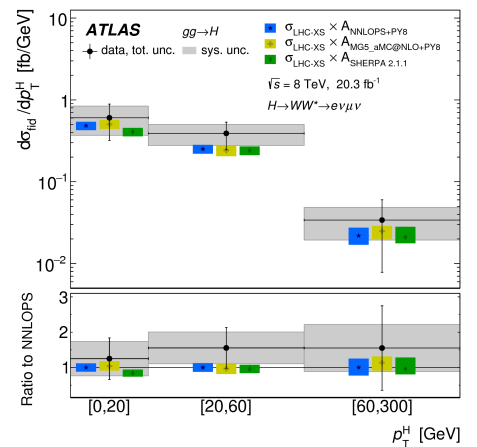

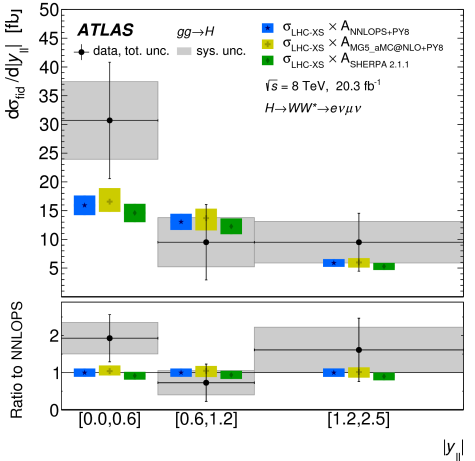

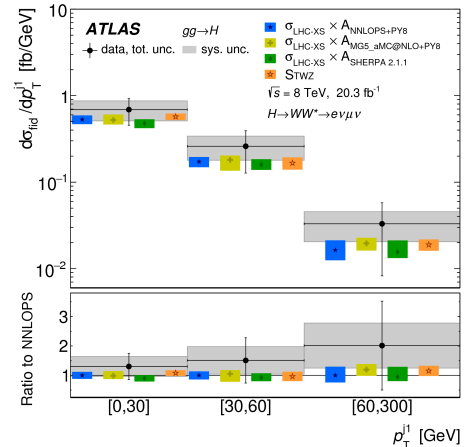

ATLAS and CMS combination Run I

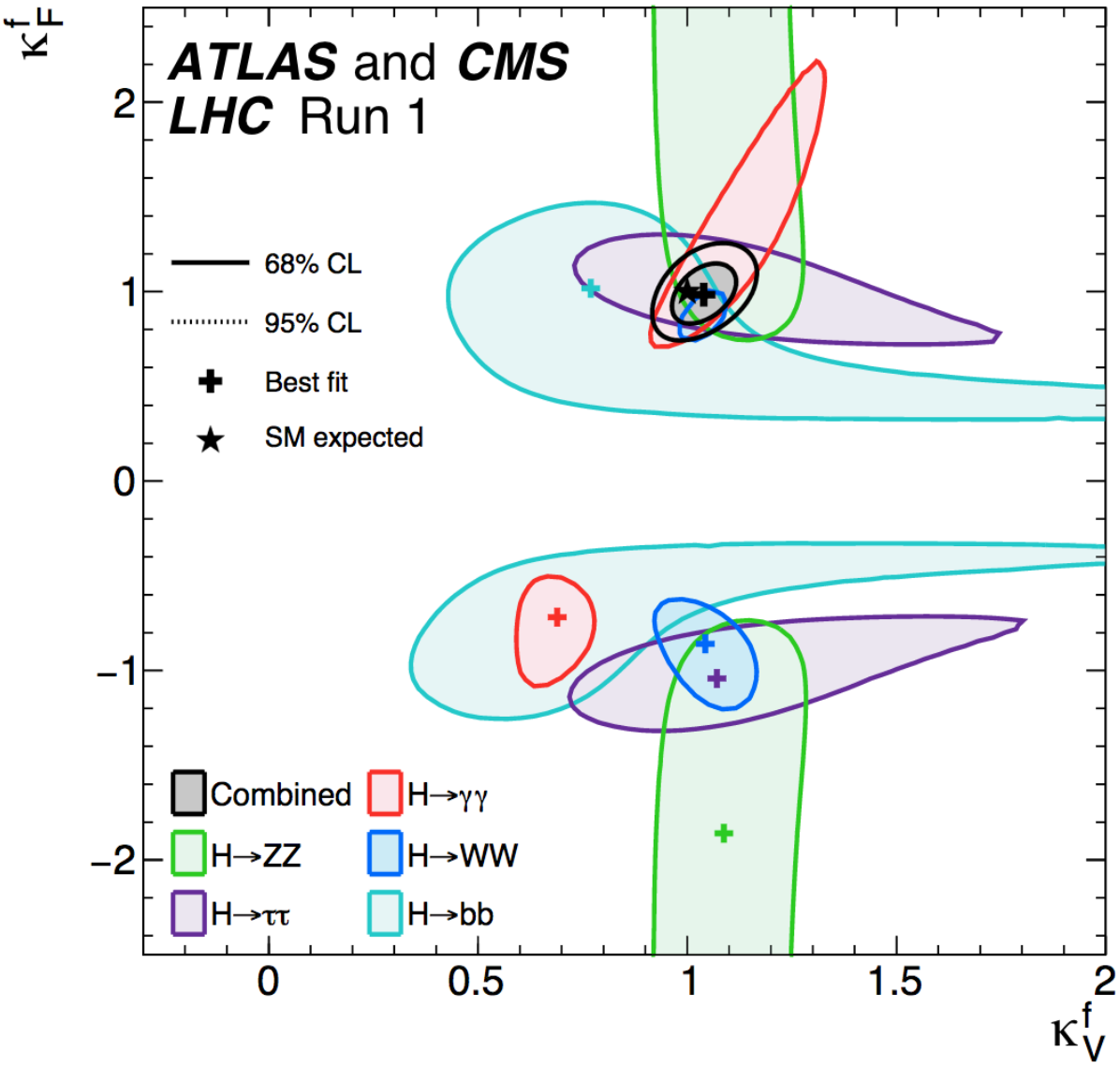

tH^+, with t hadronic $H^+ \to \tau_{had}\nu$ 13 TeV (2).

[Accepted to PLB arXiv:1603.09203]

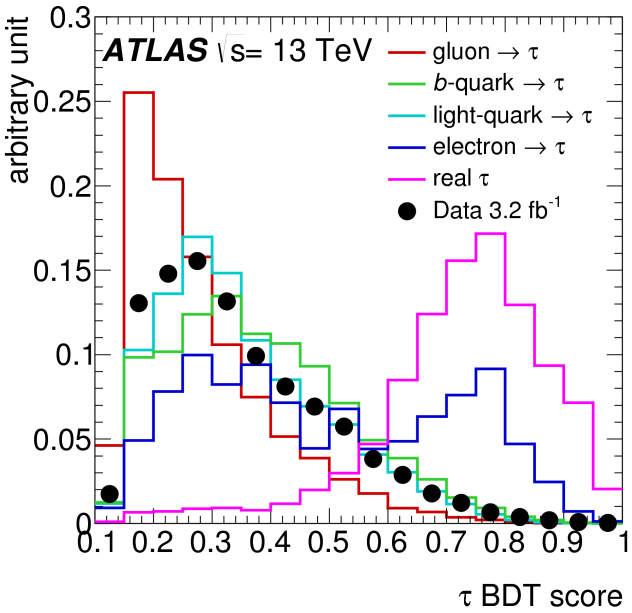

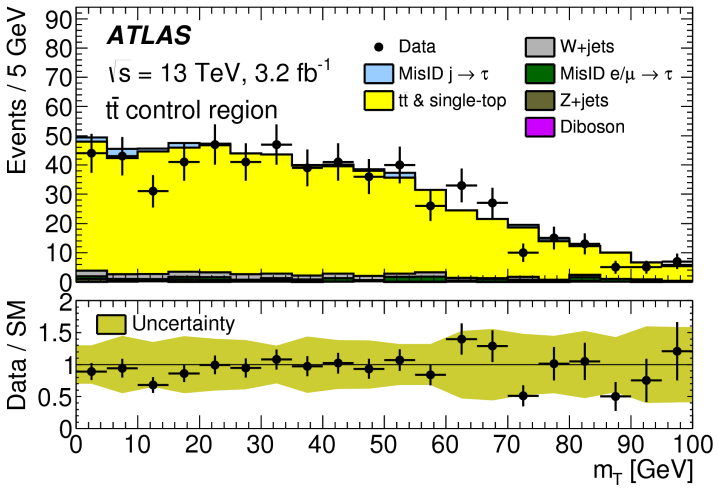

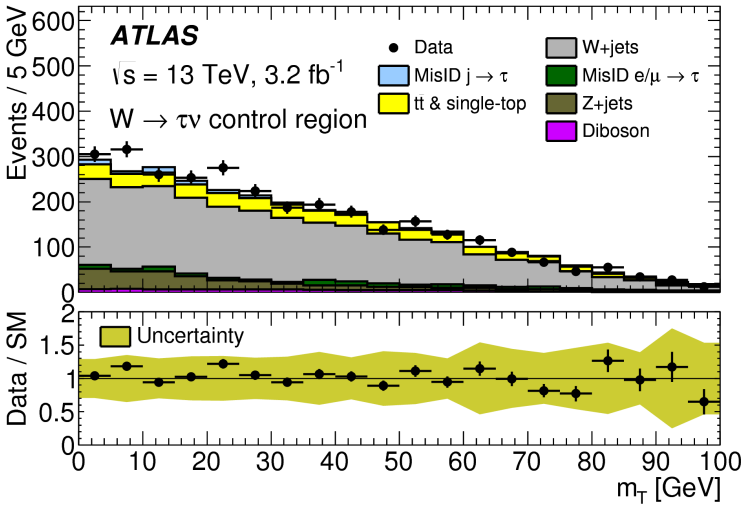

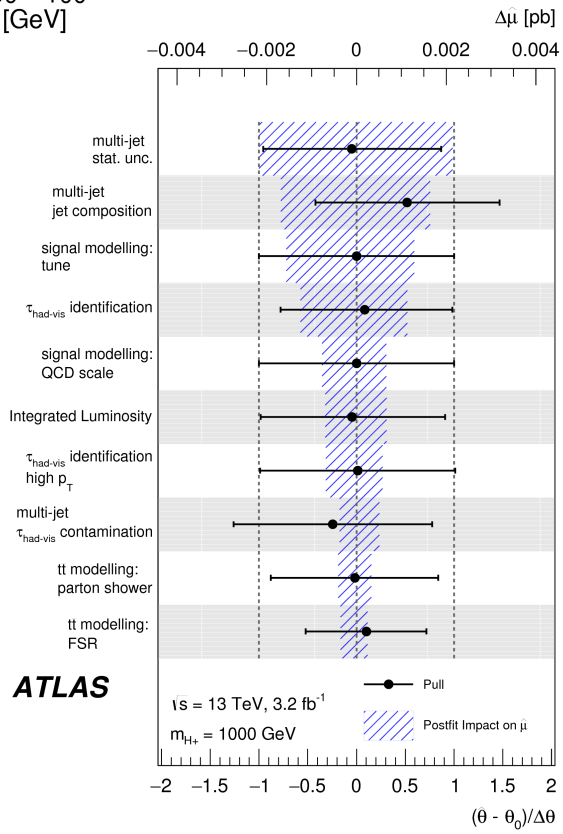

ATLAS and CMS studied almost all combinations of Higgs boson production and decay channels.

Decay	ggF	VBF	VH	Papers
H to bb	- -	- Yes	Yes Yes	in ATLAS internal review; JHEP 1501, 069 (2015) Phys. Rev. D92, 032008 (2015); Phys. Rev. D89, 012003 (2014)
H to ττ	Yes Yes	Yes Yes	Yes Yes	JHEP 1504, 117 (2015) JHEP 1405, 104 (2014)
H to WW	Yes Yes	Yes Yes	Yes Yes	Phys. Rev. D92, 012006 (2015); JHEP 1508, 137 (2015) JHEP 1401, 096 (2014)
H to ZZ	Yes Yes	Yes Yes	Yes Yes	Phys. Rev. D91, 012006 (2015) Phys. Rev. D89, 092007 (2014)
H to γγ	Yes Yes	Yes Yes	Yes Yes	Phys. Rev. D90, 112015 (2014) Eur. Phys. J. C74, 3076 (2014)
H to μμ	Yes Yes	Yes Yes	- Yes	Phys. Lett. B738, 68 (2014) Phys. Lett. B744, 184 (2015)
H to inv	- -	Yes Yes	Yes Yes	Eur. Phys. J. C75, 337 (2015); arXiv:1508.07869 Eur. Phys. J. C74, 2980 (2014)

ATLAS and CMS measured the signal strengths.

Decay	Signal strength for production mechanisms
H to bb	VH (0.52+-0.32+-0.24) VH (1.0+-0.5), VBF (2.8+1.6-1.4)
H to ττ	ggF (2.1+-0.9-0.8), VBF (1.2+-0.4) 0jet (0.34+-1.09), 1jet (1.07+-0.46), 2jet VBF (0.94+-0.41), other (-0.33+-1.02)
H to WW	ggF (1.02+-0.19+-0.22), VBF (1.27+-0.44+-0.40), VH (3.0+-1.3+-1.0) 0/1jet (0.74+-0.22), 2jet VBF (0.60+-0.57), 2jet VH (0.39+-1.97), WH (0.56+1.27-0.95)
H to ZZ	ggF+bbH+ttH (1.66+0.45-0.41+0.25-0.15), VBF+VH (0.26+1.60-0.91+0.36-0.23) ggF+ttH (0.8+0.46-0.36), VBF+VH (1.7+2.2-2.1)
H to γγ	ggF (1.32+-0.38), VBF (0.8+-0.7), WH (1.0 +-1.6), ZH (0.1+3.7-0.1), ttH (1.6+2.7-1.8) ggF (1.12+-0.37), VBF (1.58+-0.77), VH (-0.16+1.16-0.79), ttH (2.69+2.51-1.81)
H to μμ	95% CL limit 7xSM 95% CL limit 7xSM
H to inv	VBF 95% CL limit VBF (0.65), ZH (0.81), VBF+ZH (0.58)

ATLAS and CMS measured the signal strengths. For H to μμ and H to invisible only limits are set.

Decay	Signal strength for production mechanisms
H to bb	VH (0.52+-0.32+-0.24) VH (1.0+-0.5), VBF (2.8+1.6-1.4)
H to ττ	ggF (2.1+-0.9-0.8), VBF (1.2+-0.4) 0jet (0.34+-1.09), 1jet (1.07+-0.46), 2jet VBF (0.94+-0.41), other (-0.33+-1.02)
H to WW	ggF (1.02+-0.19+-0.22), VBF (1.27+-0.44+-0.40), VH (3.0+-1.3+-1.0) 0/1jet (0.74+-0.22), 2jet VBF (0.60+-0.57), 2jet VH (0.39+-1.97), WH (0.56+1.27-0.95)
H to ZZ	ggF+bbH+ttH (1.66+0.45-0.41+0.25-0.15), VBF+VH (0.26+1.60-0.91+0.36-0.23) ggF+ttH (0.8+0.46-0.36), VBF+VH (1.7+2.2-2.1)
H to γγ	ggF (1.32+-0.38), VBF (0.8+-0.7), WH (1.0 +-1.6), ZH (0.1+3.7-0.1), ttH (1.6+2.7-1.8) ggF (1.12+-0.37), VBF (1.58+-0.77), VH (-0.16+1.16-0.79), ttH (2.69+2.51-1.81)
H to μμ	95% CL limit 7xSM 95% CL limit 7xSM
H to inv	VBF 95% CL limit VBF (0.65), ZH (0.81), VBF+ZH (0.58)

Only limits.

ATLAS and CMS measured the signal strengths. For H to ZZ and H to ττ, ggF is best, rest negligible.

Decay	Signal strength for production mechanisms
H to bb	VH (0.52+-0.32+-0.24) VH (1.0+-0.5), VBF (2.8+1.6-1.4)
H to ττ	ggF (2.1+-0.9-0.8), VBF (1.2+-0.4) 0jet (0.34+-1.09), 1jet (1.07+-0.46), 2jet VBF (0.94+-0.41), other (-0.33+-1.02)
H to WW	ggF (1.02+-0.19+-0.22), VBF (1.27+-0.44+-0.40), VH (3.0+-1.3+-1.0) 0/1jet (0.74+-0.22), 2jet VBF (0.60+-0.57), 2jet VH (0.39+-1.97), WH (0.56+1.27-0.95)
H to ZZ	ggF+bbH+ttH (1.66+0.45-0.41+0.25-0.15), VBF+VH (0.26+1.60-0.91+0.36-0.23) ggF+ttH (0.8+0.46-0.36), VBF+VH (1.7+2.2-2.1)
H to γγ	ggF (1.32+-0.38), VBF (0.8+-0.7), WH (1.0 +-1.6), ZH (0.1+3.7-0.1), ttH (1.6+2.7-1.8) ggF (1.12+-0.37), VBF (1.58+-0.77), VH (-0.16+1.16-0.79), ttH (2.69+2.51-1.81)
H to μμ	95% CL limit 7xSM 95% CL limit 7xSM
H to inv	VBF 95% CL limit VBF (0.65), ZH (0.81), VBF+ZH (0.58)

ggF is best, the rest negligible.

ATLAS and CMS measured the signal strengths. For H to WW, ggF best, VBF matters too, VH too.

Decay	Signal strength for production mechanisms
H to bb	VH (0.52+-0.32+-0.24) VH (1.0+-0.5), VBF (2.8+1.6-1.4)
H to ττ	ggF (2.1+-0.9-0.8), VBF (1.2+-0.4) 0jet (0.34+-1.09), 1jet (1.07+-0.46), 2jet VBF (0.94+-0.41), other (-0.33+-1.02)
H to WW	ggF (1.02+-0.19+-0.22), VBF (1.27+-0.44+-0.40), VH (3.0+-1.3+-1.0) 0/1jet (0.74+-0.22), 2jet VBF (0.60+-0.57), 2jet VH (0.39+-1.97), WH (0.56+1.27-0.95)
H to ZZ	ggF+bbH+ttH (1.66+0.45-0.41+0.25-0.15), VBF+VH (0.26+1.60-0.91+0.36-0.23) ggF+ttH (0.8+0.46-0.36), VBF+VH (1.7+2.2-2.1)
H to γγ	ggF (1.32+-0.38), VBF (0.8+-0.7), WH (1.0 +-1.6), ZH (0.1+3.7-0.1), ttH (1.6+2.7-1.8) ggF (1.12+-0.37), VBF (1.58+-0.77), VH (-0.16+1.16-0.79), ttH (2.69+2.51-1.81)
H to μμ	95% CL limit 7xSM 95% CL limit 7xSM
H to inv	VBF 95% CL limit VBF (0.65), ZH (0.81), VBF+ZH (0.58)

ggF is best, VBF and VH matter too.

ATLAS and CMS measured the signal strengths. For H to ττ, ggF helps, but VBF is dominant, though.

Decay	Signal strength for production mechanisms
H to bb	VH (0.52+-0.32+-0.24) VH (1.0+-0.5), VBF (2.8+1.6-1.4)
H to ττ	ggF (2.1+-0.9-0.8), VBF (1.2+-0.4) 0jet (0.34+-1.09), 1jet (1.07+-0.46), 2jet VBF (0.94+-0.41), other (-0.33+-1.02)
H to WW	ggF (1.02+-0.19+-0.22), VBF (1.27+-0.44+-0.40), VH (3.0+-1.3+-1.0) 0/1jet (0.74+-0.22), 2jet VBF (0.60+-0.57), 2jet VH (0.39+-1.97), WH (0.56+1.27-0.95)
H to ZZ	ggF+bbH+ttH (1.66+0.45-0.41+0.25-0.15), VBF+VH (0.26+1.60-0.91+0.36-0.23) ggF+ttH (0.8+0.46-0.36), VBF+VH (1.7+2.2-2.1)
H to γγ	ggF (1.32+-0.38), VBF (0.8+-0.7), WH (1.0 +-1.6), ZH (0.1+3.7-0.1), ttH (1.6+2.7-1.8) ggF (1.12+-0.37), VBF (1.58+-0.77), VH (-0.16+1.16-0.79), ttH (2.69+2.51-1.81)
H to μμ	95% CL limit 7xSM 95% CL limit 7xSM
H to inv	VBF 95% CL limit VBF (0.65), ZH (0.81), VBF+ZH (0.58)

ggF helps. VBF is dominant, though.

ATLAS and CMS measured the signal strengths. For H to bb, ggF doesn't help, VH and VBF dominant.

Decay	Signal strength for production mechanisms
H to bb	VH (0.52+-0.32+-0.24) VH (1.0+-0.5), VBF (2.8+1.6-1.4)
H to ττ	ggF (2.1+-0.9-0.8), VBF (1.2+-0.4) 0jet (0.34+-1.09), 1jet (1.07+-0.46), 2jet VBF (0.94+-0.41), other (-0.33+-1.02)
H to WW	ggF (1.02+-0.19+-0.22), VBF (1.27+-0.44+-0.40), VH (3.0+-1.3+-1.0) 0/1jet (0.74+-0.22), 2jet VBF (0.60+-0.57), 2jet VH (0.39+-1.97), WH (0.56+1.27-0.95)
H to ZZ	ggF+bbH+ttH (1.66+0.45-0.41+0.25-0.15), VBF+VH (0.26+1.60-0.91+0.36-0.23) ggF+ttH (0.8+0.46-0.36), VBF+VH (1.7+2.2-2.1)
H to γγ	ggF (1.32+-0.38), VBF (0.8+-0.7), WH (1.0 +-1.6), ZH (0.1+3.7-0.1), ttH (1.6+2.7-1.8) ggF (1.12+-0.37), VBF (1.58+-0.77), VH (-0.16+1.16-0.79), ttH (2.69+2.51-1.81)
H to μμ	95% CL limit 7xSM 95% CL limit 7xSM
H to inv	VBF 95% CL limit VBF (0.65), ZH (0.81), VBF+ZH (0.58)

ggF doesn't help. VH and VBF dominant.

ATLAS+CMS Run I 7+8 TeV combination. Submitted to JHEP arXiv:1606.02266

Data consistent with SM. Total μ = 1.09 ± 0.11.

Production process	Cross section [pb] $\sqrt{s}$ = 7 TeV	Cross section [pb] $\sqrt{s}$ = 8 TeV	Order of calculation
ggF	15.0 ± 1.6	19.2 ± 2.0	NNLO(QCD) + NLO(EW)
VBF	1.22 ± 0.03	1.58 ± 0.04	NLO(QCD+EW) + APPROX. NNLO(QCD)
WH	0.577 ± 0.016	0.703 ± 0.018	NNLO(QCD) + NLO(EW)
ZH	0.334 ± 0.013	0.414 ± 0.016	NNLO(QCD) + NLO(EW)
$[ggZH]$	0.023 ± 0.007	0.032 ± 0.010	NLO(QCD)
ttH	0.086 ± 0.009	0.129 ± 0.014	NLO(QCD)
tH	0.012 ± 0.001	0.018 ± 0.001	NLO(QCD)
bbH	0.156 ± 0.021	0.203 ± 0.028	5FS NNLO(QCD) + 4FS NLO(QCD)
Total	17.4 ± 1.6	22.3 ± 2.0	

Production process	Event generator ATLAS	Event generator CMS
ggF	POWHEG [79–83]	POWHEG
VBF	POWHEG	POWHEG
WH	PYTHIA8 [84]	PYTHIA6.4 [85]
ZH ($qq \to ZH$ or $qg \to ZH$)	PYTHIA8	PYTHIA6.4
$ggZH$ ($gg \to ZH$)	POWHEG	See text
ttH	POWHEL [87]	PYTHIA6.4
tHq ($qb \to tHq$)	MADGRAPH [89]	aMC@NLO [78]
tHW ($gb \to tHW$)	aMC@NLO	aMC@NLO
bbH	PYTHIA8	PYTHIA6.4, aMC@NLO

Decay mode	Branching fraction [%]
$H \to bb$	57.5 ± 1.9
$H \to WW$	21.6 ± 0.9
$H \to gg$	8.56 ± 0.86
$H \to \tau\tau$	6.30 ± 0.36
$H \to cc$	2.90 ± 0.35
$H \to ZZ$	2.67 ± 0.11
$H \to \gamma\gamma$	0.228 ± 0.011
$H \to Z\gamma$	0.155 ± 0.014
$H \to \mu\mu$	0.022 ± 0.001

ATLAS coupling strengths consistent with the SM: with bosons (VH+VBF) and fermions (ggF+ttH).

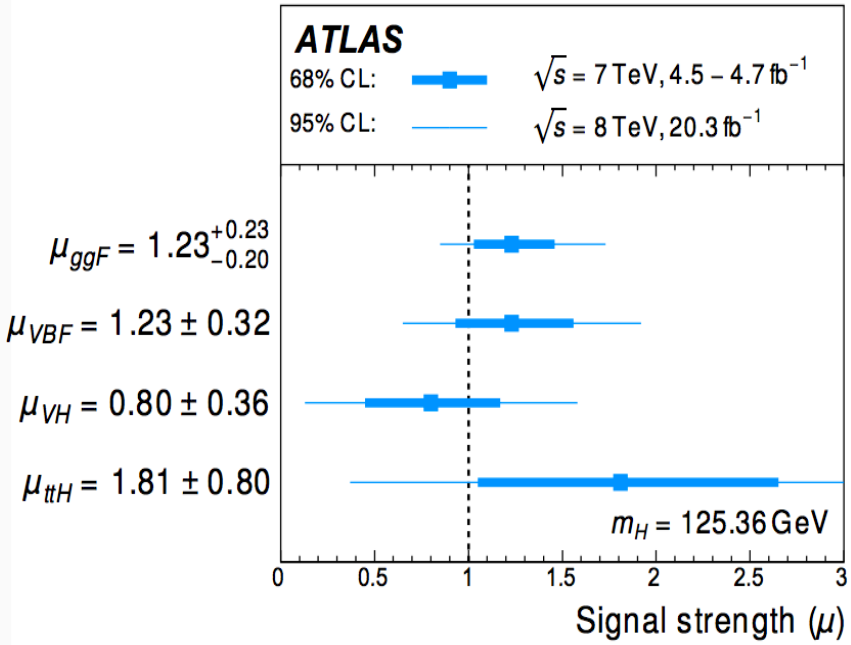

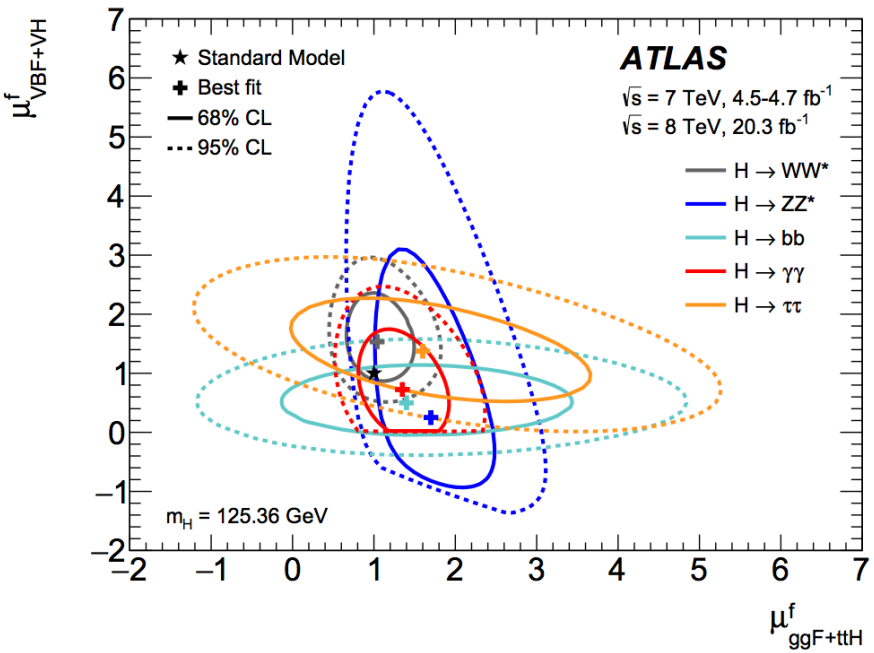

VH, H->bb, 8 TeV, has three VH topologies based on number of leptons.

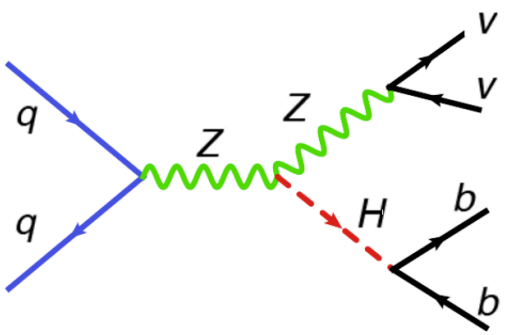

MET+bb

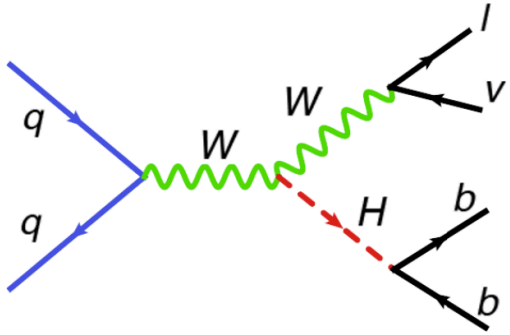

l+MET+bb

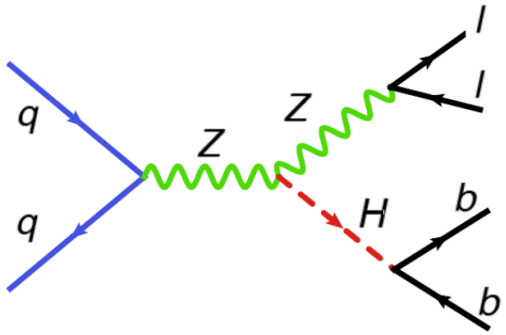

ll+bb

To increase the sensitivity even more, the analysis channels are split further by p_T^V.

ATLAS also splits further by the number of jets and b-tagging discriminant.

The event selection is chosen for each category.

The event selection is chosen for each category.

Variable	Dijet-mass analysis					Multivariate analysis	
Common selection							
p_{T}^{V} [GeV]	0–90	90$^{(*)}$–120	120–160	160–200	> 200	0–120	> 120
$\Delta R(\mathrm{jet}_1, \mathrm{jet}_2)$	0.7–3.4	0.7–3.0	0.7–2.3	0.7–1.8	< 1.4	> 0.7 (p_{T}^{V}<200 GeV)	
0-lepton selection							
$p_{\mathrm{T}}^{\mathrm{miss}}$ [GeV]	NU	> 30	> 30			NU	> 30
$\Delta\phi(\boldsymbol{E}_{\mathrm{T}}^{\mathrm{miss}}, \boldsymbol{p}_{\mathrm{T}}^{\mathrm{miss}})$		$< \pi/2$	$< \pi/2$				$< \pi/2$
$\min[\Delta\phi(\boldsymbol{E}_{\mathrm{T}}^{\mathrm{miss}}, \mathrm{jet})]$		–	> 1.5				> 1.5
$\Delta\phi(\boldsymbol{E}_{\mathrm{T}}^{\mathrm{miss}}, \mathrm{dijet})$		> 2.2	> 2.8				–
$\sum_{i=1}^{N_{\mathrm{jet}}=2(3)} p_{\mathrm{T}}^{\mathrm{jet}_i}$ [GeV]		> 120 (NU)	> 120 (150)				> 120 (150)
1-lepton selection							
m_{T}^{W} [GeV]	< 120					–	
H_{T} [GeV]	> 180		–			> 180	–
$E_{\mathrm{T}}^{\mathrm{miss}}$ [GeV]	–		> 20		> 50	–	> 20
2-lepton selection							
$m_{\ell\ell}$ [GeV]	83-99					71-121	
$E_{\mathrm{T}}^{\mathrm{miss}}$ [GeV]	< 60					–	

Table 2. Event topological and kinematic selections. NU stands for 'Not Used'. (∗) In the 0-lepton channel, the lower edge of the second p_{T}^{V} interval is set at 100 GeV instead of 90 GeV. For the 1-lepton channel, only the 1-muon sub-channel is used in the $p_{\mathrm{T}}^{V} < 120$ GeV intervals.

The main backgrounds are ttbar, V+jets and QCD. The search sensitivity increases with the P_T^V bin.

ATLAS m_{bb} 0 leptons, 2 jets, 2 b-tags, different p_T^V bins.

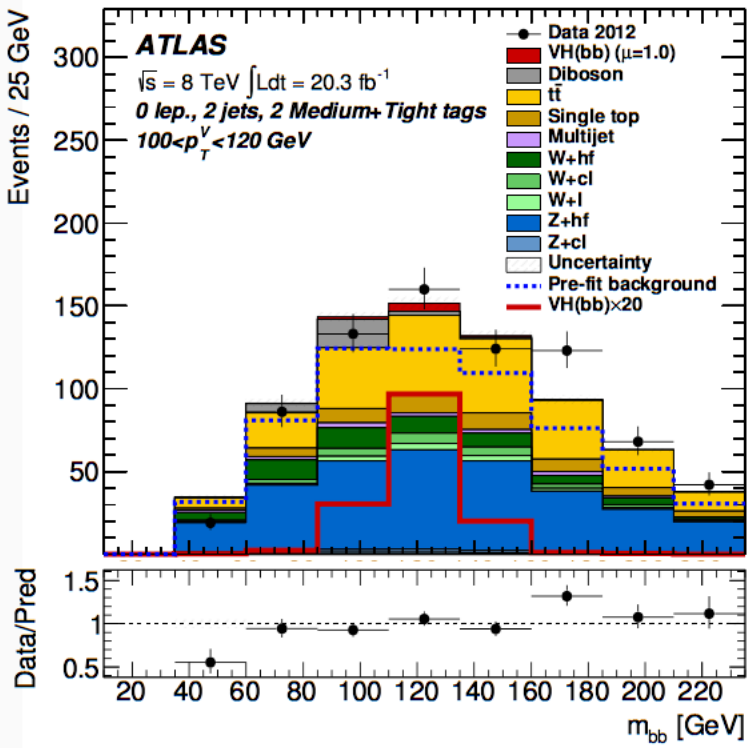

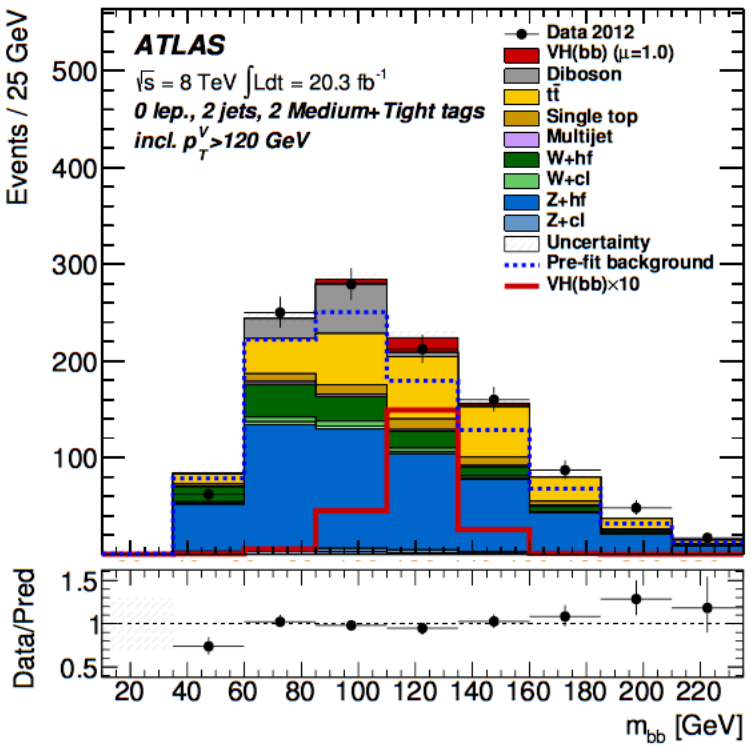

ttbar and V+jets have shapes taken from simulation and normalization from data.

QCD jets background is fully data driven.

Di-b-jet invariant mass is the best signal to background discriminant.

b-jets need extra energy calibrations to account for muons, neutrinos, non closure, jet pT spectrum.

EM → JES → GS → Muon → Resolution

"Raw" energy

Jet energy scale

Global sequential

Muon-in-jet

Pt Reco

Designed for all jets.

Two official calibrations derived to improve the scale and resolution of all jets.

JES: ATLAS-CONF-2015-017

GSC: ATLAS-CONF-2015-002

Event selection

Designed for b jets.

For jets that contain a muon from semileptonic decays (12% of b jets).

For all jets, derived from the Pt spectrum of H->bb at 125 GeV.

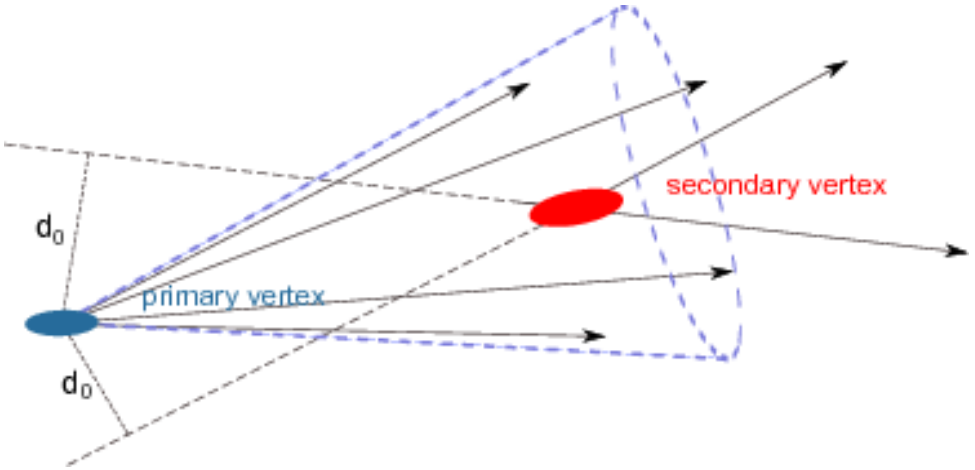

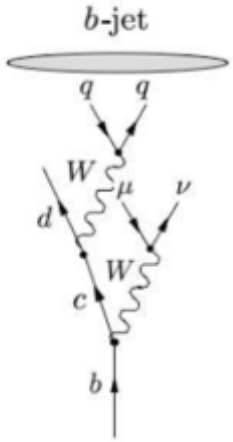

12% have muon

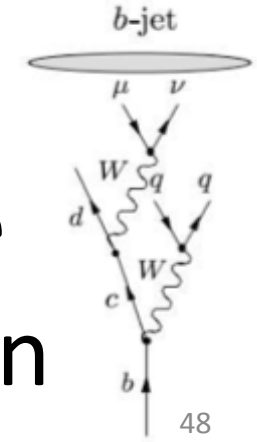

In Run I VH, after a muon-in-jet corr, PtReco was used in vvbb and lvbb, and a Kinematic Fit in llbb.

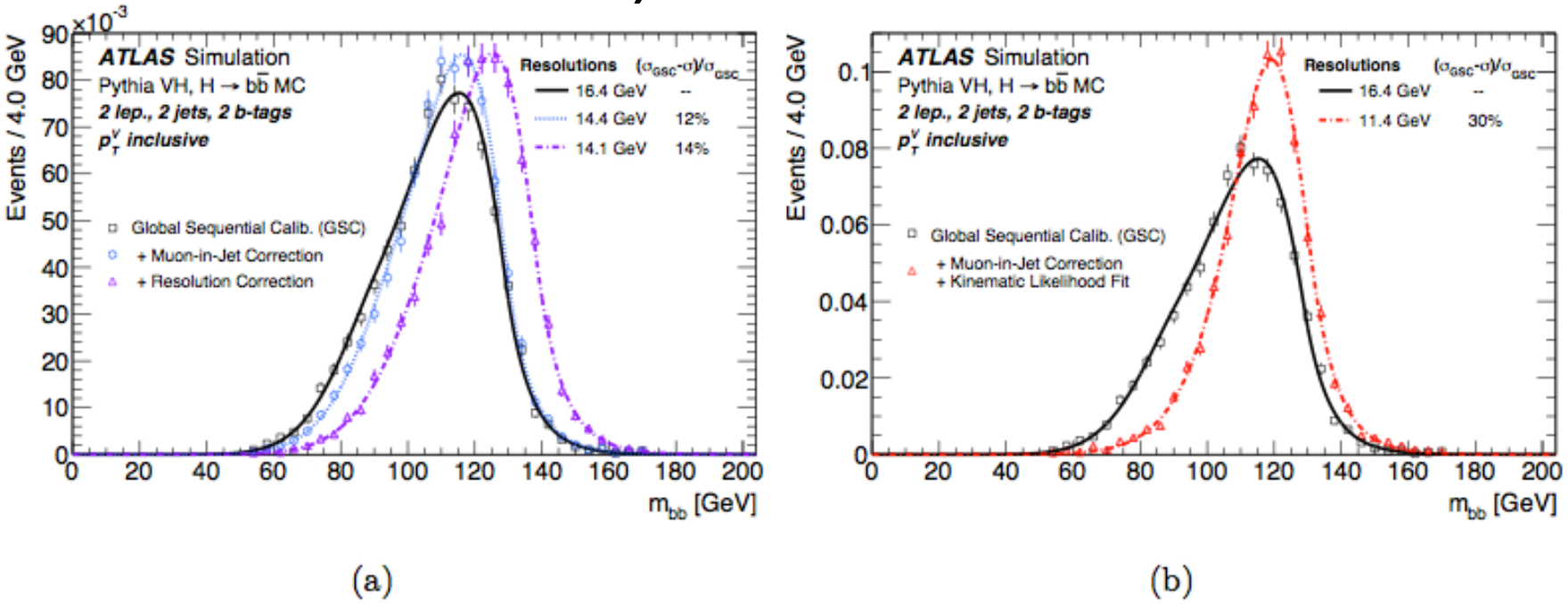

Figure 1. Dijet-invariant-mass distribution for the decay products of a Higgs boson with $m_H = 125$ GeV in the 2-lepton MVA selection. The distributions are shown (a) using jets after global sequential calibration (GSC, solid), and after adding muons inside jets (dotted) and after correcting for resolution effects specific to the kinematics of the decay of a Higgs boson with $m_H = 125$ GeV (dash-dotted); (b) using jets after global sequential calibration (GSC, solid), and after adding muons inside jets and applying the kinematic fit (dash-dotted). The distributions are fit to the Bukin function [68] and the parameter representing the width of the core of the distribution is shown in the figures, as well as the relative improvement in the resolution with respect to jets after the global sequential calibration.

m_{bb} and other event quantities are used to train an MVA S to B discriminant, which is used for limits.

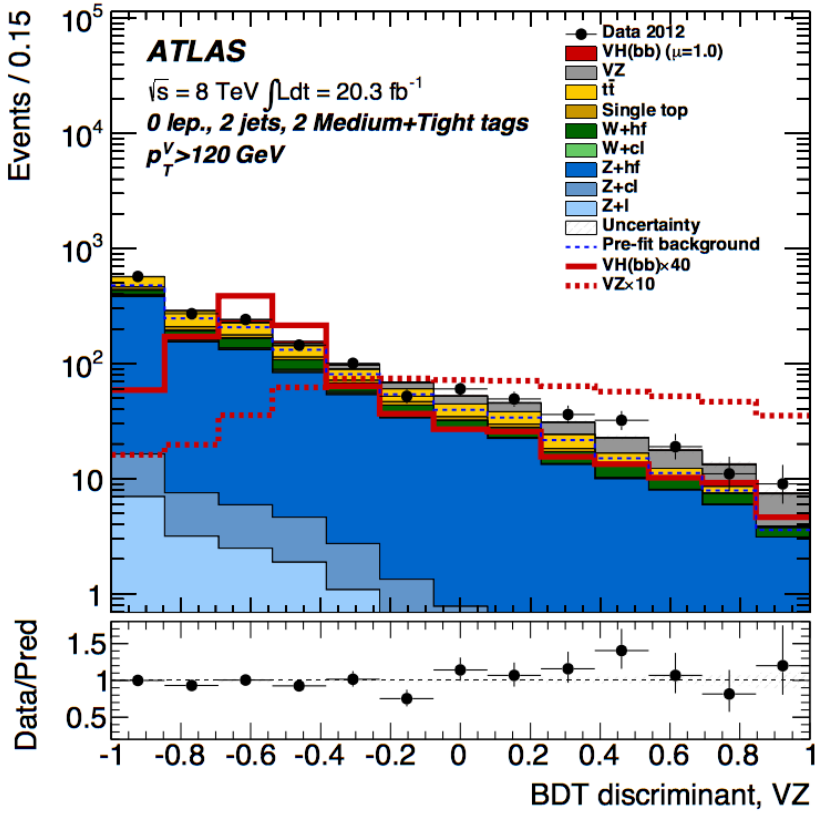

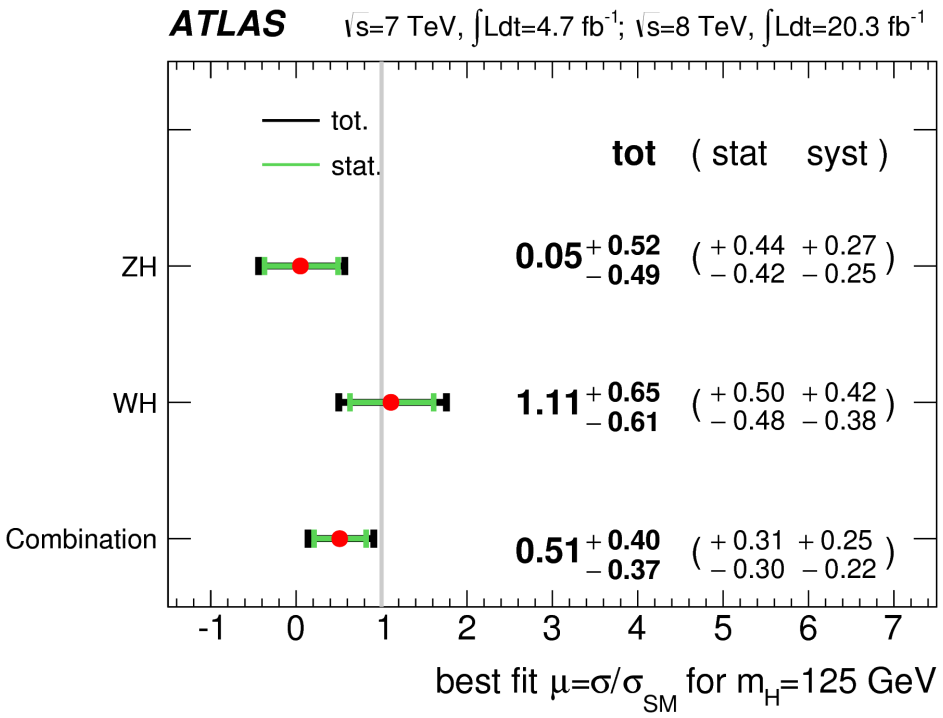

BDT trained for each lepton category.

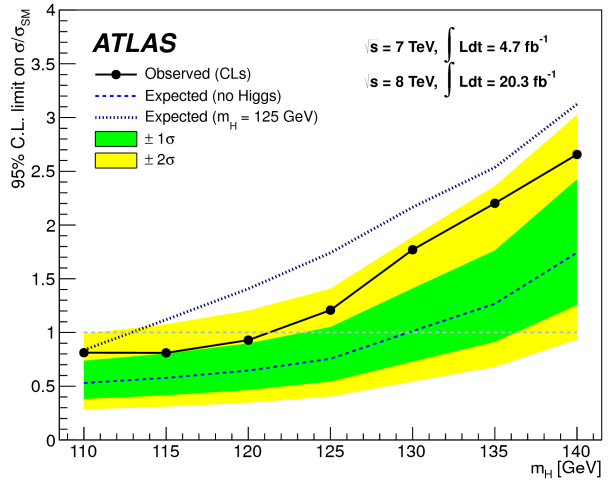

Signal strength consistent with one.
Analysis statistically limited.

VH with H to WW channel.
It reveals the tree-level H to V coupling strength.

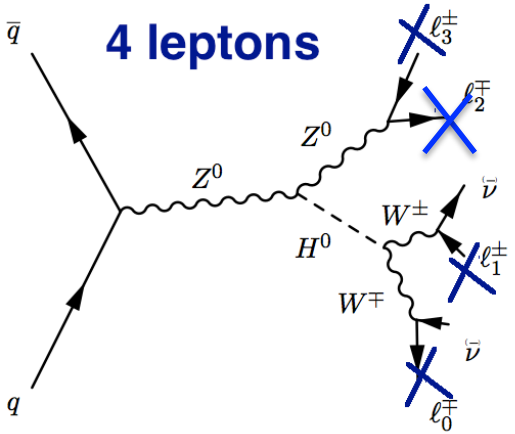

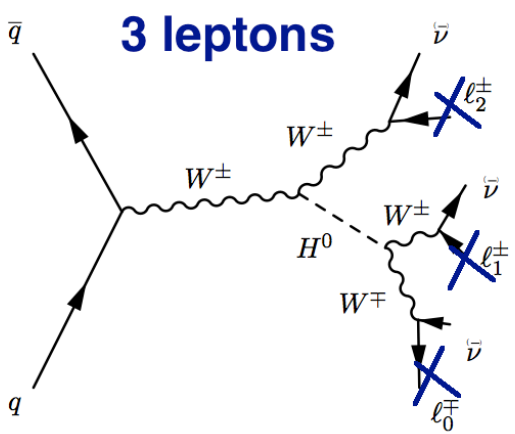

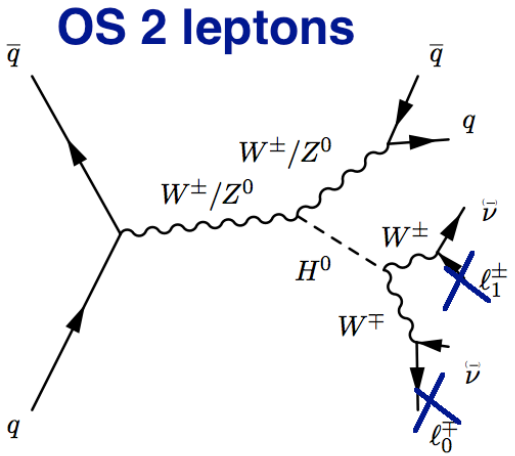

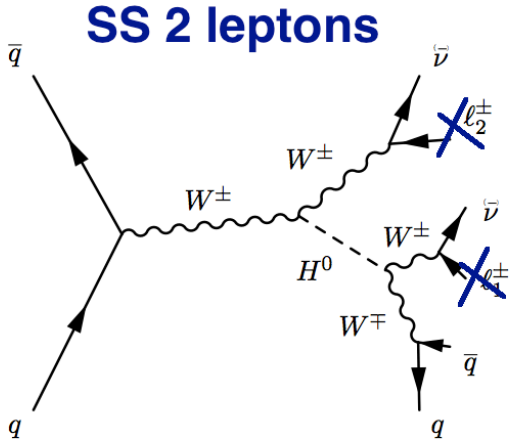

Event selection is optimised for each category based on lepton multiplicity and electric charge.

ATLAS VH H to WW event selection as a function of categories based on lepton multiplicity and charge.

Channel	4ℓ		3ℓ			2ℓ		
Category	2SFOS	1SFOS	3SF	1SFOS	0SFOS	DFOS	SS2jet	SS1jet
Trigger	single-lepton triggers		single-lepton triggers			single-lepton & dilepton triggers		
Num. of leptons	4	4	3	3	3	2	2	2
$p_{\mathrm{T,leptons}}$ [GeV]	$> 25, 20, 15$	$> 25, 20, 15$	> 15	> 15	> 15	$> 22, 15$	$> 22, 15$	$> 22, 15$
Total lepton charge	0	0	± 1	± 1	± 1	0	± 2	± 2
Num. of SFOS pairs	2	1	2	1	0	0	0	0
Num. of jets	≤ 1	≤ 1	≤ 1	≤ 1	≤ 1	≥ 2	2	1
$p_{\mathrm{T,jets}}$ [GeV]	> 25 (30)	> 25 (30)	> 25 (30)	> 25 (30)	> 25 (30)	> 25 (30)	> 25 (30)	> 25 (30)
Num. of b-tagged jets	0	0	0	0	0	0	0	0
$E_{\mathrm{T}}^{\mathrm{miss}}$ [GeV]	> 20	> 20	> 30	> 30	—	> 20	> 50	> 45
$p_{\mathrm{T}}^{\mathrm{miss}}$ [GeV]	> 15	> 15	> 20	> 20	—	—	—	—
$\lvert m_{\ell\ell} - m_Z \rvert$ [GeV]	< 10 ($m_{\ell_2\ell_3}$)	< 10 ($m_{\ell_2\ell_3}$)	> 25	> 25	—	—	> 15	> 15
Min. $m_{\ell\ell}$ [GeV]	> 10 ($m_{\ell_0\ell_1}$)	> 10 ($m_{\ell_0\ell_1}$)	> 12	> 12	> 6	> 10	> 12 ($ee, \mu\mu$) > 10 ($e\mu$)	> 12 ($ee, \mu\mu$) > 10 ($e\mu$)
Max. $m_{\ell\ell}$ [GeV]	< 65 ($m_{\ell_0\ell_1}$)	< 65 ($m_{\ell_0\ell_1}$)	< 200	< 200	< 200	< 50	—	—
$m_{4\ell}$ [GeV]	> 140	—	—	—	—	—	—	—
$p_{\mathrm{T},4\ell}$ [GeV]	> 30	—	—	—	—	—	—	—
$m_{\tau\tau}$ [GeV]	—	—	—	—	—	$< (m_Z - 25)$	—	—
$\Delta R_{\ell_0\ell_1}$	—	—	< 2.0	< 2.0	—	—	—	—
$\Delta\phi_{\ell_0\ell_1}$ [rad]	< 2.5 ($\Delta\phi_{\ell_0\ell_1}^{\mathrm{boost}}$)	< 2.5 ($\Delta\phi_{\ell_0\ell_1}^{\mathrm{boost}}$)	—	—	—	< 1.8	—	—
m_{T} [GeV]	—	—	—	—	—	< 125	—	> 105 ($m_{\mathrm{T}}^{\mathrm{lead}}$)
Min. $m_{\ell_i j(j)}$ [GeV]	—	—	—	—	—	—	< 115	< 70
Min. $\phi_{\ell_i j}$ [rad]	—	—	—	—	—	—	< 1.5	< 1.5
Δy_{jj}	—	—	—	—	—	< 1.2	—	—
$\lvert m_{jj} - 85 \rvert$ [GeV]	—	—	—	—	—	< 15	—	—

There is an excess observed of 2.5σ while 0.9σ is expected. The signal strength is $\mu = 3.0^{+1.3}_{-1.1}{}^{+1.0}_{-0.7}$.

Category	Signal significance Z_0 Exp. Z_0	Obs. Z_0	Obs. Z_0	Observed signal strength μ μ	Tot. err. +	Tot. err. −	Syst. err. +	Syst. err. −	μ
ggF	4.4	4.2		**0.98**	0.29	0.26	0.22	0.18	
VBF	2.6	3.2		**1.28**	0.55	0.47	0.32	0.25	
VH	0.93	2.5		**3.0**	1.6	1.3	0.95	0.65	
WH only	0.77	1.4		**2.1**	1.9	1.6	1.2	0.79	
ZH only	0.30	2.0		**5.1**	4.3	3.1	1.9	0.89	
ggF+VBF+VH	5.9	6.5		**1.16**	0.24	0.21	0.18	0.15	

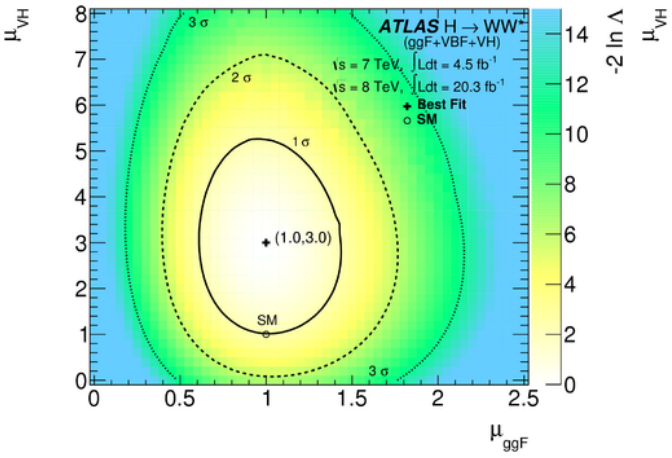

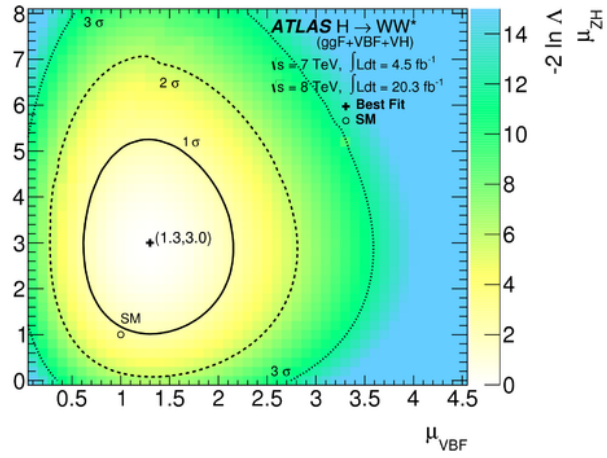

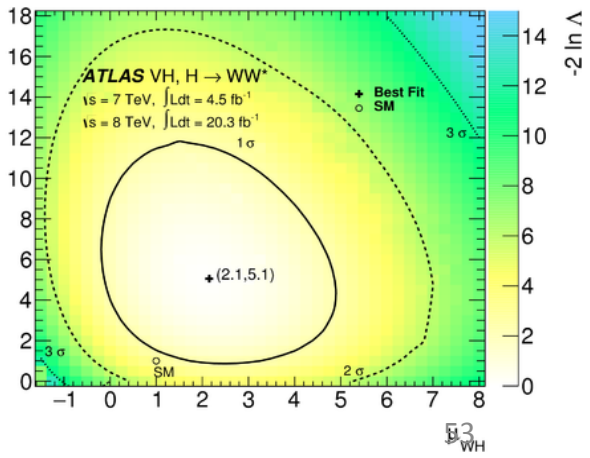

First direct observation of Higgs decay into fermion pair. Significance: 4.5 (3.4) for observed (expected).

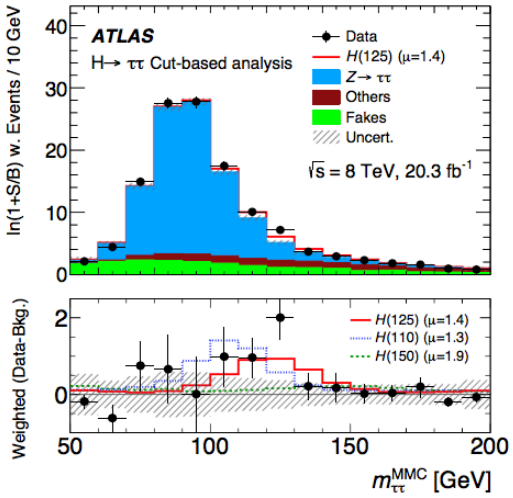

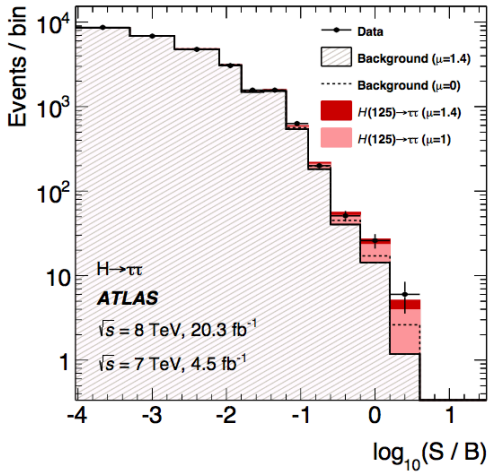

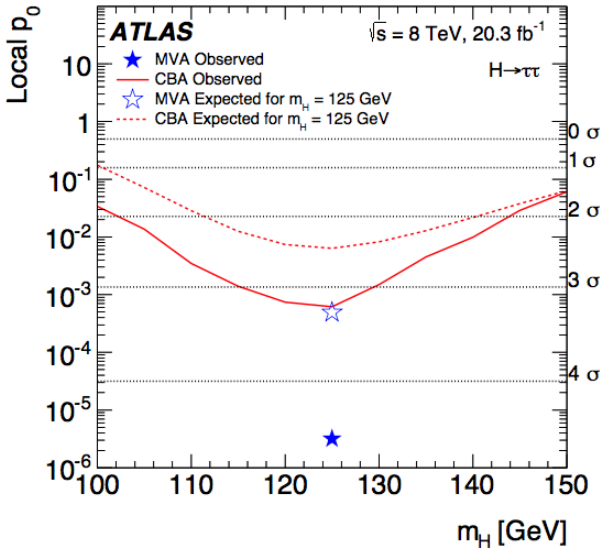

There are many many H to ττ final states.

gg+VBF	ee, eμ, μμ, $e\tau_{had}$, $\mu\tau_{had}$ and $\tau_{had}\tau_{had}$
WH	$e\mu\tau_{had}$, $\mu\tau_{had}\tau_{had}$ and $e\tau_{had}\tau_{had}$
ZH	$\mu\mu\mu\tau_{had}$, $eee\tau_{had}$, $\mu\mu\tau_{had}\tau_{had}$ and $ee\tau_{had}\tau_{had}$

Two categories: VBF and ggF (boosted).
For VBF the following list: 2 jets,
$pT_{j1} > 50$ GeV,
$pT_{j2} > 30$ GeV,
$|\Delta\eta(j1,j2)|$ is large

First direct observation of Higgs decay into fermion pair. Significance: 4.5 (3.4) for observed (expected).

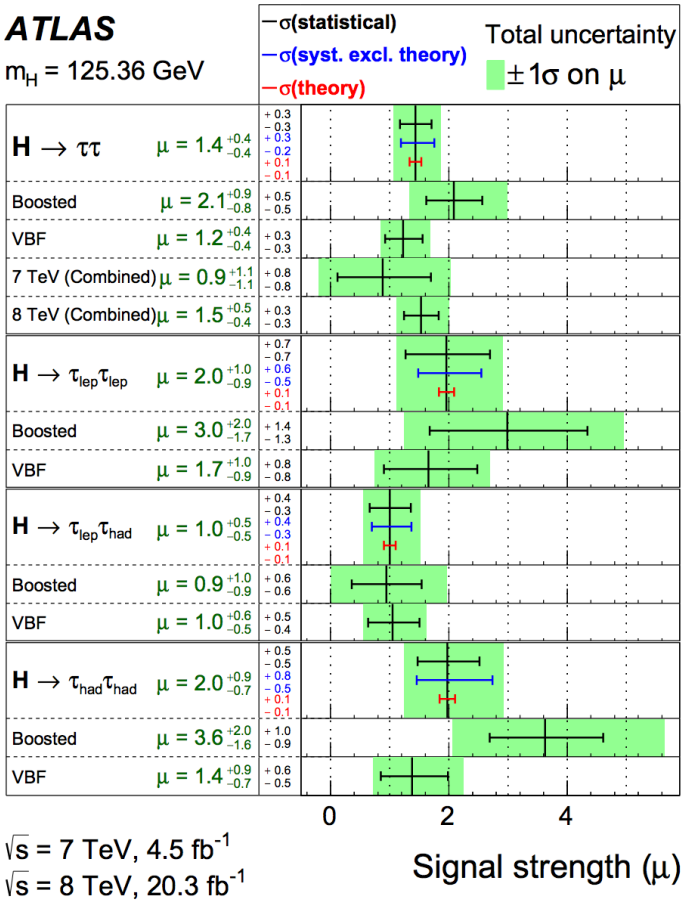

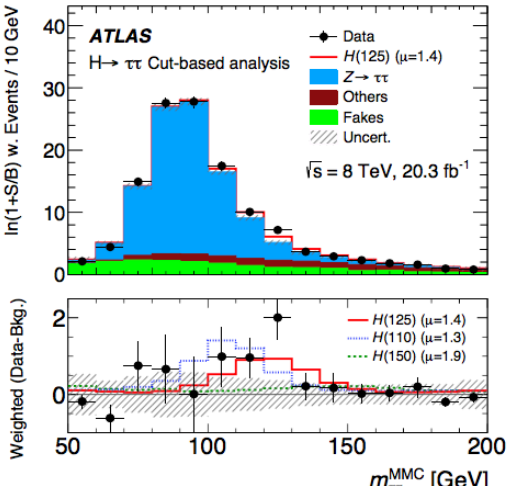

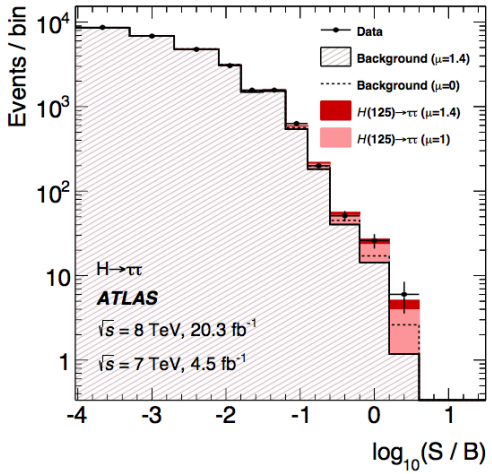

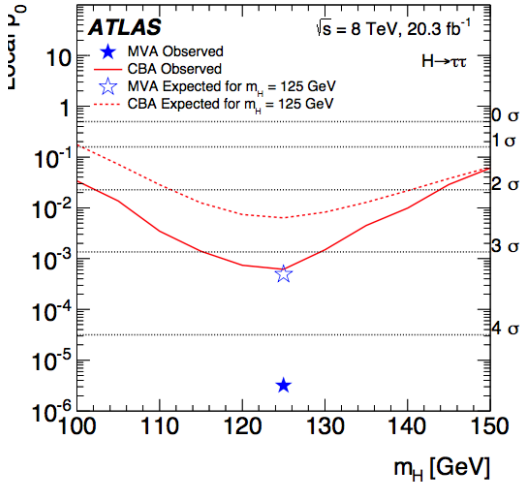

ATLAS μ=1.4+/- 0.4

gg+VBF ee, eμ, μμ, $e\tau_{had}$, $\mu\tau_{had}$ and $\tau_{had}\tau_{had}$

Two categories: VBF and ggF (boosted).

The new ATLAS VH H to ττ result is μ=2.3+/-1.6.

newly made public

WH $e\mu\tau_{had}$, $\mu\tau_{had}\tau_{had}$ and $e\tau_{had}\tau_{had}$

ZH $\mu\mu\mu\tau_{had}$, $eee\tau_{had}$, $\mu\mu\tau_{had}\tau_{had}$ and $ee\tau_{had}\tau_{had}$

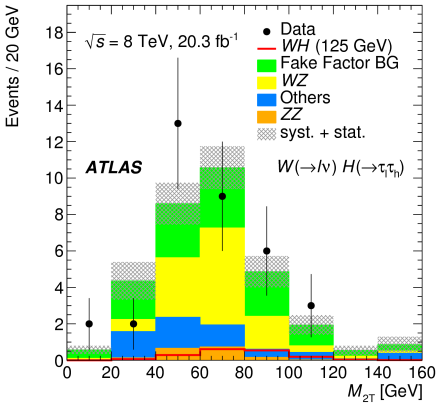

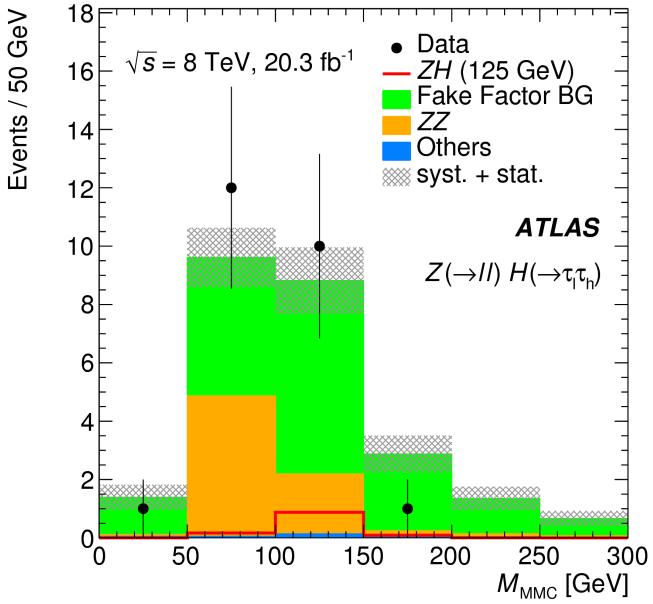

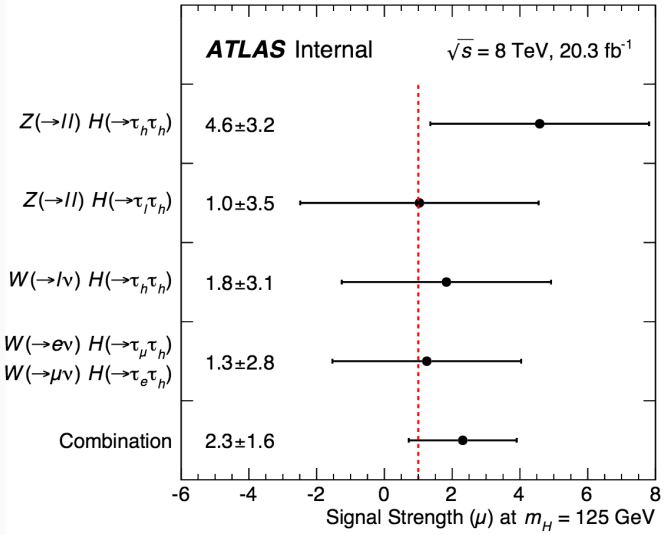

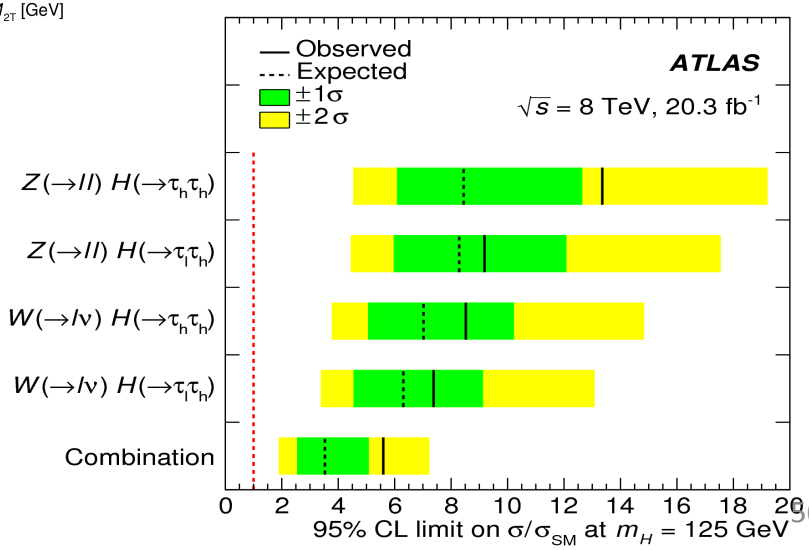

Heavy di-boson resonances (1). Combination of X->WW, X->WZ, X->ZZ.

[Submitted to JHEP: arXiv:1606.04833]

13 TeV limits improved upon 8 TeV ones.
One hadronic channes: qqqq.
Three semileptonic channels: vvqq, lvqq, llqq.
Only boosted R=1.0 jets used.

Three signal models:

1. Scalar (heavy, CP-even scalar singlet)
2. HVT (heavy vector boson triplet),
3. RSG* (bulk Randall-Sundrum Graviton, spin 2

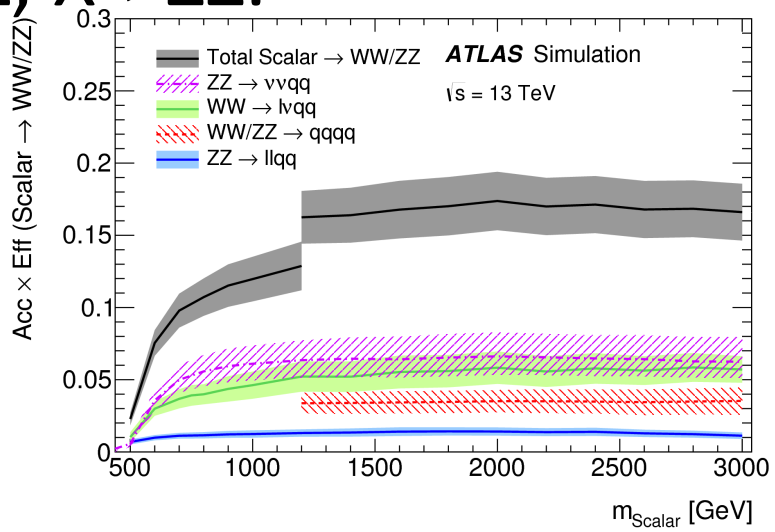

Selection level	Channel			
	$qqqq$	$\nu\nu qq$	$\ell\nu qq$	$\ell\ell qq$
Trigger	Large-R jet, $p_{\mathrm{T}} > 360$ GeV	$E_{\mathrm{T}}^{\mathrm{miss}}$	$E_{\mathrm{T}}^{\mathrm{miss}}(\mu\nu qq)$ or single electron $(e\nu qq)$	single electron or muon
Large-R jet	≥ 2, $N_{\mathrm{trk}} < 30$, $p_{\mathrm{T},J_1} > 450$ GeV, $p_{\mathrm{T},J_2} > 200$ GeV	≥ 1, $p_{\mathrm{T},J} > 200$ GeV		
Baseline leptons	0	0	≥ 1	≥ 2
Good leptons	0	0	1 medium μ or tight† e	2 e or 2 μ, loose + medium
Topology	$E_{\mathrm{T}}^{\mathrm{miss}} < 250$ GeV, $\lvert y_{J_1} - y_{J_2}\rvert < 1.2$, $\frac{p_{\mathrm{T},J_1} - p_{\mathrm{T},J_2}}{p_{\mathrm{T},J_1} + p_{\mathrm{T},J_2}} < 0.15$	$E_{\mathrm{T}}^{\mathrm{miss}} > 250$ GeV, $p_{\mathrm{T}}^{\mathrm{miss}} > 30$ GeV, $\lvert\Delta\phi(\mathbf{E}_{\mathrm{T}}^{\mathrm{miss}}, p_{\mathrm{T}}^{\mathrm{miss}})\rvert < \frac{\pi}{2}$, $\lvert\Delta\phi(\mathbf{E}_{\mathrm{T}}^{\mathrm{miss}}, j)\rvert > 0.6$	no b-jet with $\Delta R(j, J) < 1.0$, $E_{\mathrm{T}}^{\mathrm{miss}} > 100$ GeV, $p_{\mathrm{T},\ell\nu} > 200$ GeV, $p_{\mathrm{T},J}/m_{\ell\nu J} > 0.4$, $p_{\mathrm{T},\ell\nu}/m_{\ell\nu J} > 0.4$	$p_{\mathrm{T},J}/m_{\ell\ell J} > 0.4$, $p_{\mathrm{T},\ell\ell}/m_{\ell\ell J} > 0.4$, $83 < m_{ee}/\,\mathrm{GeV} < 99$, $66 < m_{\mu\mu}/\,\mathrm{GeV} < 116$
Discriminant	m_{JJ}	m_{T}	$m_{\ell\nu J}$	$m_{\ell\ell J}$

† The electron, if over 300 GeV in p_{T}, need only be medium.

Heavy di-boson resonances (2) for three signals: scalar, HVT, RSG*.

[Submitted to JHEP: arXiv:1606.04833]

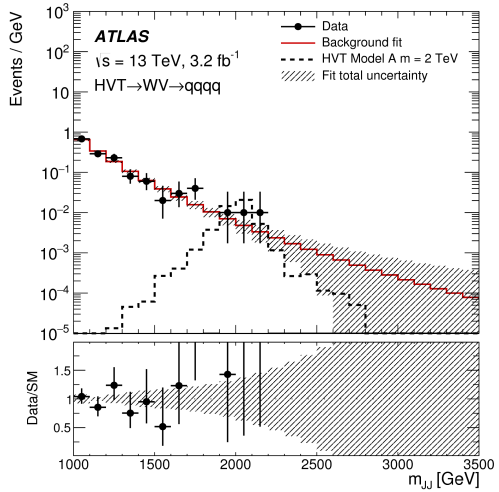

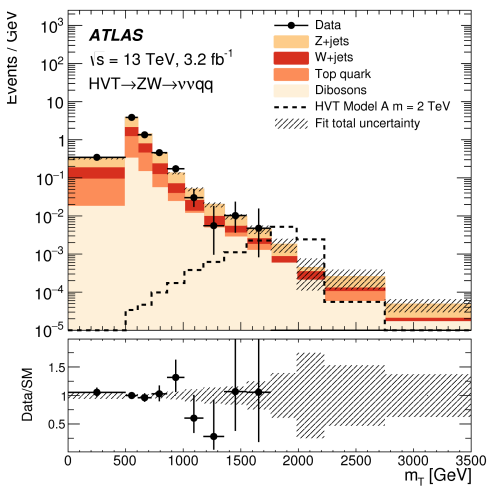

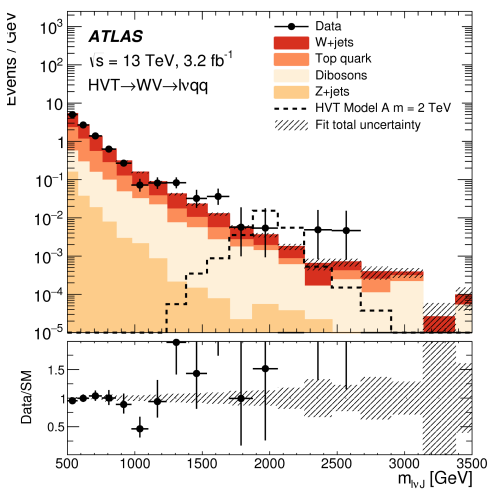

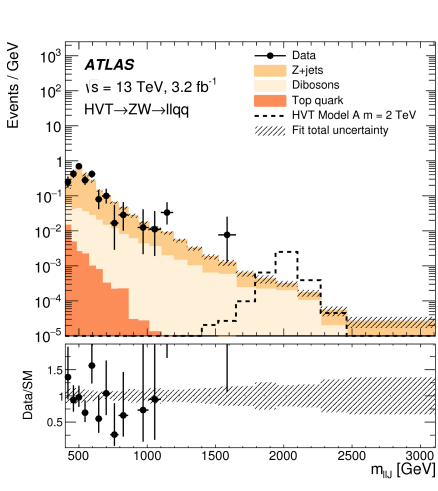

No excess of data above background found. 95% C.L. lower limits were set on m_X for Scalar, HVT and RSG* as 2650, 2600 and 1100 GeV, respectively.

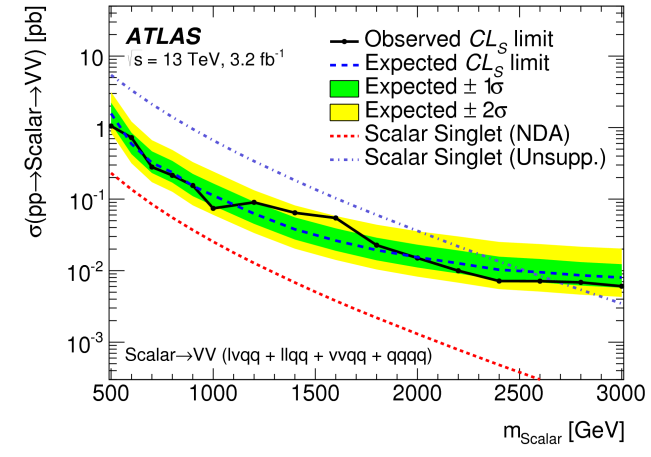

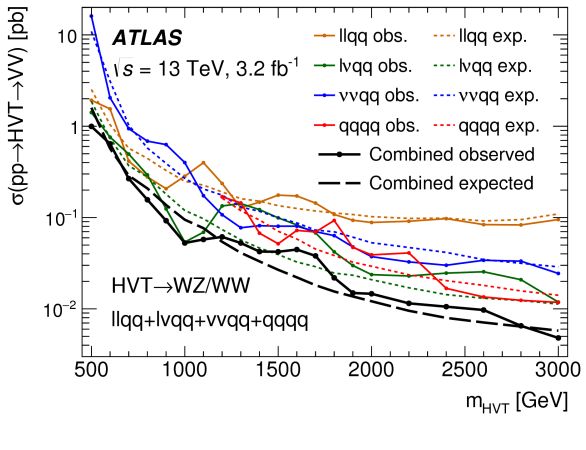

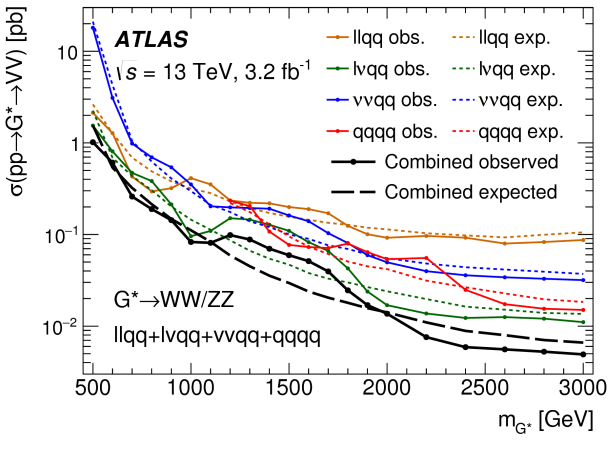

Di-photon resonances.
An excess at 750 GeV with 50 GeV width is seen.

[Submitted to JHEP
arXiv:1606.03833]

Clean experimental signature.
Excellent invariant mass resolution.
Moderate background.

Two types of signal searched:
spin-2 particle, RSG*, for $m_X > 500$ GeV.
spin-0 particle, SM-Higgs like, for $m_X > 200$ GeV.

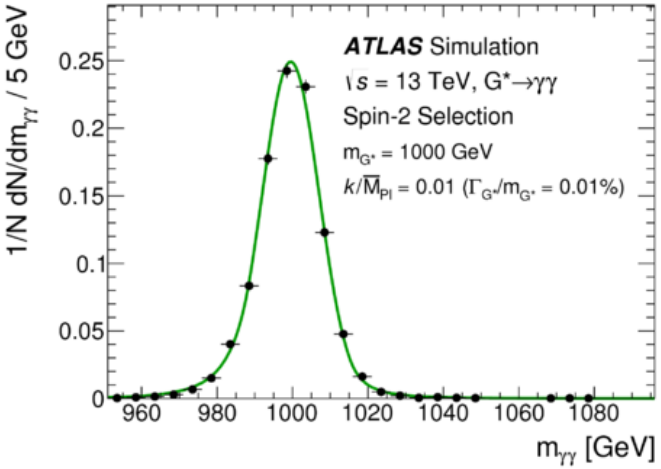

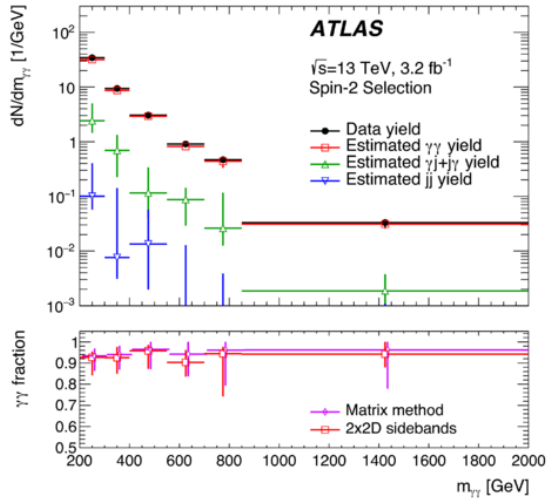

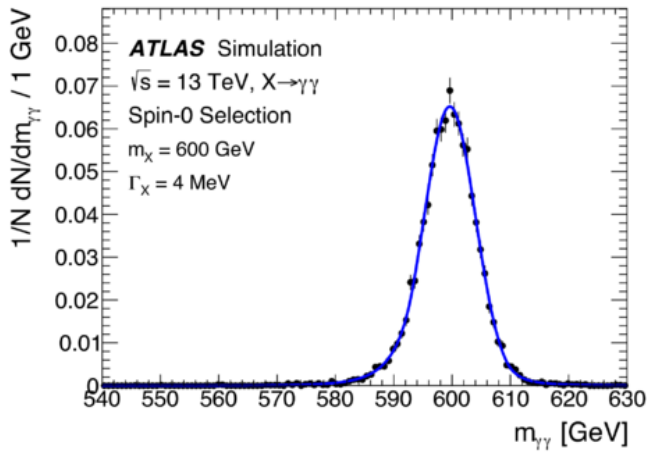

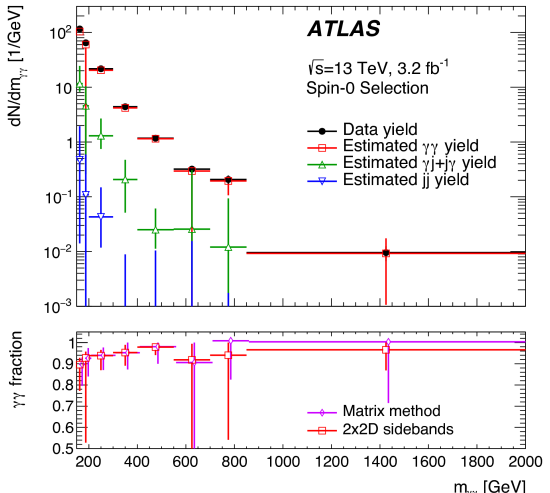

Looser
kinematic properties
for spin 2

Excess at 750 GeV with width 50 GeV seen in Run II, but not at all in reanalysed Run II data.

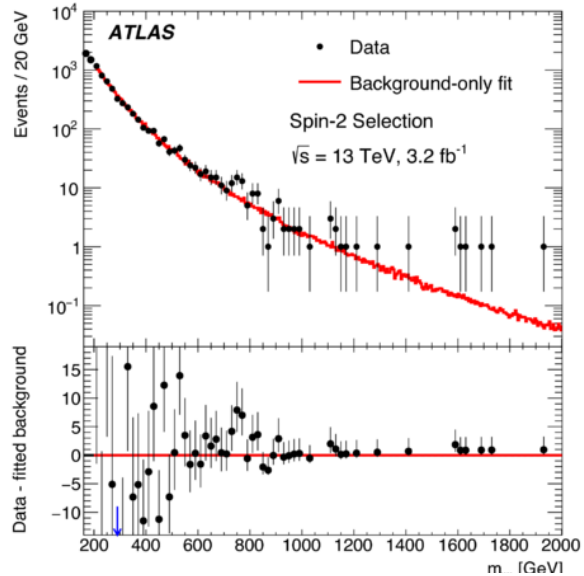

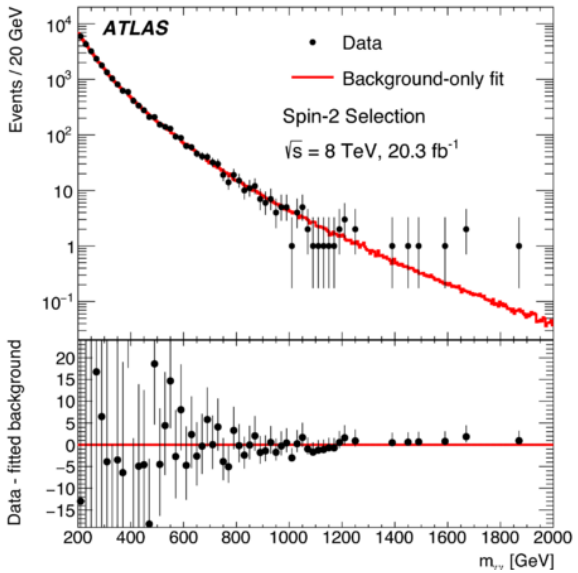

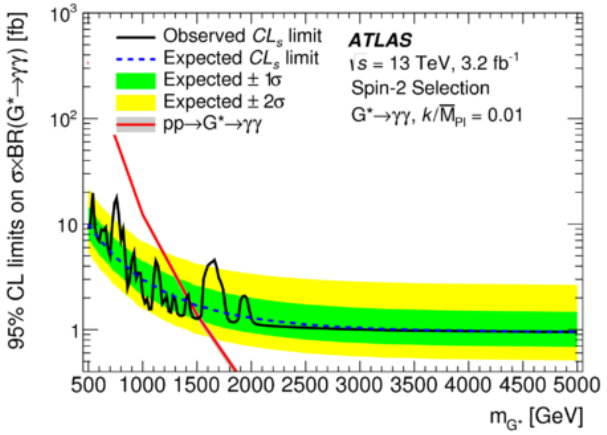

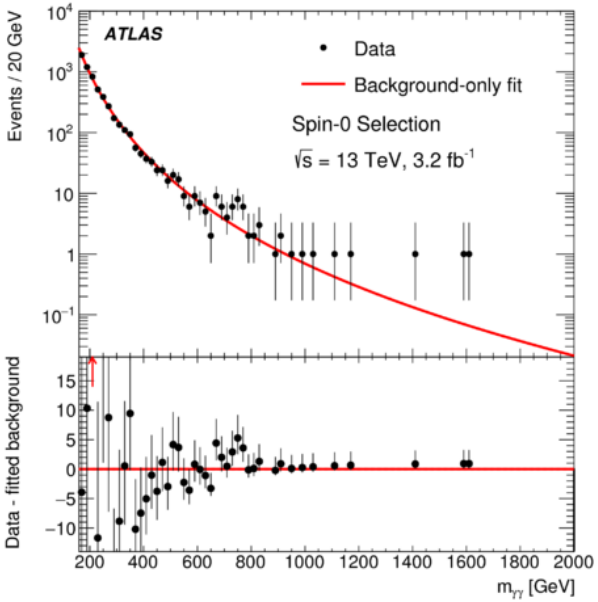

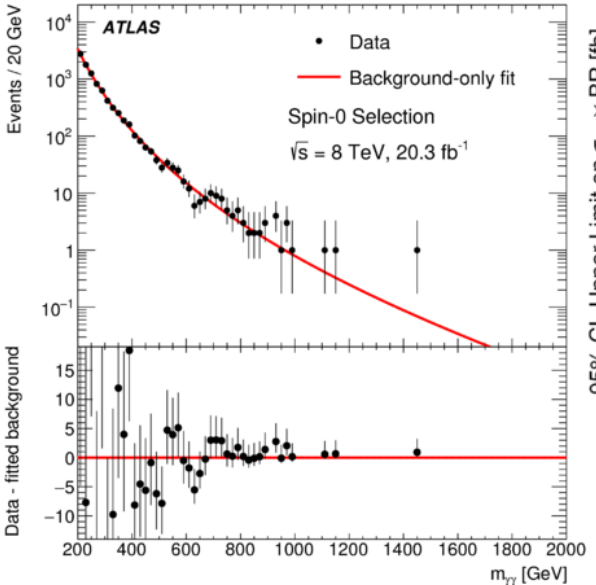

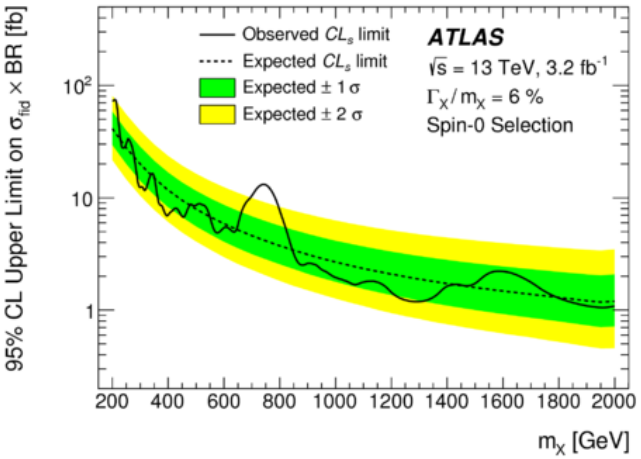

Di-photon event display with mass around 750 GeV.

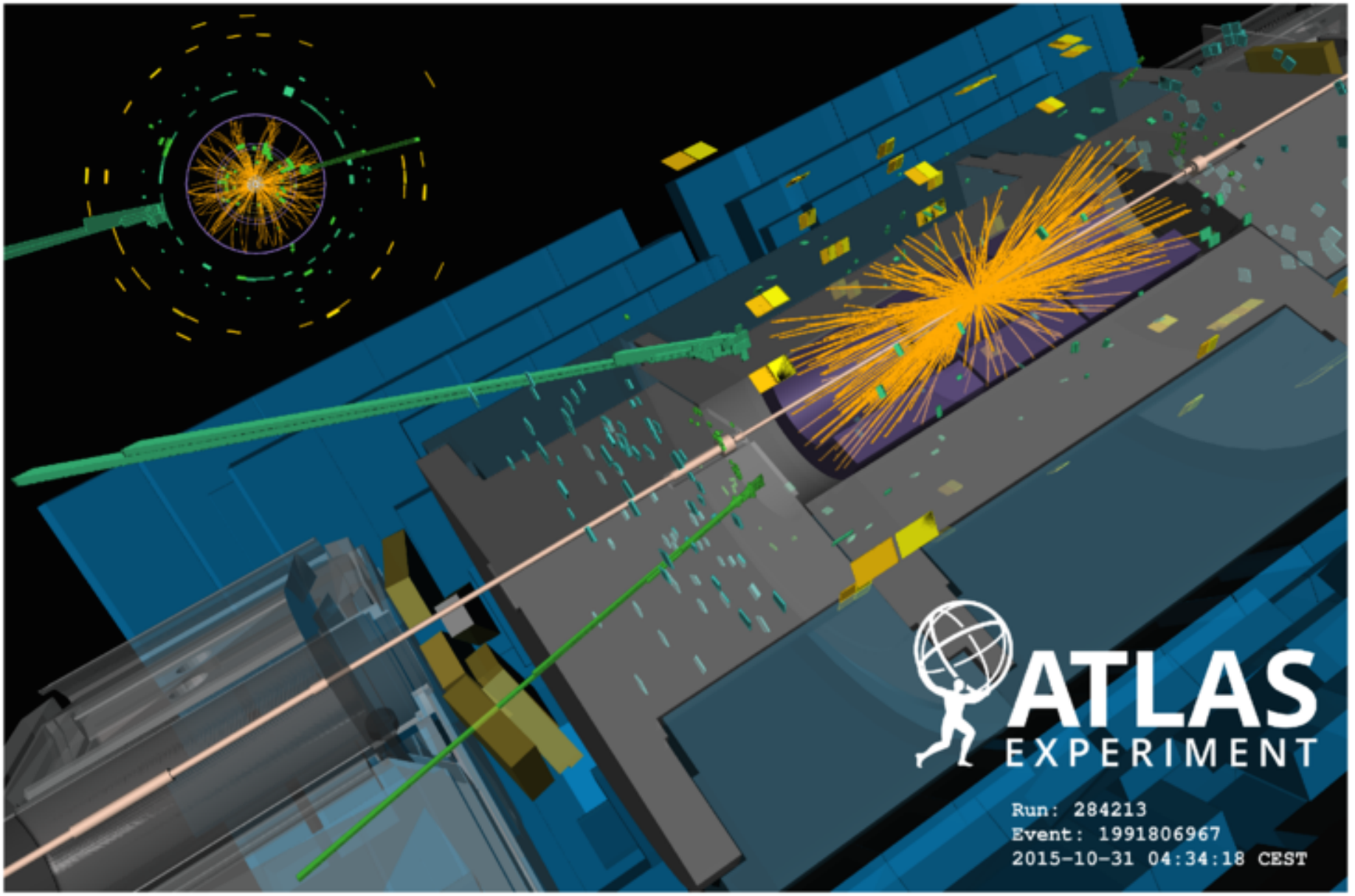

Di-photon resonance search details.

Investigated signal region	Background from MC extrapolation	Background from functional form
$m = 750$ GeV, $\Gamma/m = 6\%$		
720–780 GeV, spin-2 selection	$20.1 \pm 0.3 \pm 0.7$	$21.9 \pm 1.2 \pm 0.4$
720–780 GeV, spin-0 selection	$6.7 \pm 0.1 \pm 0.4$	$6.8 \pm 0.7 \pm 0.3$
$m = 1500$ GeV, $\Gamma/m = 6\%$		
1440–1560 GeV, spin-2 selection	$1.14 \pm 0.02 \pm 0.09$	$1.51 \pm 0.27 \pm 0.08$
1440–1560 GeV, spin-0 selection	$0.32 \pm 0.01 \pm 0.04$	$0.33 \pm 0.11 \pm 0.04$

	Spin-2 Selection		Spin-0 Selection	
	Free width	Narrow width	Free width	Narrow width
	13 TeV			
Mass for the largest excess	750 GeV	770 GeV	750 GeV	750 GeV
Width over mass for the largest excess	8%	-	6%	-
Local significance	3.8	3.3	3.9	2.9
Global significance	2.1		2.1	
	8 TeV			
Local significance (at 13 TeV best-fit)	-		1.9	
	8 TeV - 13 TeV Compatibility			
Gluon–gluon scaling (4.7)	2.7	2.2	1.2	1.5
Quark–antiquark scaling (2.7)	3.3	2.4	2.1	2.0

VH and VBF production signatures reject most of the QCD jet background, especially needed for H to bb and H to ττ.

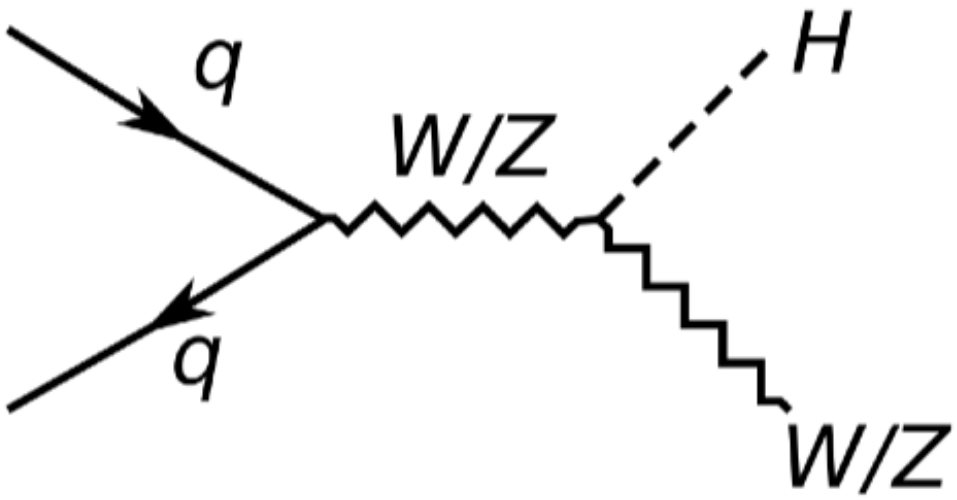

W or Z boson, decaying to leptons.

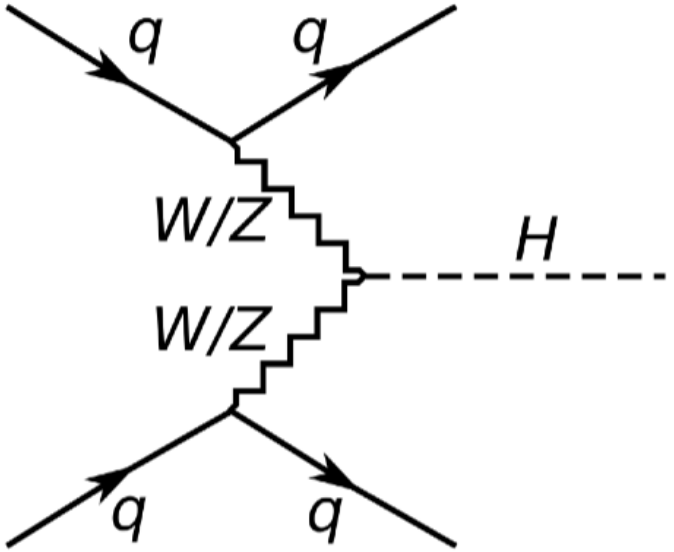

Two forward jets with
Large $|\Delta\eta|$ between them,
and large dijet invariant mass.

VH H to bb is expected to improve after 10 years of High Luminosity LHC L=3000fb^{-1} & μ=140.

		One-lepton	Two-lepton	One+Two-lepton
Stat-only	Significance	7.7	7.5	10.7
	$\hat{\mu}_{\text{Stats}}$ error	+0.13 −0.13	+0.14 −0.13	+0.09 −0.09
Theory-only	$\hat{\mu}_{\text{Theory}}$ error	+0.09 −0.07	+0.07 −0.08	+0.07 −0.07
Scenario I	Significance	1.8	5.6	5.9
	$\hat{\mu}_{\text{w/Theory}}$ error	+0.56 −0.54	+0.20 −0.19	+0.19 −0.19
	$\hat{\mu}_{\text{wo/Theory}}$ error	+0.54 −0.54	+0.18 −0.18	+0.18 −0.17
Scenario II	Significance	3.2	-	6.4
	$\hat{\mu}_{\text{w/Theory}}$ error	+0.33 −0.32	-	+0.18 −0.17
	$\hat{\mu}_{\text{wo/Theory}}$ error	+0.32 −0.32	-	+0.16 −0.16

CERN-LHCC-2015-020; CERN-LHCC-2015-10

ATLAS VH H to bb generators

Process	Generator
Signal$^{(\star)}$	
$q\bar{q} \to ZH \to \nu\nu bb/\ell\ell bb$	PYTHIA8
$gg \to ZH \to \nu\nu bb/\ell\ell bb$	POWHEG+PYTHIA8
$q\bar{q} \to WH \to \ell\nu bb$	PYTHIA8
Vector boson + jets	
$W \to \ell\nu$	SHERPA 1.4.1
$Z/\gamma* \to \ell\ell$	SHERPA 1.4.1
$Z \to \nu\nu$	SHERPA 1.4.1
Top-quark	
$t\bar{t}$	POWHEG+PYTHIA
t-channel	ACERMC+PYTHIA
s-channel	POWHEG+PYTHIA
Wt	POWHEG+PYTHIA
Diboson$^{(\star)}$	POWHEG+PYTHIA8
WW	POWHEG+PYTHIA8
WZ	POWHEG+PYTHIA8
ZZ	POWHEG+PYTHIA8

Table 1. The generators used for the simulation of the signal and background processes. ($\star$) For the analysis of the 7 TeV data, PYTHIA8 is used for the simulation of the $gg \to ZH$ process, and HERWIG for the simulation of diboson processes.

ATLAS VH bb systematics

Signal	
Cross section (scale)	1% ($q\bar{q}$), 50% (gg)
Cross section (PDF)	2.4% ($q\bar{q}$), 17% (gg)
Branching ratio	3.3 %
Acceptance (scale)	1.5%–3.3%
3-jet acceptance (scale)	3.3%–4.2%
p_{T}^{V} shape (scale)	S
Acceptance (PDF)	2%–5%
p_{T}^{V} shape (NLO EW correction)	S
Acceptance (parton shower)	8%–13%
Z+jets	
Zl normalisation, 3/2-jet ratio	5%
Zcl 3/2-jet ratio	26%
Z+hf 3/2-jet ratio	20%
Z+hf/Zbb ratio	12%
$\Delta\phi(\mathrm{jet}_1,\mathrm{jet}_2)$, p_{T}^{V}, m_{bb}	S
W+jets	
Wl normalisation, 3/2-jet ratio	10%
Wcl, W+hf 3/2-jet ratio	10%
Wbl/Wbb ratio	35%
Wbc/Wbb, Wcc/Wbb ratio	12%
$\Delta\phi(\mathrm{jet}_1,\mathrm{jet}_2)$, p_{T}^{V}, m_{bb}	S
$t\bar{t}$	
3/2-jet ratio	20%
High/low-p_{T}^{V} ratio	7.5%
Top-quark p_{T}, m_{bb}, $E_{\mathrm{T}}^{\mathrm{miss}}$	S
Single top	
Cross section	4% (s-,t-channel), 7% (Wt)
Acceptance (generator)	3%–52%
m_{bb}, $p_{\mathrm{T}}^{b_1}$	S
Diboson	
Cross section and acceptance (scale)	3%–29%
Cross section and acceptance (PDF)	2%–4%
m_{bb}	S
Multijet	
0-, 2-lepton channels normalisation	100%
1-lepton channel normalisation	2%–60%
Template variations, reweighting	S

Table 5. Summary of the systematic uncertainties on the signal and background modelling. An

ATLAS H to ττ systematics

Table 8. Impact of systematic uncertainties on the total signal, S, (sum of all production modes) and on the sum of all background estimates, B, for each of the three channels and the two signal categories for the analysis of the data taken at $\sqrt{s} = 8$ TeV. Each systematic uncertainty is assumed to be correlated across the analysis channels, except those marked with a *. Uncertainties that affect the shape of the BDT-output distribution in a non-negligible way are marked with a †. All values are given before the global fit. The notation UE/PS refers to the underlying event and parton shower modelling.

Source	Relative signal and background variations [%]											
	$\tau_{\text{lep}}\tau_{\text{lep}}$ VBF		$\tau_{\text{lep}}\tau_{\text{lep}}$ Boosted		$\tau_{\text{lep}}\tau_{\text{had}}$ VBF		$\tau_{\text{lep}}\tau_{\text{had}}$ Boosted		$\tau_{\text{had}}\tau_{\text{had}}$ VBF		$\tau_{\text{had}}\tau_{\text{had}}$ Boosted	
	S	B	S	B	S	B	S	B	S	B	S	B
Experimental												
Luminosity	±2.8	±0.1	±2.8	±0.1	±2.8	±0.1	±2.8	±0.1	±2.8	±0.1	±2.8	±0.1
Tau trigger*	–	–	–	–	–	–	–	–	$^{+7.7}_{-8.8}$	< 0.1	$^{+7.8}_{-8.9}$	< 0.1
Tau identification	–	–	–	–	±3.3	±1.2	±3.3	±1.8	±6.6	±3.8	±6.6	±5.1
Lepton ident. and trigger*	$^{+1.4}_{-2.1}$	$^{+1.3}_{-1.7}$	$^{+1.4}_{-2.1}$	$^{+1.1}_{-1.5}$	±1.8	±0.5	±1.8	± 0.8	–	–	–	–
b-tagging	±1.3	±1.6	±1.6	±1.6	< 0.1	±0.2	±0.4	±0.2	–	–	–	–
τ energy scale†	–	–	–	–	±2.4	±1.3	±2.4	±0.9	±2.9	±2.5	±2.9	±2.5
Jet energy scale and resolution†	$^{+8.5}_{-9.1}$	±9.2	$^{+4.7}_{-4.9}$	$^{+3.7}_{-3.0}$	$^{+9.5}_{-8.7}$	±1.0	±3.9	±0.4	$^{+10.1}_{-8.0}$	±0.3	$^{+5.1}_{-6.2}$	±0.2
$E_{\text{T}}^{\text{miss}}$ soft scale & resolution	$^{+0.0}_{-0.2}$	$^{+0.0}_{-1.2}$	$^{+0.0}_{-0.1}$	$^{+0.0}_{-1.2}$	$^{+0.8}_{-0.3}$	±0.2	±0.4	< 0.1	±0.5	±0.2	±0.1	< 0.1
Background Model												
Modelling of fake backgrounds*†	–	± 1.2	–	±1.2	–	±2.6	–	±2.6	–	±5.2	–	±0.6
Embedding†	–	$^{+3.8}_{-4.3}$	–	$^{+6.0}_{-6.5}$	–	±1.5	–	±1.2	–	±2.2	–	±3.3
$Z \to \ell\ell$ normalisation*	–	± 2.1	–	±0.7	–	–	–	–	–	–	–	–
Theoretical												
Higher-order QCD corrections†	$^{+11.3}_{-9.1}$	±0.2	$^{+19.8}_{-15.3}$	±0.2	$^{+9.7}_{-7.6}$	±0.2	$^{+19.3}_{-14.7}$	±0.2	$^{+10.7}_{-8.2}$	< 0.1	$^{+20.3}_{-15.4}$	< 0.1
UE/PS	± 1.8	< 0.1	± 5.9	< 0.1	±3.8	< 0.1	±2.9	< 0.1	±4.6	< 0.1	±3.8	< 0.1
Generator modelling	±2.3	< 0.1	±1.2	< 0.1	±2.7	< 0.1	±1.3	< 0.1	±2.4	< 0.1	±1.2	< 0.1
EW corrections	±1.1	< 0.1	±0.4	< 0.1	±1.3	< 0.1	±0.4	< 0.1	±1.1	< 0.1	±0.4	< 0.1
PDF†	$^{+4.5}_{-5.8}$	± 0.3	$^{+6.2}_{-8.0}$	± 0.2	$^{+3.9}_{-3.6}$	± 0.2	$^{+6.6}_{-6.1}$	± 0.2	$^{+4.3}_{-4.0}$	± 0.2	$^{+6.3}_{-5.8}$	± 0.1
BR ($H \to \tau\tau$)	± 5.7	–	±5.7	–	±5.7	–	±5.7	–	± 5.7	–	±5.7	–

It's easier to identify electrons and muons than jets originating from quarks.

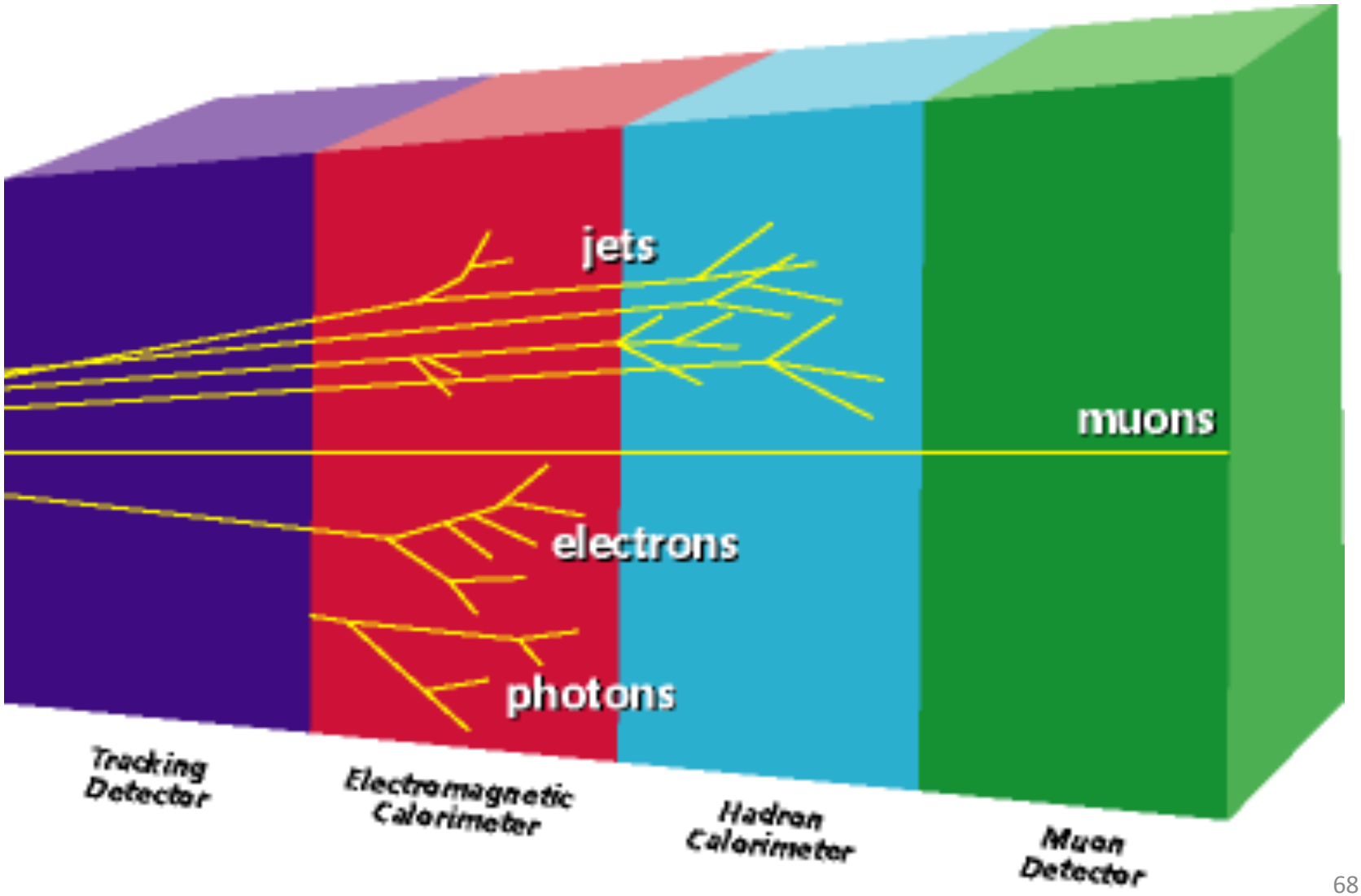

Main background processes have a W boson and jets.

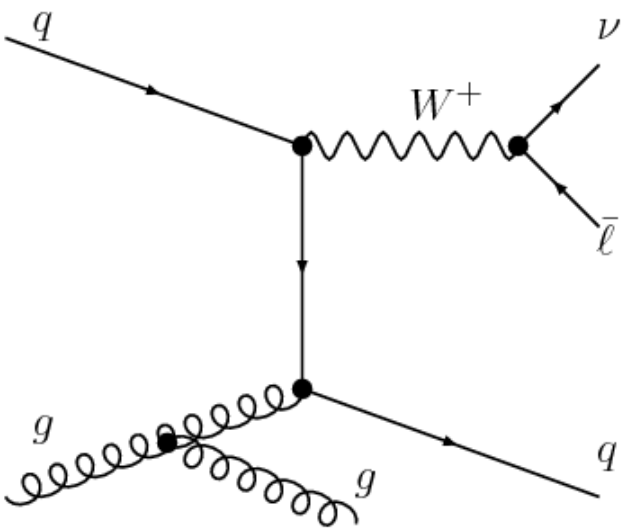

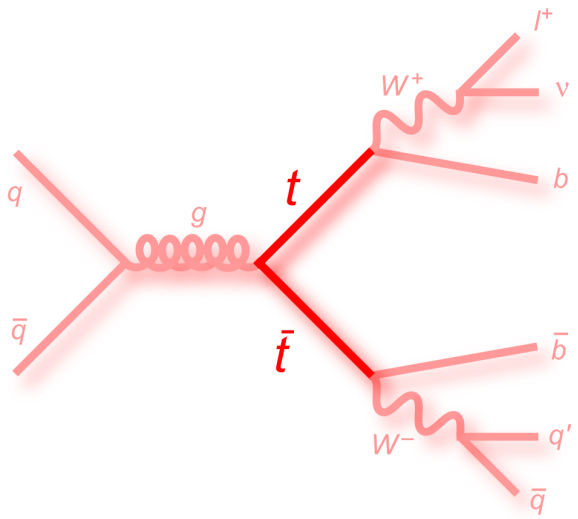

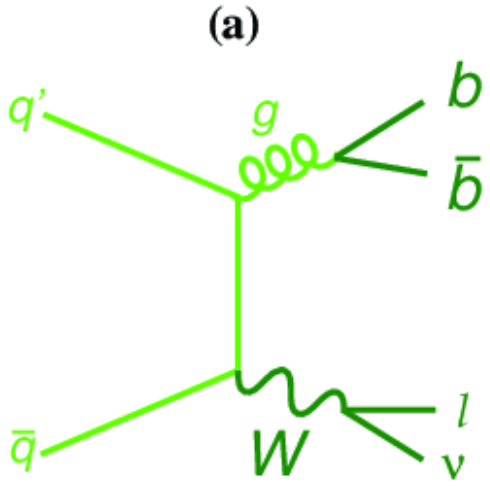

Reducible in time with more work on detector understanding
Different final state particles

Irreducible
Same final state particles

Invariant mass of the two b jets has
different shape between signal and backgrounds.

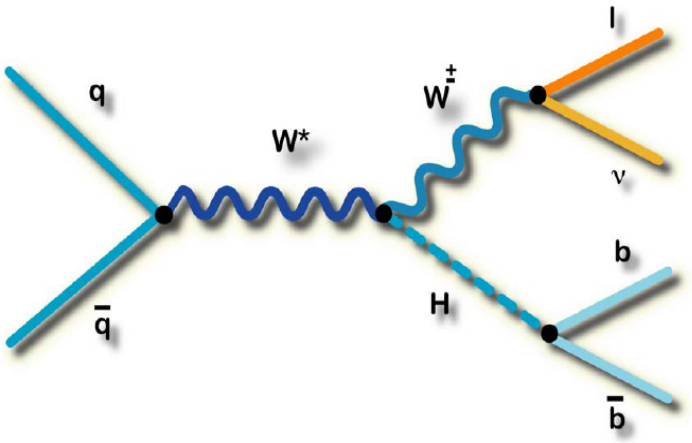

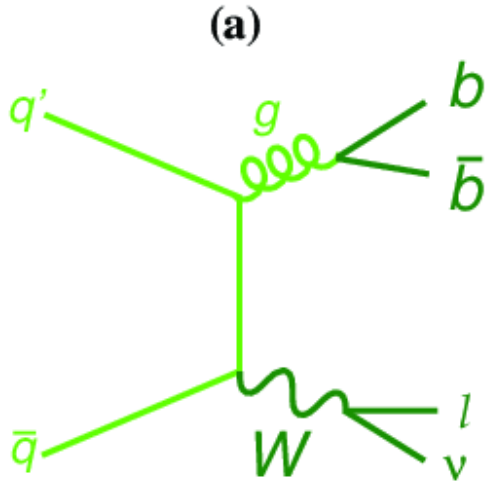

Higgs mass 125 GeV

gluon mass 0 GeV

We measure Higgs candidate mass better
by measuring jet energies better,
aka calibrating our detector better.

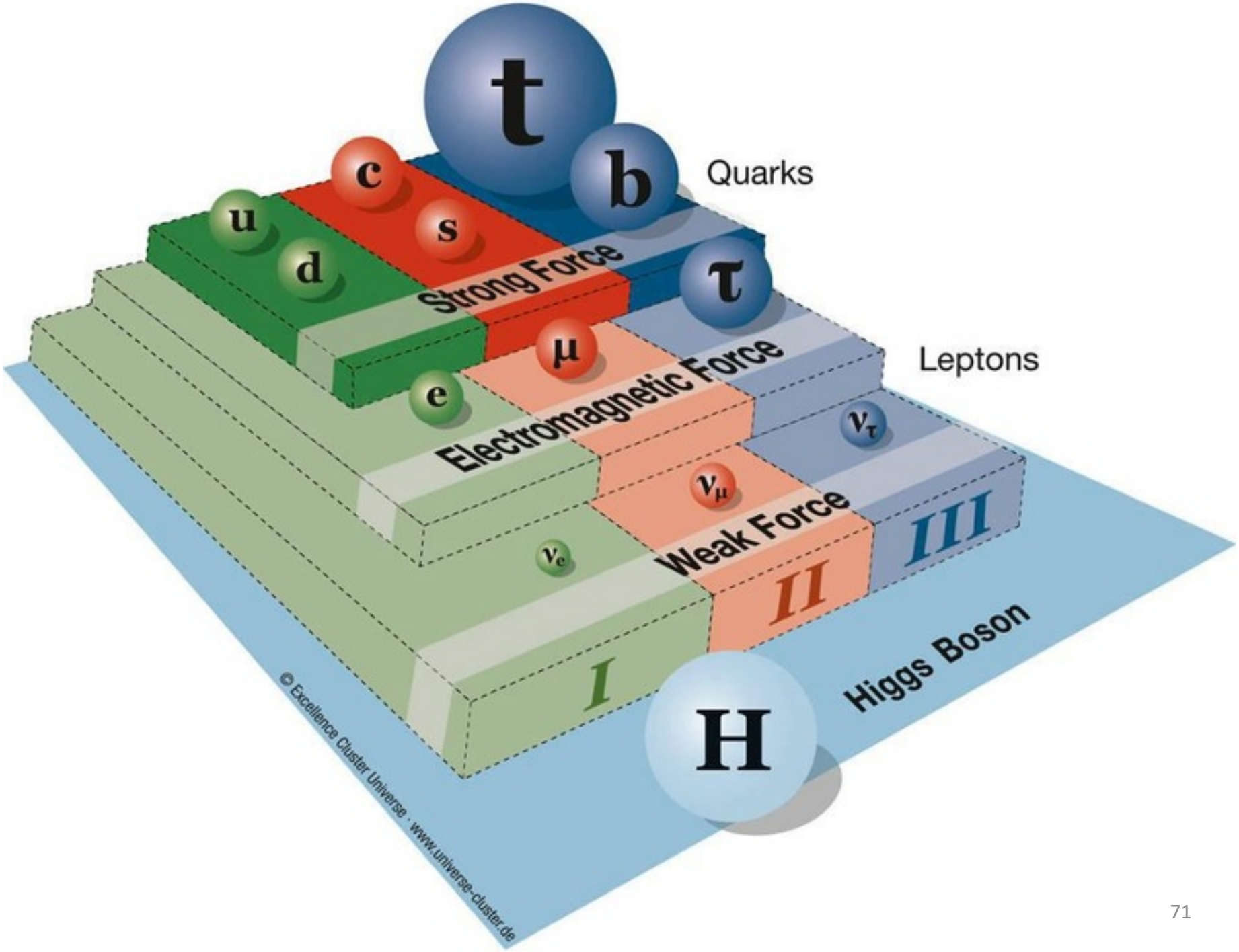
t
b
c
s
u
d
Quarks
Strong Force
τ
μ
e
Electromagnetic Force
Leptons
ν_τ
ν_μ
ν_e
Weak Force
III
II
I
H
Higgs Boson
© Excellence Cluster Universe · www.universe-cluster.de

Outline

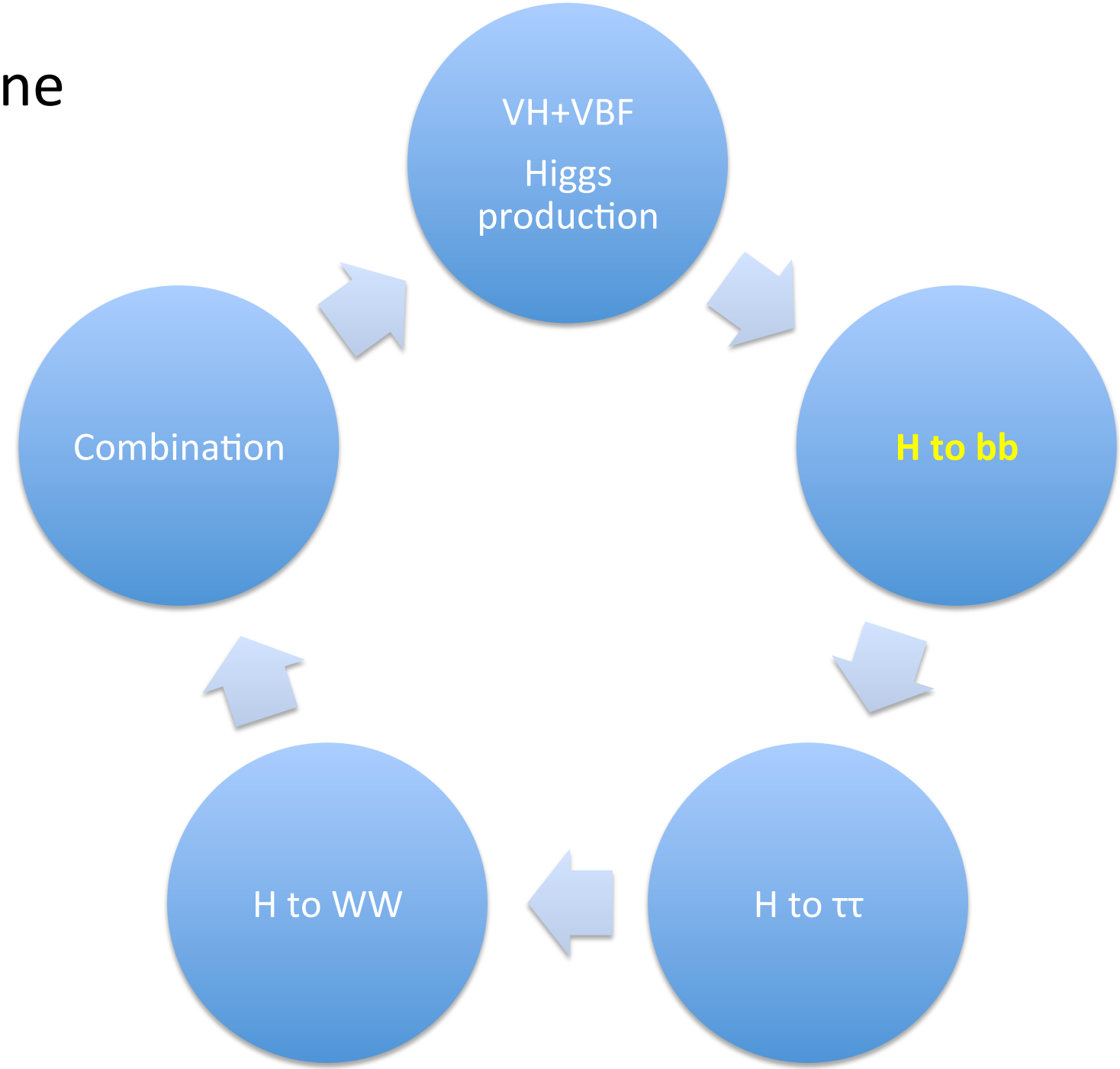

Higgs boson mass shift due to interferences in gg->H->ϒϒ at 8 TeV

[Public note 15 April 2016](#)
[ATL-PHYS-PUB-2016-009](#)

Mass of Higgs boson is key parameter to measure precisely.
8 TeV H->ϒϒ and H->ZZ*->4l measured with an 0.2% error, meaning 250 MeV.
The true mass value is shifted due to interferences of processes that have same initial and final state:

- Non-resonant background gg->ϒϒ
- Resonant Higgs production of gg->H->ϒϒ

Interference has two effects:

- Imaginary part reduced signal yield by 2%, but taken into account in current analysis.
- Real part induces a shift in mass, not taken into account and never evaluated before.

Result: Shift is of 35 MeV ± 9 MeV,
an order of magnitude below the experimental error of 250 MeV.

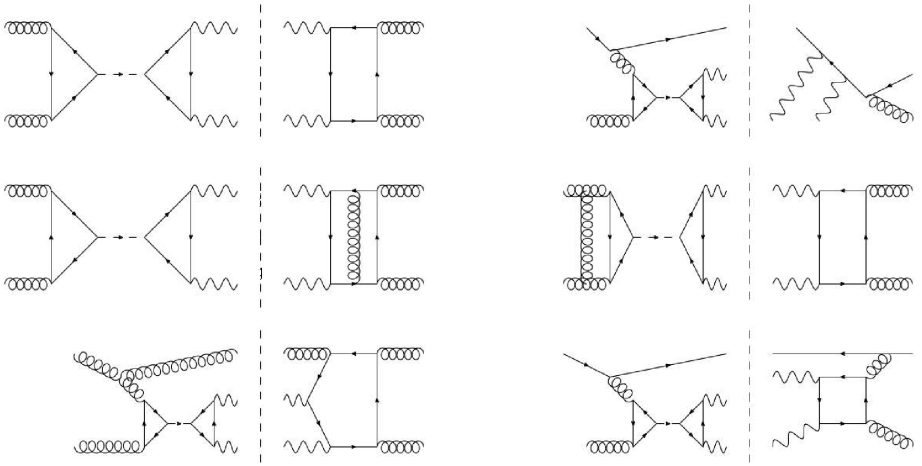

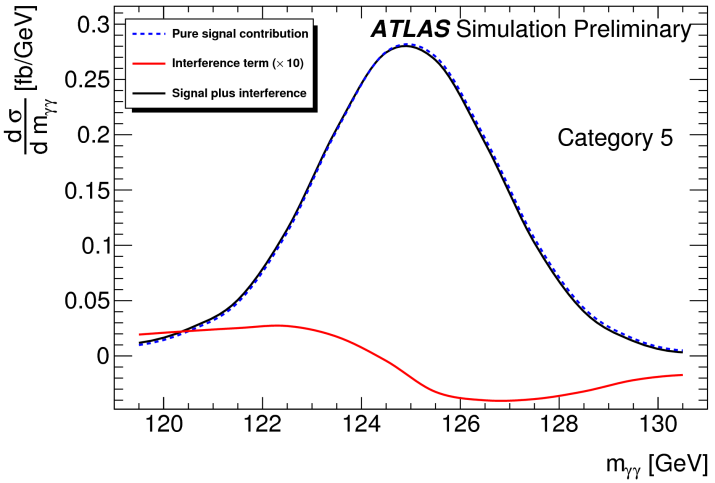

Higher order QCD correction for gg->H*->VV at 8 TeV

[Public note 29 Jan 2016](#)
[ATL-PHYS-PUB-2015-006](#)

Import to measure also off-shell strength of the Higgs boson.
Change k factor for unknown bkgs gg->ZZ, gg->WW for higher order QCD corrections.
Assumption of Higgs coupling independent of energy scale of Higgs production.
Compare LO generators with Sherpa+OpenLoops
A 20% difference is observed in the pT of the VV system
It affects both kinematic shapes and acceptance.
Suggestion: reweight LO generators to Sherpa+OpenLoops weights of the pT of VV system.

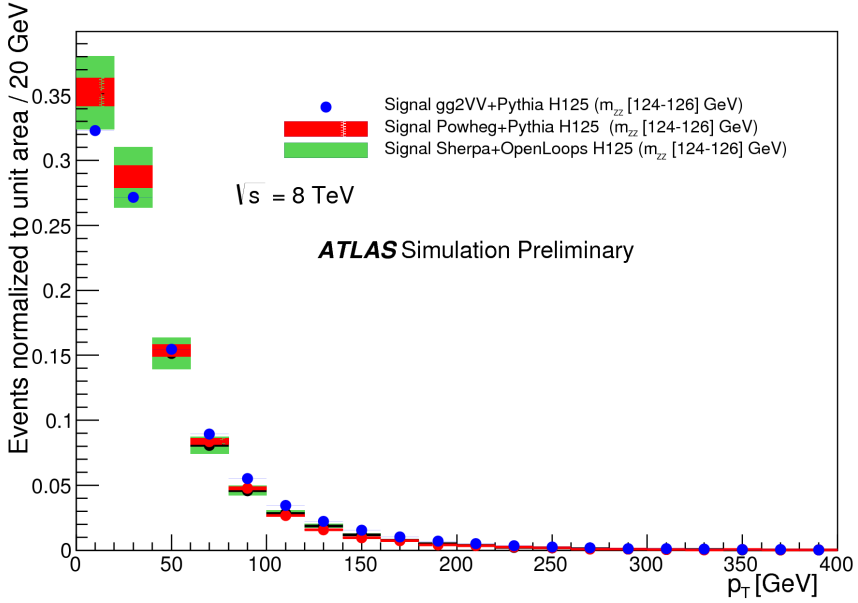

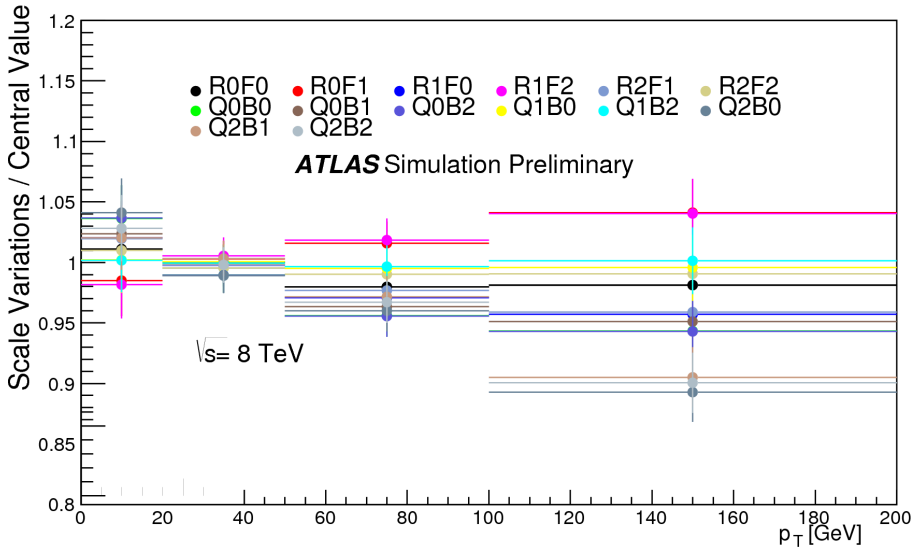

Prospects at HL-LHC for HH->bbττ.

[Public note 10 Nov 2015](#)
[ATL-PHYS-PUB-2015-046](#)

Higgs tri-linear coupling λ_{HHH}.
14 TeV, 3000 fb_{-1}, <μ>=140.
Three channels: $\tau_{lep}\tau_{lep}$ $\tau_{lep}\tau_{had}$ $\tau_{had}\tau_{had}$
Irreducible bkgs: Z(->ττ)+ jets and ttbar.
Cut and count analysis.
b-jet energy correction of TruthWZ to b Parton.
m_{bb} = [95-145] GeV
$M_{\tau\tau}$ = [80,158] GeV
Limit of 4 x SM can be achieved.
For BSM, we can exclude at 95% CL
$\lambda_{HHH}/\lambda_{SM}$ < -4 and $\lambda_{HHH}/\lambda_{SM}$ >= 12

Decay Channel	Branching Ratio	Total Yield (3000 fb^{-1})
$b\bar{b}+b\bar{b}$	33%	4.1×10^4
$b\bar{b}+W^+W^-$	25%	3.1×10^4
$b\bar{b}+\tau^+\tau^-$	7.4%	9.0×10^3
$W^+W^-+\tau^+\tau^-$	5.4%	6.6×10^3
$ZZ+b\bar{b}$	3.1%	3.8×10^3
$ZZ+W^+W^-$	1.2%	1.4×10^3
$\gamma\gamma+b\bar{b}$	0.3%	3.3×10^2
$\gamma\gamma+\gamma\gamma$	0.0010%	1

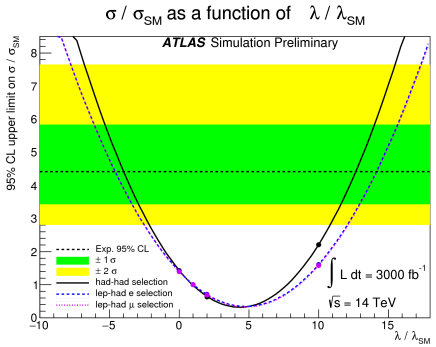

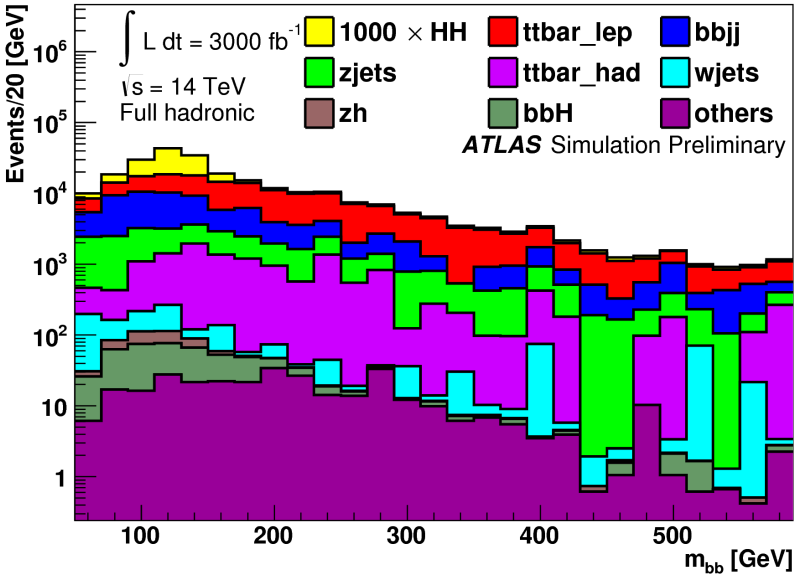

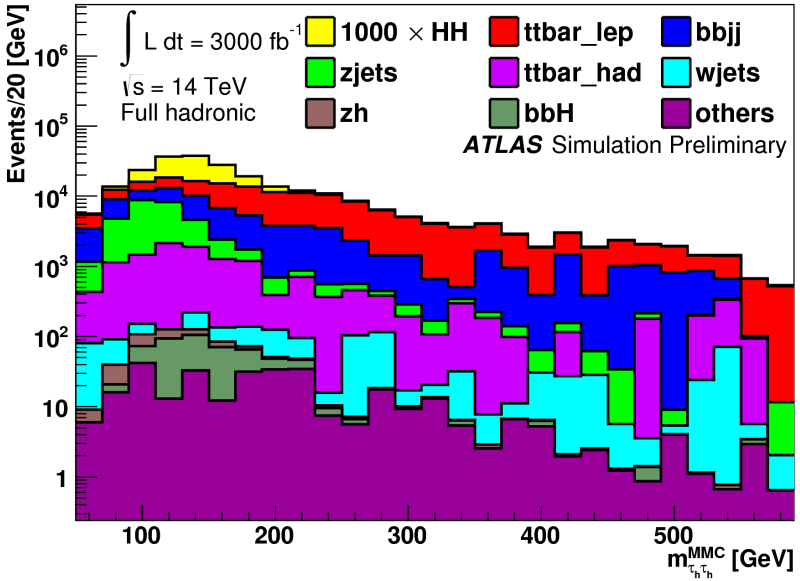

Prospects at HL-LHC for VBF, H->4l.

[Public note 11 Apr 2016](#)
[ATL-PHYS-PUB-2016-008](#)

Three detector layouts compared.
<μ> = 200
Pile-up efficiency = 0.02
ggF and qqZZ are backgrounds
BDT trained to separate S and B
Training on smeared hard scatter-jets

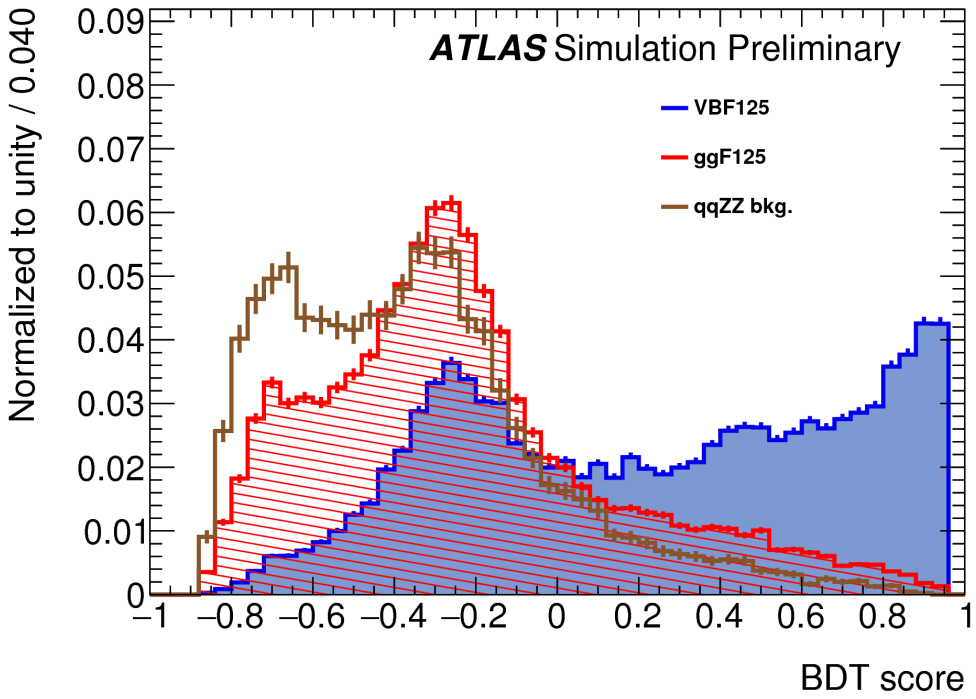

Sample	Expected events after $4l$ selection	Expected events after dijet selection
ggF (POWHEG)	7812	621
VBF (POWHEG)	720	358

Sample	Full sample events	Full event weights	Weights after $4l$ cuts	After dijet cuts
ggF (POWHEG)	4 919 000	2.23×10^8	4.09×10^7	3.25×10^6
VBF (POWHEG)	9.8×10^5	9.8×10^5	193 036	95 768

ATLAS+CMS Run I 7+8 TeV combination.

Submitted to JHEP
arXiv:1606.02266

Data consistent with SM. Total μ = 1.09 ± 0.11.

Production process		Decay mode											
		$H \to \gamma\gamma$ [fb]			$H \to ZZ$ [fb]			$H \to WW$ [pb]			$H \to \tau\tau$ [fb]			$H \to bb$ [pb]		
		Best fit value	Uncertainty Stat	Uncertainty Syst	Best fit value	Uncertainty Stat	Uncertainty Syst	Best fit value	Uncertainty Stat	Uncertainty Syst	Best fit value	Uncertainty Stat	Uncertainty Syst	Best fit value	Uncertainty Stat	Uncertainty Syst
*gg*F	Measured	$48.0\ ^{+10.0}_{-9.7}$	$^{+9.4}_{-9.4}$	$^{+3.2}_{-2.3}$	$580\ ^{+170}_{-160}$	$^{+170}_{-160}$	$^{+40}_{-40}$	$3.5\ ^{+0.7}_{-0.7}$	$^{+0.5}_{-0.5}$	$^{+0.5}_{-0.5}$	$1300\ ^{+700}_{-700}$	$^{+400}_{-400}$	$^{+500}_{-500}$		–	
		$(^{+9.7}_{-9.5})$	$(^{+9.4}_{-9.4})$	$(^{+2.5}_{-1.6})$	$(^{+150}_{-130})$	$(^{+140}_{-130})$	$(^{+30}_{-20})$	$(^{+0.7}_{-0.7})$	$(^{+0.5}_{-0.5})$	$(^{+0.5}_{-0.5})$	$(^{+700}_{-700})$	$(^{+400}_{-400})$	$(^{+500}_{-500})$		–	
	Predicted	44 ±5			510 ±60			4.1 ±0.5			1210 ±140			11.0 ±1.2		
	Ratio	$1.10\ ^{+0.23}_{-0.22}$	$^{+0.22}_{-0.21}$	$^{+0.07}_{-0.05}$	$1.13\ ^{+0.34}_{-0.31}$	$^{+0.33}_{-0.30}$	$^{+0.09}_{-0.07}$	$0.84\ ^{+0.17}_{-0.17}$	$^{+0.12}_{-0.12}$	$^{+0.12}_{-0.11}$	$1.0\ ^{+0.6}_{-0.6}$	$^{+0.4}_{-0.4}$	$^{+0.4}_{-0.4}$		–	
VBF	Measured	$4.6\ ^{+1.9}_{-1.8}$	$^{+1.8}_{-1.7}$	$^{+0.6}_{-0.5}$	$3\ ^{+46}_{-26}$	$^{+46}_{-25}$	$^{+7}_{-7}$	$0.39\ ^{+0.14}_{-0.13}$	$^{+0.13}_{-0.12}$	$^{+0.07}_{-0.05}$	$125\ ^{+39}_{-37}$	$^{+34}_{-32}$	$^{+19}_{-18}$		–	
		$(^{+1.8}_{-1.6})$	$(^{+1.7}_{-1.6})$	$(^{+0.5}_{-0.4})$	$(^{+60}_{-39})$	$(^{+60}_{-39})$	$(^{+8}_{-5})$	$(^{+0.15}_{-0.13})$	$(^{+0.13}_{-0.12})$	$(^{+0.07}_{-0.06})$	$(^{+39}_{-37})$	$(^{+34}_{-32})$	$(^{+19}_{-18})$		–	
	Predicted	3.60 ±0.20			42.2 ±2.0			0.341 ±0.017			100 ±6			0.91 ±0.04		
	Ratio	$1.3\ ^{+0.5}_{-0.5}$	$^{+0.5}_{-0.5}$	$^{+0.2}_{-0.1}$	$0.1\ ^{+1.1}_{-0.6}$	$^{+1.1}_{-0.6}$	$^{+0.2}_{-0.2}$	$1.2\ ^{+0.4}_{-0.4}$	$^{+0.4}_{-0.3}$	$^{+0.2}_{-0.2}$	$1.3\ ^{+0.4}_{-0.4}$	$^{+0.3}_{-0.3}$	$^{+0.2}_{-0.2}$		–	
WH	Measured	$0.7\ ^{+2.1}_{-1.9}$	$^{+2.1}_{-1.8}$	$^{+0.3}_{-0.3}$		–		$0.24\ ^{+0.18}_{-0.16}$	$^{+0.15}_{-0.14}$	$^{+0.10}_{-0.08}$	$-64\ ^{+64}_{-61}$	$^{+55}_{-50}$	$^{+32}_{-34}$	$0.42\ ^{+0.21}_{-0.20}$	$^{+0.17}_{-0.16}$	$^{+0.12}_{-0.11}$
		$(^{+1.9}_{-1.8})$	$(^{+1.9}_{-1.8})$	$(^{+0.1}_{-0.1})$		–		$(^{+0.16}_{-0.14})$	$(^{+0.14}_{-0.13})$	$(^{+0.08}_{-0.07})$	$(^{+67}_{-64})$	$(^{+60}_{-54})$	$(^{+30}_{-32})$	$(^{+0.22}_{-0.21})$	$(^{+0.18}_{-0.17})$	$(^{+0.12}_{-0.11})$
	Predicted	1.60 ±0.09			18.8 ±0.9			0.152 ±0.007			44.3 ±2.8			0.404 ±0.017		
	Ratio	$0.5\ ^{+1.3}_{-1.2}$	$^{+1.3}_{-1.1}$	$^{+0.2}_{-0.2}$		–		$1.6\ ^{+1.2}_{-1.0}$	$^{+1.0}_{-0.9}$	$^{+0.6}_{-0.5}$	$-1.4\ ^{+1.4}_{-1.4}$	$^{+1.2}_{-1.1}$	$^{+0.7}_{-0.8}$	$1.0\ ^{+0.5}_{-0.5}$	$^{+0.4}_{-0.4}$	$^{+0.3}_{-0.3}$
ZH	Measured	$0.5\ ^{+2.9}_{-2.4}$	$^{+2.8}_{-2.3}$	$^{+0.5}_{-0.2}$		–		$0.53\ ^{+0.23}_{-0.20}$	$^{+0.21}_{-0.19}$	$^{+0.10}_{-0.07}$	$58\ ^{+56}_{-47}$	$^{+52}_{-44}$	$^{+20}_{-16}$	$0.08\ ^{+0.09}_{-0.09}$	$^{+0.08}_{-0.08}$	$^{+0.04}_{-0.04}$
		$(^{+2.3}_{-1.9})$	$(^{+2.3}_{-1.9})$	$(^{+0.1}_{-0.1})$		–		$(^{+0.17}_{-0.14})$	$(^{+0.16}_{-0.14})$	$(^{+0.05}_{-0.04})$	$(^{+49}_{-40})$	$(^{+46}_{-38})$	$(^{+16}_{-12})$	$(^{+0.10}_{-0.09})$	$(^{+0.09}_{-0.08})$	$(^{+0.05}_{-0.04})$
	Predicted	0.94 ±0.06			11.1 ±0.6			0.089 ±0.005			26.1 ±1.8			0.238 ±0.012		
	Ratio	$0.5\ ^{+3.0}_{-2.5}$	$^{+3.0}_{-2.5}$	$^{+0.5}_{-0.2}$		–		$5.9\ ^{+2.6}_{-2.2}$	$^{+2.3}_{-2.1}$	$^{+1.1}_{-0.8}$	$2.2\ ^{+2.2}_{-1.8}$	$^{+2.0}_{-1.7}$	$^{+0.8}_{-0.6}$	$0.4\ ^{+0.4}_{-0.4}$	$^{+0.3}_{-0.3}$	$^{+0.2}_{-0.2}$
ttH	Measured	$0.64\ ^{+0.48}_{-0.38}$	$^{+0.48}_{-0.38}$	$^{+0.07}_{-0.04}$		–		$0.14\ ^{+0.05}_{-0.05}$	$^{+0.04}_{-0.04}$	$^{+0.03}_{-0.03}$	$-15\ ^{+30}_{-26}$	$^{+26}_{-22}$	$^{+15}_{-15}$	$0.08\ ^{+0.07}_{-0.07}$	$^{+0.04}_{-0.04}$	$^{+0.06}_{-0.06}$
		$(^{+0.45}_{-0.34})$	$(^{+0.44}_{-0.33})$	$(^{+0.10}_{-0.05})$		–		$(^{+0.04}_{-0.04})$	$(^{+0.04}_{-0.04})$	$(^{+0.02}_{-0.02})$	$(^{+31}_{-26})$	$(^{+26}_{-22})$	$(^{+16}_{-13})$	$(^{+0.07}_{-0.06})$	$(^{+0.04}_{-0.04})$	$(^{+0.06}_{-0.05})$
	Predicted	0.294 ±0.035			3.4 ±0.4			0.0279 ±0.0032			8.1 ±1.0			0.074 ±0.008		
	Ratio	$2.2\ ^{+1.6}_{-1.3}$	$^{+1.6}_{-1.3}$	$^{+0.2}_{-0.1}$		–		$5.0\ ^{+1.8}_{-1.7}$	$^{+1.5}_{-1.5}$	$^{+1.0}_{-0.9}$	$-1.9\ ^{+3.7}_{-3.3}$	$^{+3.2}_{-2.7}$	$^{+1.9}_{-1.8}$	$1.1\ ^{+1.0}_{-1.0}$	$^{+0.5}_{-0.5}$	$^{+0.8}_{-0.8}$

Higgs bosons can be produced by coupling with bosons (VH, VBF) or with fermions (ggF, ttH).